





Article

A Vision of 6th Generation of Fixed Networks (F6G): Challenges and Proposed Directions

Dimitris Uzunidis ¹, Konstantinos Moschopoulos ¹, Charalampos Papapavlou ¹, Konstantinos Paximadis ¹,
Dan M. Marom ², Moshe Nazarathy ³, Raul Muñoz ⁴ and Ioannis Tomkos ^{1,*}

¹ Department of Electrical and Computer Engineering, University of Patras, 26504 Patras, Greece; paximadis.konstantinos@ac.eap.gr (K.P.)

² Department of Applied Physics, Hebrew University of Jerusalem, Jerusalem 91904, Israel; danmarom@mail.huji.ac.il

³ Faculty of Electrical and Computer Engineering, Technion, Israel Institute of Technology, Haifa 32000, Israel; nazarat@ee.technion.ac.il

⁴ Centre Tecnologic de Telecomunicacions de Catalunya (CTTC/CERCA), 08860 Castelldefels, Spain

* Correspondence: itom@ece.upatras.gr

Abstract: Humankind has entered a new era wherein a main characteristic is the convergence of various technologies providing services and exerting a major impact upon all aspects of human activity, be it social interactions with the natural environment. Fixed networks are about to play a major role in this convergence, since they form, along with mobile networks, the backbone that provides access to a broad gamut of services, accessible from any point of the globe. It is for this reason that we introduce a forward-looking approach for fixed networks, particularly focused on Fixed 6th Generation (F6G) networks. First, we adopt a novel classification scheme for the main F6G services, comprising six categories. This classification is based on the key service requirements, namely latency, capacity, and connectivity. F6G networks differ from those of previous generations (F1G–F5G) in that they concurrently support multiple key requirements. We then propose concrete steps towards transforming the main elements of fixed networks, such as optical transceivers, optical switches, etc., such that they satisfy the new F6G service requirements. Our study categorizes the main networking paradigm of optical switching into two categories, namely ultra-fast and ultra-high capacity switching, tailored to different service categories. With regard to the transceiver physical layer, we propose (a) the use of all-optical processing to mitigate performance barriers of analog-to-digital and digital-to-analog converters (ADC/DAC) and (b) the exploitation of optical multi-band transmission, space division-multiplexing, and the adoption of more efficient modulation formats.

Keywords: fixed networks; F6G; optical switching; capacity scaling; optical networks; network services; optical transceivers; optical transmission; telecom industry; all-optical processing



Citation: Uzunidis, D.; Moschopoulos, K.; Papapavlou, C.; Paximadis, K.; Marom, D.M.; Nazarathy, M.; Muñoz, R.; Tomkos, I. A Vision of 6th Generation of Fixed Networks (F6G): Challenges and Proposed Directions. *Telecom* **2023**, *4*, 758–815. <https://doi.org/10.3390/telecom4040035>

Academic Editor: Barbara M. Masini

Received: 7 June 2023

Revised: 27 July 2023

Accepted: 9 October 2023

Published: 7 November 2023



Copyright: © 2023 by the authors. Licensee MDPI, Basel, Switzerland. This article is an open access article distributed under the terms and conditions of the Creative Commons Attribution (CC BY) license (<https://creativecommons.org/licenses/by/4.0/>).

1. Introduction

Modern telecommunications are the direct offspring of the Second Industrial Revolution, which commenced with the deployment of the Public Switched Telephone Network (PSTN) in the second half of the 19th century. The Third Industrial Revolution led to great advances in electronics and the introduction of new services, especially Internet services, exerting a profound impact on the way people communicate, work, and live. Nowadays, we have entered the Fourth Industrial Revolution (I4.0), which has led to the convergence of various processes, like fixed/wireless communication, computing, and sensing, into a single network entity. The forthcoming transformed network, and especially its access part, will concurrently serve as a communication medium, sensor, and super-computer, providing services to wield major impacts on all aspects of human activity and the forms of social interaction, as well as their interaction with the natural environment [1]. I4.0 marks the dawn of a completely new Epoch where its main characteristic is the convergence,

and eventually the fusion, of those technologies that define our technosphere into a single technological continuum [2–4].

Social interactions are about to deepen through a broad gamut of novel services to be offered to end-users by service/network providers and will be emerging in the context of the 6th Generation of Fixed networks (F6G). The work of [5] presented the evolution of services as well as the various network layers over the first five fixed-network generations (F1G–F5G), based on a layered approach to enable deeper understanding of the key drivers underlying the evolution. More specifically, ref. [5] examined and reviewed the key technological advances, standards, enablers, and limitations in fixed telecommunication networks over the past 50 years. The starting point of [5] was 1970 and the ending point is 2020, examining the impact of the third Industrial Revolution on the various layers of the telecommunications ecosystem. In the current work, we are examining the impact of the fourth Industrial Revolution on the various layers of the telecommunications ecosystem particularly focusing on F6G services and their requirements, following a dialectical procedure and observing that the limitations of F5G are becoming the novelties of F6G.

The main aim of the work of [5] and the current visionary work is to shed light particularly on the fixed part of the network, as the wireless part of the network and its generations have been extensively investigated in the literature. For telecommunications, fixed constitutes one pillar and wireless the other; for this reason, from the end users' perspectives, they are of equal importance, as they can exploit one or the other pillar to access the network and enjoy the offered services. Both fixed and wireless parts of the network have specific Key Performance Indicators (KPIs) and requirements, which need to be satisfied in order to ensure seamless operation of the 6G/F6G demanding services during the entire service life-cycle; the most important can be found in [6].

In this work, our methodology for presenting our vision is as follows. First, we explore the strict requirements demanded of the service/network providers, such as high bit-rate, low latency, dense connectivity, and more (Section 2). These requirements will aid in defining the research objectives and the outstanding challenges and proposing stratagems to aid in successfully fulfilling them in a cost- and energy-efficient way. Next, based on these requirements, we elaborate our vision in three directions: (a) Discuss state-of-the-art transceivers along with novel techniques to scale the bit rate flexibly up to 2 Tb/s (Section 3); (b) propose and elaborate on different options to enhance the transportation capacity and node connectivity as well as analyze the interplay between transported capacity and transparent reach (Section 4); and (c) analyze optical switching in the F6G era by proposing alternatives to satisfy ultra-high capacity and ultra-low latency demands, while enabling scalability from operating down to a fraction of the spectrum of a channel up to the full spectral capacity of the optical fiber, whereby channels fully occupy the available bands (Section 5). The presentation of our vision in these three directions will highlight the key challenges of F6G networks and explore solutions to address them at various levels of the network, as well as use prior knowledge to make informed predictions up to 2030 about the foreseeable evolution of key metrics such as attainable per-fiber capacity, data rate per-channel, etc. For each of the three directions, a thorough literature review is performed while the pros and cons of important published research works are highlighted and elaborated in order to designate what it is needed in order to seamlessly support the F6G services.

This vision of the article is organized as follows. In Section 2, the key services of the F6G ecosystem along with their requirements are analyzed. Next, in Section 3, a thorough examination of the literature on optical transceivers is performed. Next, all-optical processing is addressed, proposing concrete steps for how 'to get there' in light of the pros and cons of ADCs and DACs. In Section 4, the barriers to optical transmission are examined, emphasizing how to push F6G capacity even higher, considering methodologies to attain spectrally efficient modulation formats, increased channel counts, and opening up additional transmission degrees-of-freedom by means of space division multiplexing (SDM) via the use of extra fibers, modes, or cores. Based on the relevant literature, we also pro-

vide predictions about the transported capacity per channel and per single mode fiber up to 2030. In Section 5, a thorough examination of the literature on optical switching is performed. Subsequently, the issue of optical switching is investigated regarding the needs of the F6G ecosystem for both cases of switching, namely ultra-fast vs. ultra-high capacity switching, each one tailored to different performance criteria. Finally, a summary of the key findings is provided in Section 6.

2. Services and Requirements for F6G

2.1. Classification of Services

According to the F5G group timeline [7,8], today we have entered the 5th generation of fixed networks (F5G), which paves the way for various fresh services, such as augmented and cloud virtual reality, smart city, ultra-high definition (UHD) video streaming, etc., and discussions about the 6th generation (F6G) are already taking place. F6G is expected to majorly transform the overall network ecosystem in various dimensions, in order to underpin the stringent requirements of the forthcoming F6G services. Key components for F6G are expected to be (a) the industrial sector, e.g., through digital representation of the physical world (digital twin), (b) the field of entertainment/communications, e.g., through holograms, internet of senses, and mixed reality, and (c) the transportation sector, mainly through the use of ultra-smart infrastructures, such as airports, ports, highways, cities, and railways. To further understand the evolution of services, we illustrate the three key services for each of the six generations of fixed networks in Figure 1.

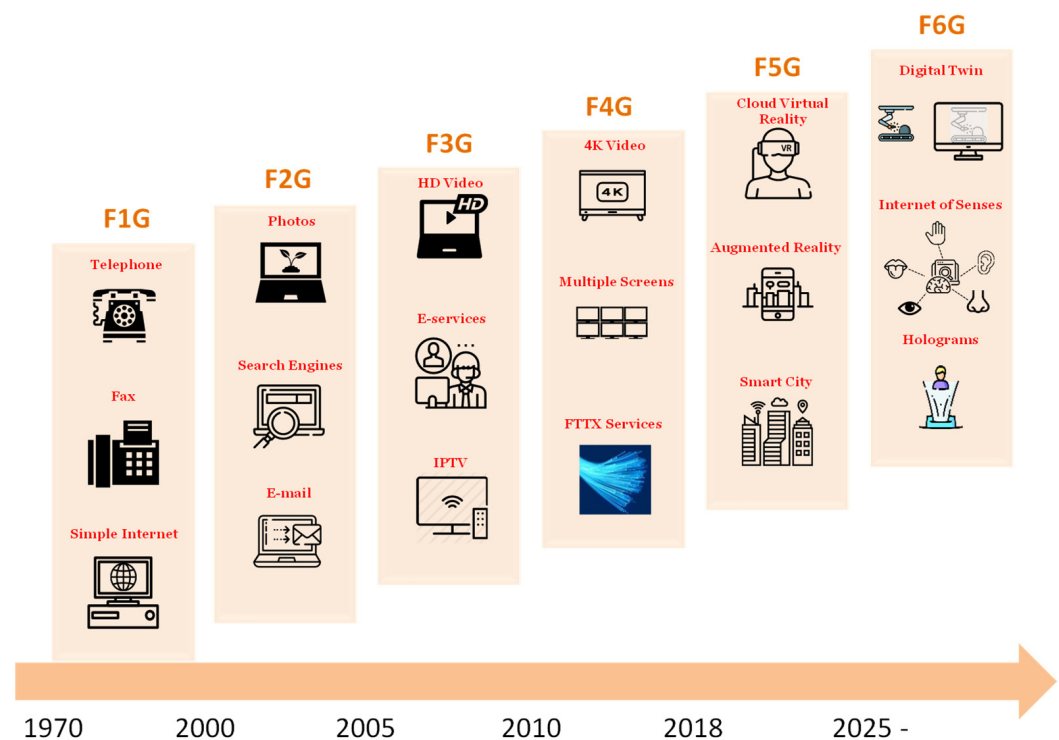


Figure 1. Representative services over the six fixed network generations as a result of 3rd and 4th Industrial Revolutions.

The main difference in F6G services compared with F5G ones, which poses major challenges to network providers, is that they need various strict requirements to be satisfied *concurrently* in order to ensure a seamless service operation during the entire service life cycle. For example, industrial services such as digital twins require high densification, high bit rate, low latency, and high reliability at the same time. In order to ensure this, a significant amount of research work needs to be performed, and the network needs to be transformed accordingly in order to attain (based on the service) increased capacity, lower latency, higher reliability, greater availability, higher densification, lower jitter, etc., and all

these using low-cost and low-power-consumption platforms. These requirements can be satisfied through many options, each with its own merits; some indicatives are new optical wavelength bands, space division multiplexing, high-capacity and ultra-low latency optical switching, free-space optical communications, new integration schemes, and the use of all-optical processing techniques in Tx/Rx, as well as the integration of Artificial Intelligence (AI)/Machine Learning (ML) with the overall network ecosystem. These options and their feasibility, along with their advantages, are discussed in the current work.

In the next sub-sections of this chapter, we elaborate on the F6G services and their requirements, then we present our vision of the F6G ecosystem and, finally, we analyze the network transformation that needs to be realized in order to support all the new types of services with their requirements.

2.2. Upcoming Categories of Services and Their Requirements

As shown in Figure 1, network evolution is service driven, and network operators and service providers continuously try to introduce “fresh” services to users in order to capitalize their investments on their network upgrades/transformations. Consequently, the service needs are always increasing with time. As in this paper we focus mainly on F6G, we tabulate a list with the most representative categories and services for the F6G ecosystem (Table 1). We classify the services into six categories based on three key requirements, which are bit-rate, fiber density, and latency. Three categories require only one of these requirements to be met in order to operate without disruptions and are named Enhanced Fiber BroadBand (eFBB), Full Fiber Connection (FFC), and Guaranteed Reliable Experience (GRE) [7]. The main key requirement for each category is a high bit rate, high densification, and low latency, respectively. Further, three more categories require a combination of the aforementioned three key requirements and are named Full Fiber BroadBand Connection (FFBC), requiring both high fiber density and high bit rate; Guaranteed Reliable Fiber Broadband (GRFB), requiring both low latency and high bit rate, and; Guaranteed Reliable Full Fiber Experience (GRFFE), requiring both high fiber density and low latency. It is worth mentioning, that some services may require *all the three key requirements to be met concurrently*, as they need to collect bandwidth-consuming signals and data (e.g., video) from various network points in order to process them in real time and inform the respective element in order to make a decision. Indicative services for this category are ultra-smart ports, airports, railways, and autonomous truck and taxi-fleets. Our vision of the F6G ecosystem incorporating the six service categories is pictorially described in Figure 2.

The categorization scheme for the 6G services presented in Figure 2 is equivalent to the scheme proposed in [9], which focuses mainly on the categories supported by the wireless part of the network. In the current work, the proposed scheme includes 6G services underpinned by the fixed part of the network. Both schemes complement each other in order to offer all service categories to the users at any point on the globe and regardless of the technology the users exploit to access the network. The equivalent categories of services accessed using the wireless part of the network are designated in Figure 2 in parentheses in red.

Another classification that can be made regarding F6G services is based on the domain of operation. The first domain includes I4.0 services, such as digital twins, automated operations in a harsh environment, collaborative robots (cobots), Augmented Reality (AR), and AI synergy with cloud computing, which aims to improve the quality of decisions on the production line. These services require high bandwidth, low latency, high reliability, and medium fiber density in order to operate efficiently. The second category includes entertainment/communication services, such as holograms, immersive extended reality, and internet of senses. There is a dissimilarity regarding the requirements of these services (e.g., holographic communications and extended reality require a high bit rate and low latency while the internet of senses shows more relaxed needs on latency and bit rate). The third category includes ultra-smart transportation and can be introduced in various types

of mediums, such as ports, airports, city roads, highways, and railways. Safety is one of the most important requirements here, but reliability, sufficient availability, high bandwidth, and low latency are also a must. The fourth category includes e-health services, such as Telesurgery, AR field medical support, and remote areas diagnosis/consultations, which mandate low latency and very high reliability. In the fifth category, the AR-assisted remote education requires an increased bit rate in order to provide a high level of interaction between students and teachers. In addition, low latency is required in order to allow interactions in real-time. In the final category, various safety-related services can be found, such as health hazard monitoring and AI-assisted incident detection, which, depending on the target-monitored metric, may require low latency (e.g., detecting an imminent threat) or high connectivity (e.g., monitoring and sensing several places concurrently for health hazards).

2.3. The Indispensable Network Transformation in Order to Realize the F6G Vision

In order to elaborate on the requirements of each of the six categories of services presented in Figure 2, we illustrate how F6G extends the key quantities when it is compared with F5G (Figure 3). Of course, there are additional critical requirements that need to be satisfied and are usually service-dependent, such as security, operational efficiency, spectral utilization, cost/power efficiency [7], jitter, etc. However, in this work, we are focusing on the three key metrics, which are latency, bit rate, and fiber density, as at least one of them is critical for any F6G service. Figure 3 highlights that, first, the introduction of a fresh Passive Optical Network (PON) standard is required in order to reach data rates of 100 Gb/s and beyond in the access domain and support bandwidth-critical services. Further, a new densification strategy needs to be adopted in order to realize Fiber to the Everything (FTE), which aims to integrate all “Fiber to the X” concepts that are expected to be introduced during F5G into a single network entity (such as Fiber to the Home (FTTH), Fiber to the Office (FTTO), Fiber to the Room (FTTR), Fiber to the Desk (FTTD), and Fiber to the Machine (FTTM) [9]). At the same time, this densification will aid in integrating fixed and wireless networks, leading to a major network transformation through which the network will be able to concretely support the demands of both wireless-based and wired-based services. Regarding latency, the F6G infrastructure is expected to advance significantly compared with F5G in order to support services with very low latency requirements, especially those of the industrial sector, which can be down at the order of some tens of μs [10–13]. In order to attain all these very strict requirements, there is a strong need for network/service providers to upgrade their current network infrastructure both at the component and network levels, as well as to make their network fully automated in order to perform fast and accurate decisions at a μs timescale.

Towards this target, in the next three sections, this work proposes various directions and solutions that can aid in underpinning F6G services in a cost- and energy-efficient way. Indicatively, a significantly larger spectrum needs to be allocated, which can be realized either by exploiting all five low attenuation bands of the optical fiber or by performing SDM, which in essence means data transmission through bundles of fibers, multi-core fibers, multi-mode fibers, few-mode fibers, and/or their combination [14–16]. At the same time, very high-capacity switches need to be installed and operate at very high bit rates (per channel) [17–20]. Further, ultra-fast optical switching will be a must in order to attain as low an end-to-end delay as possible by eliminating delay [10,13]. In order to reduce the overall cost and power consumption, novel all-optical transceivers need to be deployed, e.g., without the need for cumbersome modules such as electronic Digital to Analog Converters (eDACs) while the introduction of wavelength band converters and comb generators will assist in removing the electronic conversion, which can lead to a lower end-to-end delay. Finally, convergence between various technologies and methods such as those in 6G and F6G, as well as an all-encompassing integration, is required. This conversion will transform the network into a sensor, communicator, and super-computer, enabling it to automatically make AI-based decisions.

Table 1. Classification of services and their requirements in the F6G ecosystem. eFBB: Enhanced Fiber BroadBand, FFC: Full Fiber Connection, GRE: Guaranteed Reliable Experience, FFBC: Full Fiber BroadBand Connection, GRFB: Guaranteed Reliable Fiber Broadband, GRFFE: Guaranteed Reliable Full Fiber Experience.

Category	Service	Service Requirements				Service Type					
		Bandwidth	Latency	Reliability	Density	eFBB	FFC	GRE	FFBC	GRFB	GRFFE
Industry 4.0	Digital twins	H	L	H	M				x		
	Harsh environment automation	M	L	H	M					x	
	Collaborative robots	H	M	H	M						x
	AR diagnostics and collaboration	H	L	H	M						x
	AI and edge computing aided decisions	H	M	H	M			x			
Entertainment/ Communications	Holographic communications	H	M	M	L	x					
	Immersive extended reality (XR)	H	M	M	L	x					
	Internet of senses	M	M	M	L	x					
Transportation	Ultra smart airport	H	L	H	H				x	x	
	Ultra smart port	H	L	H	H					x	x
	Ultra smart highway	H	L	H	H				x		
	Ultra smart city	H	L	H	H				x		
	Ultra smart railway	H	L	H	H					x	x
	Seamless monitoring, e.g., airplanes, fleet	H	L	H	H					x	x
E-Health	Telesurgery	H	L	H	L					x	
	AR field medical support	H	L	H	L					x	
	remote areas Diagnosis/consultations	H	L	H	L					x	
Education	AR-assisted remote education	H	L	H	L				x		
Safety	Health hazard monitoring	H	M	H	M		x				
	AI-assisted incident detection	H	M	H	M			x			

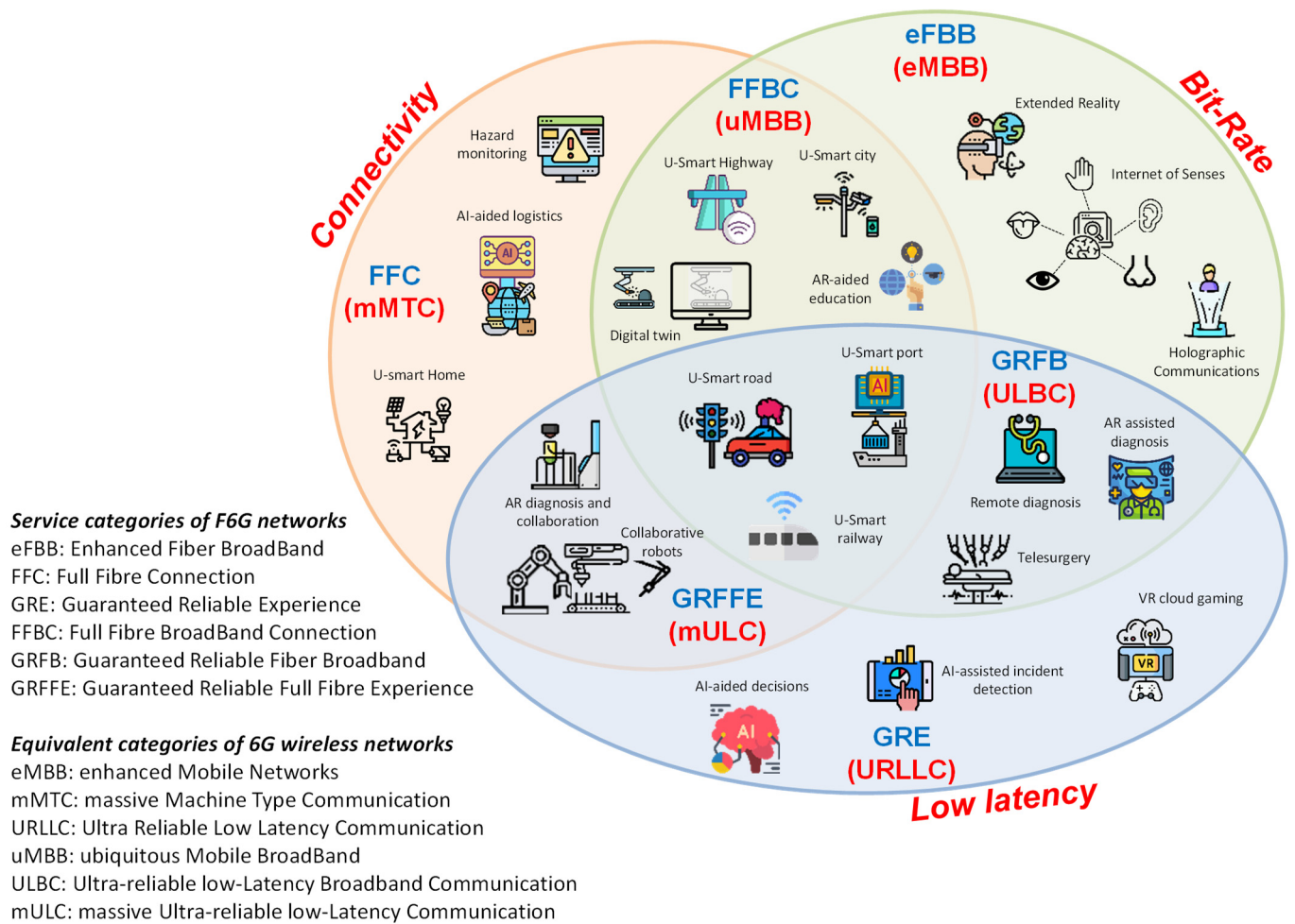
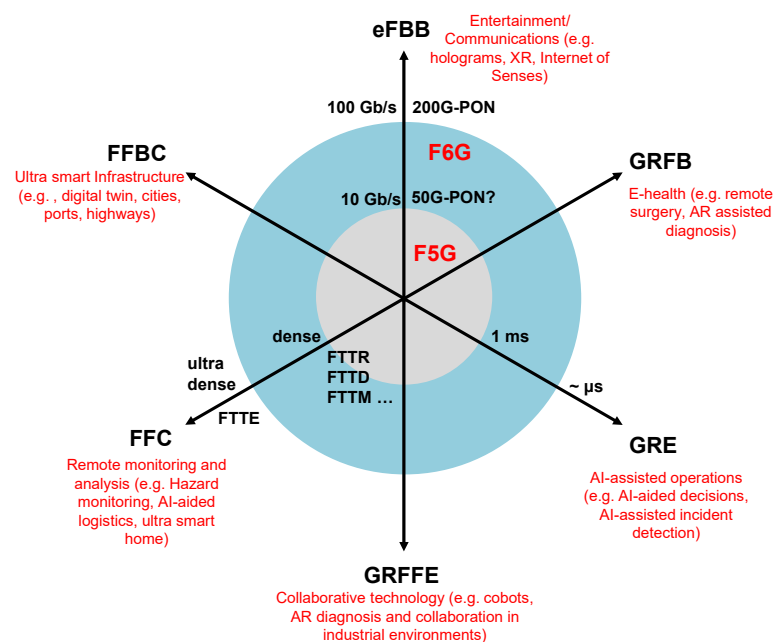


Figure 2. Our vision of the F6G ecosystem: The six categories of services based on their requirements. The equivalent categories of the 6G ecosystem are shown in parentheses in red.



3. Photonics-Based Subsystems for All-Optical Processing

In recent years, innovative approaches have emerged to address the challenge of efficient scaling of the bit-rate of the transceivers (TRx) to support the various network segments per their specific needs. From a cost and power consumption perspective, the TRx requirements of the optical access network in the 5G/6G era are quite distinct from those of core networks, and the emphasis is on further reduction of cost/power consumption of short-reach systems. Another significant feature of state-of-the-art TRxs is their capability to dynamically vary the bitrate and have them tailored to variable service demand. This feature is beneficial for network operators, as it provides significant savings in cost and energy. Hence, TRx breakthroughs enabling one to unlock bitrate up-scaling, energy/cost-efficiency, and agile programmability of parameters such as modulation format or baud rate are desirable. To attain these objectives, TRxs for fiber-optic transmission have been extensively developed for long-haul transmission, wherein the key objective is the capacity times reach maximization, whereas cost and energy efficiency are deemed secondary requirements. The energy-efficiency challenge, in particular, emerges as a key barrier precluding straightforward migration of high-bit-rate TRxs from long-reach links to short-reach 5G/6G and cloud networks/datacenter interconnects.

A major driving force boosting TRxs capabilities over the past few decades has been the tremendous advance in electronics. Unfortunately, porting those advances to the environment of short-reach communication is now proving difficult, as silicon technology approaches its energy-efficiency limits, no longer able to keep supporting the energy demands of the ever higher sought performance. In particular, state-of-the-art implementations of ultra-high-speed optical transceivers, used in coherent long-haul systems for generating and detecting Tb/s signal constellations, are based on power-hungry electronic Application-Specific Integrated Circuits (ASICs), platforms used to implement electronic DACs (eDAC), electronic ADCs (eADC), and Digital Signal Processing (DSP) functionalities. On the transmitter side, eDACs are key interfaces converting the signal from the digital to the analog domain. In high-speed optical transmitters, state-of-the-art techniques for digital-to-optical (D/O) transduction typically comprise power-consuming and costly eDAC-based data-conversion, followed by analog optical modulation. As eDAC technology is becoming more expensive in both cost and energy, next-generation TRxs are highly challenged to sustain upscaling in speed, while keeping power dissipation at bay. In particular, the rise in the pJ/b figure-of-merit is a major bottleneck in TRxs employing eDAC/eADC technologies. Therefore, innovative approaches are in high demand to enable advancing the rates to as high as 10 Tb/s per TRx at the lowest performance/capacity penalties.

Aiming for that objective, we commence by inspecting the transmitter and receiver structures (Figure 4), which comprise the main electronic section providing multiple essential functionalities. First, the electronic circuit in the transmitter processes the information bitstream in the digital domain, performing various operations, such as error-correction, signal mapping, spectrum shaping, pre-distortion, etc. Then, via a D/A converter (eDAC) typically of the current-steered type, followed by a transimpedance amplifier (TIA), the digital signal is transduced to the voltage analog domain in order to drive the optical modulator. On the receiver side, following the optical front-end, a TIA with automatic gain control feeds an A/D converter (eADC) transducing the signal to the digital domain for Digital Signal Processing (DSP). The DSP 'engine' comprises building blocks such as polarization demultiplexing, carrier frequency, phase recovery, IQ imbalance compensation clock recovery, adaptive equalization, data decoding (slicer), and error detection and correction decoding; overall, compensating for distortions and mitigating/correcting errors that arise due to the physical layer impairments along the transmission link. In both the Tx and Rx sides, the ultra-high-speed ADC/DAC and DSP functionalities, realized on state-of-the-art ASICs, are bandwidth-constrained and turn out to be extremely power-hungry, imposing significant scalability limitations. Averting the soaring costs and power consumption of TRxs in Access and intra-Data Center Interconnection (DCI) networks is a particularly challenging task put forward to the research community, requiring creative approaches to

enable conceiving novel efficient solutions, in light of worrisome models predicting that electricity use by information and communications technologies could exceed 20% of the worldwide electricity consumption by 2030, with data centers using more than one-third of that [21]. Therefore, solutions to increase or at least retain energy-efficiency, for the ever-higher bit rates, are of utmost importance.

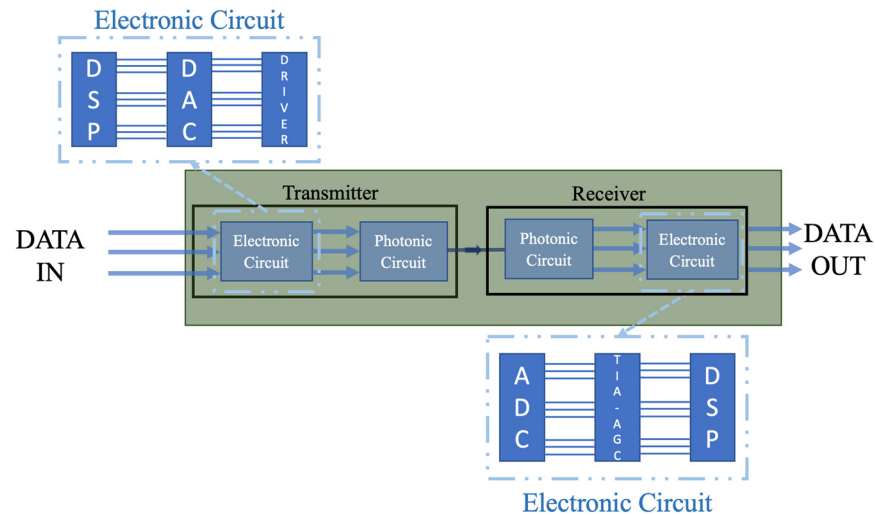


Figure 4. Conventional optical transceiver. On the transmitter side, the electronic circuit employs the DSP, DAC, and DRIVER functionalities, whereas on the receiver side, the electronic circuit employs the ADC, TIA-AGC, and DSP functionalities. The photonic circuit performs the modulation of light on the transmitter side and photodetection on the receiver side.

Efforts to develop low-cost/power interconnect solutions for short-reach networks have been sparse and mainly explored two directions: (i) All-optical DAC/ADC implementations that reduce the use of electronic DACs/ADCs [22] and (ii) all-optical implementation of coherent receivers as efficient alternatives to the power-hungry electronic DAC/ADC/DSP-chip functionalities [23]. It is worth mentioning that in short-reach interconnects, on which we are mainly focused, link lengths are constrained to less than 20–50 km for 5G/6G fronthaul and access networks and less than 2 km for intra-data center interconnects; however, the bit rate can still scale to high numbers, e.g., to some hundreds of Gb/s. In these domains, less costly methods are usually employed; this is why Direct-Detection (DD) optical interconnects have been widely utilized in such short-reach interconnects, heretofore. However, besides Intensity Modulation (IM)-DD systems, the option of adopting coherent detection-based transceivers in shorter-reach networks has been investigated with the aim to facilitate scaling up bit-rates while reducing energy-per-bit, where according to conventional wisdom, many functions employed in the DSP-chips of long-haul-oriented transceivers addressing dispersion and non-linearities of the optical fiber (which are absent or less prominent in short-reach links) can be removed in order to mitigate the cost and power consumption bottleneck of electronic circuitry.

In the following subsections of this section, we survey all-optical solutions to be harnessed to tackle the upcoming bottlenecks of increased power consumption and cost that electronics are subject to (Section 3.1). Subsequently, we describe how analog-to-digital and digital-to-analog conversion can be implemented mainly using photonic technology (Sections 3.2 and 3.3). Finally, it is suggested that research in these two systems fits within the framework of the wider domain of ‘reconfigurable photonics’, showing use cases potentially enabling lower cost and lower power consumption (Section 3.4).

3.1. All-Optical Coherent and Simplified Coherent Solutions: Challenges and Opportunities

After a long period of utilizing coherent systems for long-haul transmission, the need to exploit the same benefits in terms of offered data rates for shorter links has become

apparent. Following this path, a lot of research has been conducted lately to unravel coherent transceivers with the power consumption and cost penalties that they are attached to. In this context, two main alternatives have been extensively investigated in the literature: (a) The simplified coherent and (b) the analog coherent. In order to offer optimized performance for short links and high energy efficiency, both discard many of the digital signal processes that conventional coherent transceivers employ. The all-analog (electronic and photonic) signal processing techniques have been utilized to partially replace some of the processes of DSP and power-hungry electronics (e.g., DACs, ADCs, and electrical phase-locked loops). This is different than the lite-coherent approach where the main objective is to optimize the DSP algorithms in order to reduce the power consumption. The differences between analog and simplified coherent can be mostly found on the optical frontend, where analog coherent systems remain the same compared with the conventional architecture, while in simplified coherent systems, different architectures than those of the conventional ones have been proposed to exploit the benefits of coherent transmission. Furthermore, solutions for scaling up the capacity using direct detection schemes have been proposed as a simpler alternative. In [24,25], using a polarization demultiplexing scheme, it is described how to exploit two different polarization multiplexed intensity-modulated signals. Thus, direct detection can offer twice the rate once an analog polarization demultiplexer is realized. Along these lines, we can extend the benefits of IMDD by employing a novel PAM-M modulator that has been proposed recently using a parallel scheme of MZMs in order to relax the requirements of the eDACs [26]. In conclusion, even though simplified coherent solutions have been much more investigated and are presented in the upcoming paragraphs, a quantitative comparison between the conventional schemes, analog coherent, simplified coherent, and the two very similar architectures that share strong similarities between analog and simplified is introduced and tabulated in Table 2.

Table 2. Comparison of various parameters of four low-cost/-power transceiver schemes for short-reach transmission [26].

	Conventional IMDD PAM-4	Conventional Coherent	Simplified Coherent	Analog Coherent	Low Cost/Power Dual Polarization PAM4 IMDD3	Analog Coherent W/Novel PAM-M Implementation
LO requirements	No	DFB	No	DFB	No	Typical
Tx complexity	None	Limited by eDACs	Limited by eDACs	Limited by eDACs	Limited by eDACs	None
Rx complexity	PD	Power Hungry DSP&Electronics	None	oPLLs	None	None
DSP at Rx	Low	Heavy	None	Low	None	Low
Power Consumption	Medium	Very High	Low	Low	Low	Low
Signaling rate	Up to 100 Gbs/s	Up to 800 Gbp/s	Up to 112 Gbs/s/ λ /pol	Up to 200 Gbs/s/ λ /pol	N/A	Estimated up to 800 Gbs/s/ λ
Reach	More than 20 km	More than 1000 km	Up to 2 km	Up to 10 km	N/A	Estimated up to 10 km
Application	Access/Intra-DC	Long-Haul/Submarine	Short reach/Access	Intra-DC	Intra-DC	Inter-DC/Intra-DC/Access

The all-optical receiver has been initially presented in [26] (see Figure 5 for its high-level design), indicating the possibility of replacing the DSP chip with an all-optical analog front-end that can achieve most of the required functionality.

The novel required Rx Blocks of this scheme are: Analog optical carrier phase recovery utilizing an Optical Phase-Locked Loop (OPLL) based on a low-linewidth Laser [23,27], to optically decouple the two I and Q quadratures.

Analog optical polarization demultiplexing circuit [28], decoupling all optically the two signal polarizations.

The OPLL could be implemented at a bandwidth of ~10–100 MHz based on a high-bandwidth photodetector and a low-linewidth semiconductor laser, operating the local oscillator laser as a Current Controlled Oscillator (CCO). The Analogue Polarization Demultiplexing (PoDMUX) circuit block, depicted in Figure 5 in the polarization controller inset, consists of a cascade of several 2×2 matrix stages and is implemented based on directional couplers and phase modulators (PMs), as was experimented in [29]. It is noted

that slow (~ 10 kHz rate) precise tuning control of the phase alignments of the PMs in the cascade is required as an essential enabler for the practical polarization demux functionality of this block to which we refer to as the Analog Optical Signal Processor (AOSP). Due to the all-optical nature of signal processing in the 10–100 MHz building blocks of this transceiver, which are transparent to the ultra-high-speed optical signals modulated onto the light flowing along it, the efficient operation of the AOSP polarization demux is essentially independent of the baud rate; hence, the supported bit-rate is scalable to >800 Gb/s rates per wavelength/space lane. Moreover, multiple optical wavelengths may be served at once (polarization demultiplexed together by a single AOSP) to further scale the offered capacity. The AOSP is still followed by ADCs (slicers), albeit at a much-reduced Effective Number Of Bits (ENOB), and the DSP is reduced in cost, footprint, and power consumption, as the XY polarizations and IQ quadratures are effectively decoupled ahead of the four ADCs. Other receiver operations such as timing recovery and detection may be performed with a high-speed analog electronics stage using conventional clock and data recovery (CDR) techniques. Alternatively, these functions may be relegated to the scaled-down DSP.

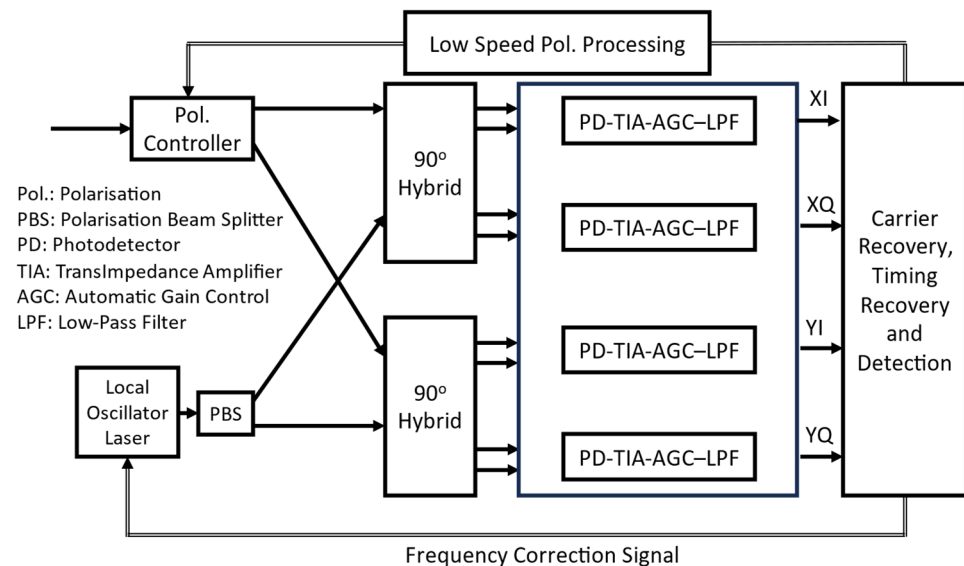


Figure 5. Block diagram of DSP-free coherent receiver (PM-QPSK) based on AOSP [29].

For basic proof-of-principle feasibility purposes, the operation of such an AOSP receiver has been demonstrated via preliminary simulations and the results are shown in Figure 6. In this particular example, operation at an aggregate rate of 400 Gb/s was considered [26]. In the simulation platform, the AOSP was constructed by considering a low-linewidth local oscillator laser and a cascade of discrete Mach–Zehnder Modulators (MZMs) and PMs for the Pol-Demux, which is not as effective as in the case where integrated elements in a Photonic Integrated Circuit (PIC) are employed. Following the all-optical AOSP-based polarization demultiplexing and phase/frequency recovery operations, the four coherently recovered analogue lanes, I_x , Q_x , I_y , and Q_y , display clear bipolar Pulse Amplitude Modulation 4 (PAM4) eye diagrams, which are detectable using conventional CDRs (based on all-analogue electronic symbol timing recovery and 4-level slicing implemented in merchant Silicon circuitry). These initial simulation results at 400 Gb/s [26] are significant, as they validate the feasibility of the all-optical analogue signal processing-based coherent transceiver.

The aforementioned all-optical solutions, besides the sufficient transmission performance, can also scale-up the capacity capabilities in order to meet the ever-growing traffic demands of the coming decade. Furthermore, they can serve as important solutions for optical interconnects in datacenters and 5G telecom infrastructures, which are the network

domains wherein the cost (measured in \$/Gbps) and power consumption (W/Tb/s) must be further reduced [26].

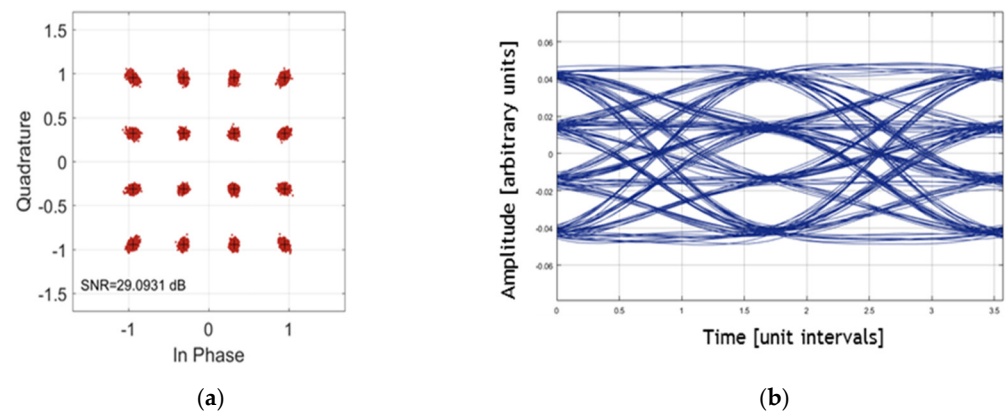


Figure 6. The 16-QAM constellation diagram is shown in (a) and the subsequent PAM4 eye diagram in (b) for one of the quadratures, attained using an AOSP-based receiver [26].

Figure 7 presents a high-level comparison between the AOSP based transceiver and other popular transceiver designs for 400 Gb/s interconnects. Evidently, the cost and power consumption using conventional coherent solutions are prohibitively large for such applications. A straightforward solution could consist of the combination of parallel fibers exploiting lower-performance transceivers in order to achieve the desired capacity. Unfortunately, the scalability of such an idea once benchmarked against alternatives, is limited by the number of fibers that can be deployed in parallel. Another potential solution is Wavelength Division Multiplexing (WDM); however, WDM is constrained in cost and power consumption due to the high complexity of deployment. As a consequence, it is becoming evident that for short-reach applications (below 10 km), the AOSP transceiver may be a competitive option as it concurrently addresses the desirable characteristics of low cost and power consumption, high data rate, low latency, high scalability, and reach of up to at least 10 km.

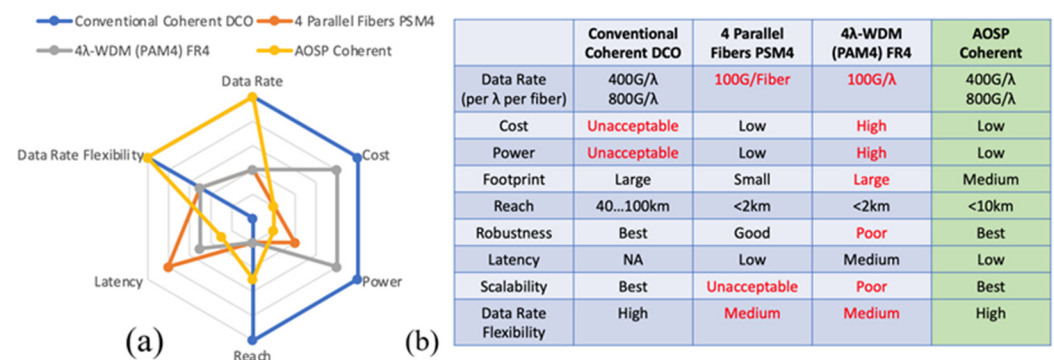


Figure 7. Comparison is shown as a star diagram (a) and through a table (b) of the AOSP with alternative implementations for various quantities [26].

Other notable options are classified in the category of ‘simplified coherent’ solutions. These solutions entail various tradeoffs between the extremes of direct-detection and coherent detection, exploiting both the amplitude and the phase of the optical signal to increase the transmitted data rate, albeit with lower complexity compared with conventional coherent transceivers, e.g., comprising a smaller number of optical elements. The main advantage of coherent technology is the benefit of up to 4-times higher bit-rate while keeping transceiver cost and power consumption at bay. To achieve this goal, new all-optical techniques are envisaged [30–32]. Using these alternatives, the cumbersome DSP

components are no longer required. These techniques target extremely low-cost applications where the requirements cannot be simply met via using direct detection techniques, whereas the cost and power consumption of fully coherent solutions would be prohibitive and the coherent performance would be an ‘overkill’.

In this category of solutions, Erkilinc et al. in [30] proposed a single polarization scheme that incorporates a polarization-time block-code signal, circumventing polarization tracking and driving a dual-polarization modulator at the transmitter. In this context, both intradyne and heterodyne architectures have been investigated and resulted in massive simplification of the receiver side, discarding polarization rotators, beam splitters, two balanced Photo-Diodes (PD), and ADCs. Next, Cano et al. [31] adopted another simplified version, first introduced by Kazovsky et al. [32], using a 3×3 coupler followed by three single-ended PDs and three ADCs for the intradyne reception. The main advantage of this solution is the polarization scrambling technique [33], attaining polarization-independent detection avoiding polarization tracking devices at the receiver. The third approach by Ciarrella [34] utilized polarization-independent reception with a polarization beam splitter (PBS) and a symmetric 3×3 coupler followed by three single-ended PDs. The 3×3 coupler incorporated the intermixing of three signals: (a) One horizontal signal, (b) one vertical polarized signal, and (c) the incoming signal. The horizontal and vertical signals are the outputs of the polarization beam splitter. In this architecture, ADCs and DSP can be completely removed; therefore, only the On Off Keying (OOK) or PAM4 signal can be detected by the receiver. The most recent work in the literature is called quasi-coherent [35,36], also classified in the category of simplified coherent approaches. Here, the signal and LO are mixed using a coupler. Then passing them through a PBS, the two resulting optical signals are fed into two PDs and, next, by performing envelope detection, they are inserted into the electronic amplifier. Based on these aforementioned techniques, we conclude that dual-polarization schemes or Quadrature Amplitude Modulation (QAM) formats can be dispensed with under certain conditions, for the sake of minimization of optical and/or electrical components, albeit the reduced data rates. That is why these coherent-like approaches are best suited for extremely low-cost and low-power consumption solutions in short-reach applications but do not typically qualify for either long-haul transmission or for high-end (inter) datacenter interconnects.

It is for this reason that new coherent approaches emerge in order to cover the white areas of the optical communication market. Based on the complexity, which directly impacts the cost and power consumption, Figure 8 maps the different options with the network domain where they can be applied.

3.2. Photonic ADCs: Challenges and Opportunities

A tremendous amount of research has been conducted on Analog-to-Digital Conversion from the beginning of modern telecommunications. The reason is apparent: The information to be exchanged among the users via the Internet is predominantly, almost exclusively, digital. Although research is focused on both electronic and photonic realizations of ADCs, heretofore only the electronic ones have been commercialized. More specifically, due to the steady decrease in transistor size (technology node), commercial solutions have exclusively focused on the development of the electronic option: eADCs. Unfortunately, in the last 10 years, transistors’ speed and size have started approaching their limits [37]. In particular, Murmann’s survey in 2021 [37] highlights that energy consumption and jitter are the main bottlenecks, which have mainly arisen from the minimization of the technology node. Figure 9 shows the Energy per Nyquist sample as a function of the Signal to Noise plus Distortion Ratio (SNDR), which is one of the most well-known FoM metrics that evaluates the performance of an ADC. SNDR is measured when the frequency of operation is set to Nyquist Rate/2. In this figure, the lines for Jitter = 0.1 psrms/1 psrms designate the performance that a fictitious sampler with only the specified jitter numbers (no other nonidealities such as quantization noise, etc.) would achieve.

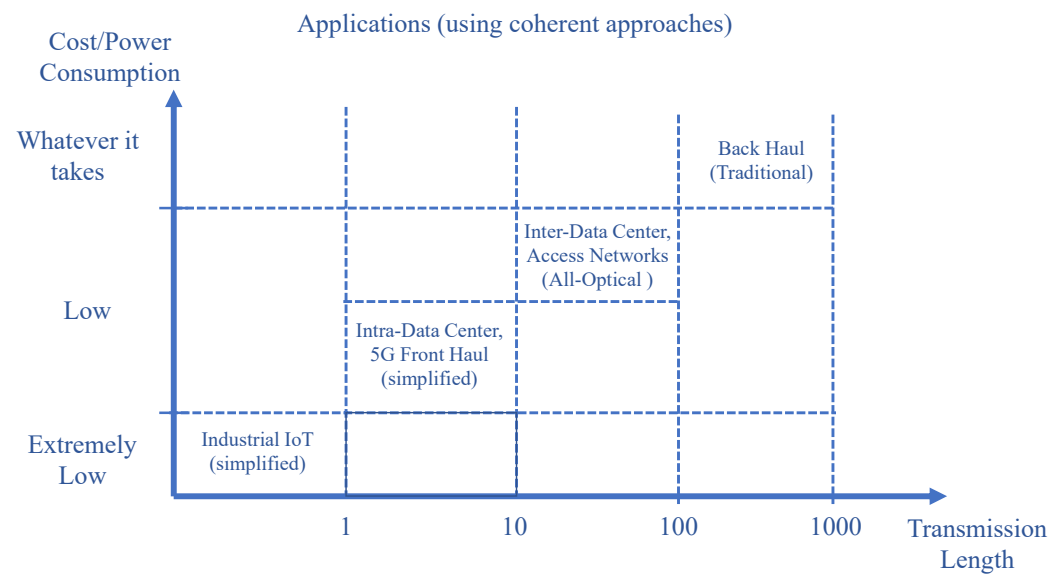


Figure 8. Coherent transceiver alternatives for the different applications based on the cost/power consumption and transmission length.

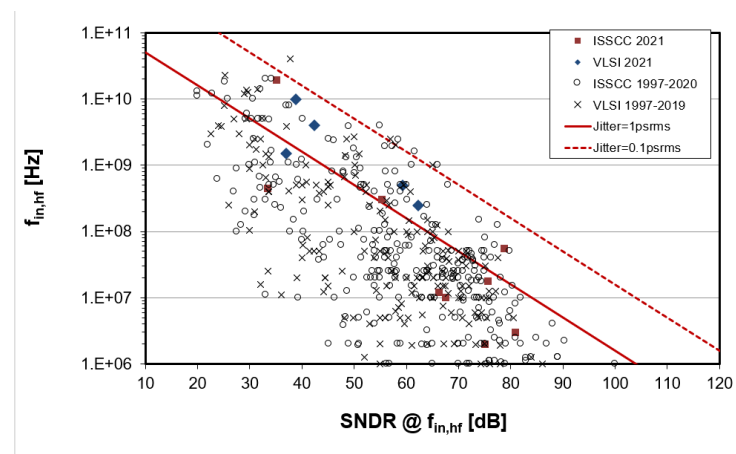


Figure 9. ADC Performance Survey 1997–2021 [37]. Illustration of the operational frequency of published ADCs vs. the SNDR FoM. With the red solid/dotted lines is shown the Jitter FoM.

On the other hand, accurate Analog to Digital (A/D) conversion of wideband multi-GHz signals has always been a problem as the use of eADCs is far from optimal and not sufficiently scalable looking forward. The reason is that digitizing analog signals in the range of 100 GHz and beyond is practically impossible because of the lack of electronic devices, which can sample the input signal with sufficient low aperture jitter at this rate, as it is shown in Figure 9. These facts kept the research of photonic ADCs active for almost 30 years, however, without yielding a practical realization at sufficient SNDR.

The origins of photonic ADCs date back to 1970 when Siegman and Kuizenga [38] were working on optical sampling of Radio Frequency (RF) signals notwithstanding that the different main targets of that work. Photonic ADCs can be classified into four broad categories as per Figure 10 [39]: In particular, photonic-assisted ADCs use optics in order to replace the track-and-hold operation on the RF input signal and perform both sampling and quantization in the electronic domain. Photonic sampled ADCs and photonic quantized ADCs use photonic technology to sample or quantize the signal (but not both), respectively. The combination of sampling and quantizing the signal with photonics is a different category that enables the optical sampling of the intensity angle.

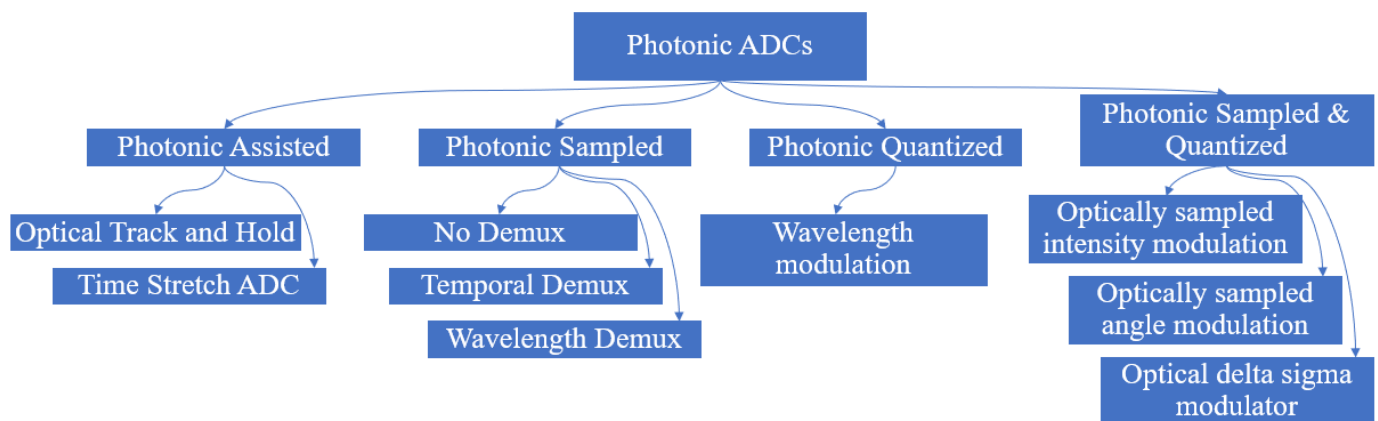


Figure 10. Four major classes of photonic ADCs with their different variants.

As the range of the different approaches for constructing a photonic ADC is huge, the most useful category is the one aiming to overcome the most significant bottleneck of high-speed eADCs. That category is the photonic-sampled ADCs, which overcome the electronic jitter limitation. A general overview of photonic ADCs can be found in the excellent review by Valley [39]. Heretofore, there have been just three State-of-the-Art photonic-sampled ADCs implemented and tested, based on a common fundamental principle of operation. The first one was proposed by a group of researchers at MIT in 2012 [40], whereby they implemented a discrete time-to-wavelength mapping approach (an approach first proposed by Yariv in [41]). The second alternative resulted from a collaboration of researchers from Rohde and Schwarz and IHP in 2017 [42], which demonstrated a monolithically integrated time-interleaved topology to relax the timing constraints at the highest sampling rates. The third and most recent one was proposed by the Institute of Integrated Photonics of Aachen University [42], demonstrated two monolithically integrated topologies; one based on time-interleaving, whereas the second one was based on frequency interleaving.

Although the target here is not to elaborate on the principle of operation of these implementations, we discuss the most important aspect, namely the optical sampling of the RF signal [43]. The main components of an optically sampled system are shown in Figure 11 and comprise a stable pulsed laser, an optical modulator, and a detector/integrator. The basic concept is that the ultra-short pulses of the laser actuate the modulator over an ultra-short and ultra-stable (low-jitter) time-window, such that the average amplitude of the analog signal over that window, an excellent approximation of a point-sample, is mapped on the amplitude of the optical signal. This mapping of the amplitude is converted into electrical variation by the photodetector and eventually quantized in the electronic domain (thus the sampling is performed by optics, the quantizing is electronic). The most significant advantage is that the overall jitter induced by the laser pulses is much smaller compared with the jitter created in its electronic counterpart. For clarification, the sampling rate is just the Mode-Locked Laser (MLL) pulse repetition period. As demonstrated in [40], with a single laser, several repetition periods can be implemented by adding a multiplexer, a dispersive fiber, and a demultiplexer. A comparative analysis of various options for the optical sampling process is summarized in Table 3.

In Table 3, a trade-off between the sample rate and the bandwidth of the optical sampling processes for RF signals is evident across these four alternatives. Alongside this trade-off, it should be pointed out that different processes to manufacture the PICs have been employed. Both bipolar complementary metal–oxide–semiconductor (BiCMOS) and silicon photonic integration may be considered. All four variants have successfully implemented a photonic-sampled ADC, with the latest option exceeding 60 GHz bandwidth and achieving the lowest power consumption and die area. These four variants validate the concept of photonic ADC and establish its great potential to enable systems aiming

to process signals in the microwave region with sufficient accuracy, made possible by the sampling photonic technology.

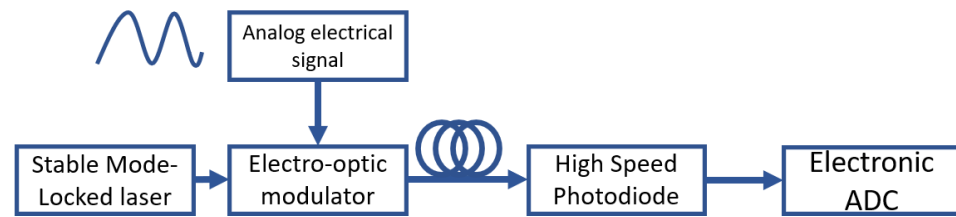


Figure 11. Photonically sampled and electronically quantized ADC. The analog electrical signal is sampled through a photonic process that employs a mode locked laser, an electro-optic modulator, and a high-speed photodetector. Then the electronic ADC performs the quantization of the corresponding electrical signal.

Table 3. Quantitative comparison of options for the optical sampling process of the RF signal [43].

Topology	Optically Clocked	MZM Sampler	MZM Sampler	Optically Clocked
Sampl. Rate	10 GS/s	2.1 GS/s	2.1 GS/s	0.25 GS/s
BW	30 GHz	41 GHz	-	65 GS/s
THD/SFDR	−39 dB/42 dBc	−/52 dBc	−/39 dBc	−38 dB/39 dBc
@ f_{in}	@32.5 GHz	@41 GHz	@10 GHz	@43 GHz
ENOB	5.57 (SNR)	7 (SINAD)	3.5 (SINAD)	5.5 (SINAD)
@ f_{in}	@10 GHz	@41 GHz	@10 GHz	@45 GHz
Power	1250 mW	-	-	506 mW
Die Area	4.84 mm ²	-	-	0.59 mm ²
Process	250 nm Photonic SiGe BiCMOS	Discrete components	Integrated silicon photonics	250 nm photonic SiGe BiCMOS

In conclusion, we deem it important to point out that as a first step, the major bottleneck of high-speed ADCs may be eliminated based on photonic technology, exceeding the performance of an electronic counterpart. The next step towards achieving a fully optically enabled ADC is to conceive a feasible method that implements photonic quantization. Although practical implementations have not been realized yet, some photonic sampled architectures through optical quantization architectures hold promise to exceed their electrical counterparts [44], as well as to reduce power consumption due to the use of optical elements. Nevertheless, a significant amount of additional work lies ahead along the road towards realizing an all-optical ADC with reduced power consumption. Moreover, the photonic ADCs surveyed above have electronic inputs and outputs. A worthy future objective would be to establish the feasibility of an oADC with optical input (carrying the information modulated signal) and electronic digitized output, embedded in a future all-optical polarization and IQ demultiplexing front-end of a coherent receiver, in order to pave the way for truly all-optical low-energy consumption systems.

3.3. Photonic DACs: Challenges and Opportunities

Electronic Digital-to-Analog Converters, abbreviated as eDACs, are key interfaces that convert the signal from the digital to the analog domain. In high-speed digital optical transmitters, the D/O translation typically comprises costly and power consuming eDAC-based data conversion, followed by analogue optical modulation. In a conventional optical link, eDACs are used to drive multilevel analog signals into the optical modulators.

As mentioned earlier in this chapter, from the viewpoints of performance, energy efficiency, complexity, and cost reduction, it would be advantageous to adopt direct D/O conversion and eliminate the eDAC intermediaries. This would be particularly useful with regard to ultra-high-speed photonic interconnects, as eDAC technology is even more expensive and is becoming increasingly challenging to keep scaling up data rates while keeping power dissipation at reasonable levels and maintaining the required ENOB performance.

To introduce optical-to-digital conversion, let us first review the conventional way of generating multi-level optical signals. For decades, IQ modulators generating optical constellation signals remained the same, e.g., the case of 64QAM is illustrated in Figure 12. The light split into two parallel optical paths is modulated using a pair of MZMs. Each MZM modulates the Continuous Wave (CW) optical signals according to the electrical voltage applied to its electrodes. As a consequence, for quantized electrical voltage levels applied to the MZM electrodes, quantized optical levels are generated (and are relatively phased 90° along the two parallel paths). However, the bandwidth of the entire transmitter is limited by the lowest bandwidth of either the DAC in the electronic driver or the MZM electrical to optical modulator transducer.

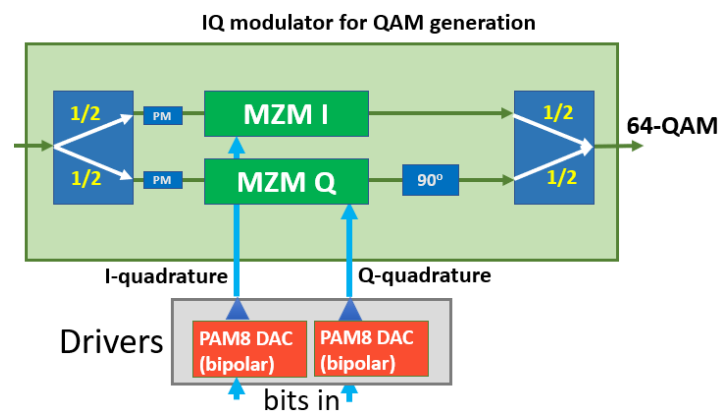


Figure 12. Conventional 64-QAM architecture where the light is split into two parallel optical paths and is modulated using a pair of MZMs.

In order to scale-up the capacity of a single-lane point-to-point optical tributary, one can either increase the baud rate or adopt formats with higher spectral efficiency. These solutions require either faster electronics or more complex DSP in the Rx. Either way, both options entail increased cost and power consumption. In addition, as silicon technology is approaching its physical limits, the use of faster electronics no longer seems a viable solution in terms of its upscaling rate, which is no longer able to keep up with the data rate scaling roadmap. This is why one of the key goals of the research community is the reduction in the energy-per-bit by conceiving a new optical transceiver architecture able to attain direct digital to optical domain conversion, the optical DAC (oDAC), eliminating power-hungry electronics and specifically doing away with conventionally expected future eADCs featuring three or more bits given their scalability problem in rate-vs.-energy-efficiency. The oDAC will still be driven by electronic D/A interfaces, but those will be highly efficient and scalable—the drivers of the oDAC will comprise arrays of decoupled 1 bit (NRZ) or, at most, 2 bits (PAM4), where signal formats are relatively mature, more energy efficient, and more amenable to upscaling than higher-order ADCs, which are about to be pushed beyond their limits in the upcoming optical interconnects roadmap.

Over the last decade, the research activity regarding the oDAC has been mainly focused on ‘serial’ structures, which are based on partitioning the electrodes of the basic MZM (Figure 13). The so-called Segmented Mach-Zehnder Modulator (SEMZM) [45–53] breaks up the MZM electrodes pair along the two MZM waveguides into multiple (shorter) electrically isolated segments. Each modulation-segment amounts to an elementary 1-bit modulation gate driven by a separate binary signal. The summation of the optical phases

induced by the array of 1-bit segments along the device generates a multilevel output optical signal. Accordingly, Figure 13 depicts an exemplary $S = 7$ segment thermometer-weighted SEMZM optical structure, aiming to implement oDAC functionality. The contiguous MZM electrodes are partitioned into S segments. Each segment acts as a “partial MZM” with a push-pull drive. Hypothetically assuming a single segment is electrically driven (the other segments grounded or removed), we would obtain a “partial” MZM modulator with a short electrode pair, inducing just a fraction of the maximum possible peak phase modulation, as attained when all segments are active. When all the segments are modulated in unison, driven by properly synchronized binary signals, the total differential phase along the device may assume a multiplicity of values, inducing, by interference in the output coupler, multiple optical amplitude (or power) levels at the device output.



Figure 13. Segmented MZM (SEMZM) 7 segments oDAC architecture-optimized thermometer-weighted DAC Structure for generation of PAM8 signals [22]. This SEMZM comprises seven segments; each segment is described as a yellow box. In red, the optical waveguide that light passes through and is modulated by each segment appropriately is shown.

As an alternative approach, a “parallel” design that employs electroabsorption modulators (EAMs) instead of MZMs has been also proposed in [54]. The compact size of the EAMs and their ease of integration with silicon photonics make them a real lucrative option. However, various works examining the ‘multi-parallel’ oDAC functionality have been proposed, e.g., via arraying in parallel a pair of 1-bit (OOK) [54] or 2-bit (QPSK) [55–58] modulation gates, fed after splitting a common optical source, with their outputs superposed in an optical combiner. The latest and state-of-the-art ‘multi-parallel’ oDAC structure is proposed in [22] introducing an architecture, which, via the combination of identical parallel paths and a variable splitter and combiner, is able to generate both direct and coherent detection constellations (Figure 14a).

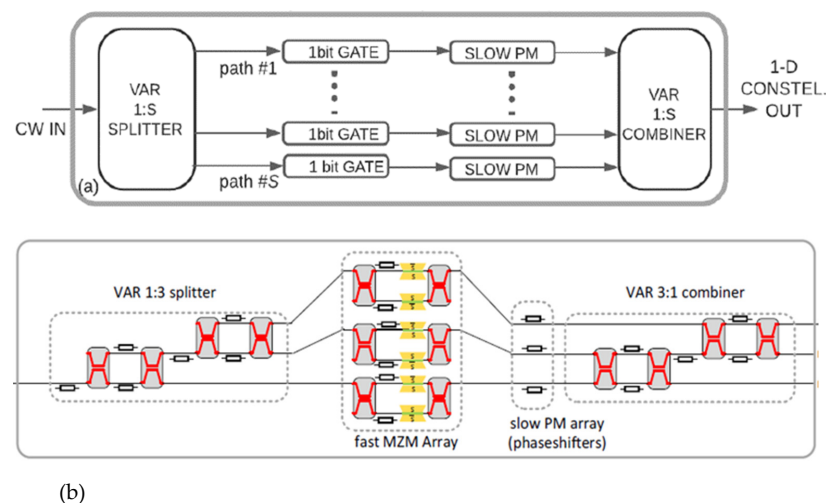


Figure 14. (a) The generalized parallel architecture proposed in [22] and (b) an implementation of a PAM8 generator that comprises a variable 1:3 splitter, a fast MZM array to modulate the light, and a variable 3:1 combiner. The slow PM array is a crucial element for the control and calibration of the o-DAC.

The basic goal of a parallel design is to generate optical multilevel PAM signals using only binary driving digital signals. As shown in Figure 14a, in this implementation, 1-bit gates are the fundamental building blocks. These blocks either let the optical signal pass through the specific path or block it and can be practically implemented using MZMs. Then, by adding all the optical paths using a combiner, optical signals with different amplitude levels can be generated. Figure 14b illustrates how a PAM8 generator can be implemented using this architecture. In practice, the variable splitters and combiners are identical and bit gates are put just in parallel, demonstrating the high scalability of this architecture. In that aspect, it is possible not only to scale the parallel paths but also the electronic PAM (ePAM) levels that drive the MZMs in order to scale the attainable data rate. It is theoretically established that by using ePAM4 in each of the two parallel paths via a two-way o-DAC, it is possible to scale the constellation up to optical 256-QAM [59]. Moreover, extensive analysis has been performed in [49] in order to demonstrate the significance of splitting and combining ratios to realize such a design. Also, in [49], control and calibration functionalities were added along the optical paths by inserting slow phase modulators. Accounting for mismatch in splitting or combining ratios occurring in the manufacturing processes, or due to environmental disturbances, this current design becomes far more robust compared with that of previously published work.

Other optical DAC solutions based on (a) silicon ring modulators [49,50], (b) III-V-on-Si electro-absorption modulated distributed feedback laser [51], and (c) polarization division multiplexing [53,54] have been also proposed. The previous generations of MZM devices might not be suited for short-reach interconnects as typically large transmission line structures are required. With ring resonators, the system becomes too dependent on temperature fluctuations and needs control systems to guarantee its stable operation. Silicon microring modulators are already implemented but they are limited to 80 Gb/s rates even with DSP on both the transmitter and receiver sides, something that contradicts the notion of the DSP-free architecture. Generally, from all the experiments demonstrated heretofore, we may conclude that although optical DAC implementations have been proposed, the results show that there is no particular implementation yielding considerably better results compared with the others. If one thing is clear, it is that control and calibration of different kinds of mismatches like phase mismatches or energy mismatches will play a key role for any type of deployed modulator. It goes without saying that the path for reducing energy consumption and achieving better performance in the near future acknowledges that electronics have come to their limits and the future seems to be purely optical. Although these designs are promising, the research community still seeks optimal scaling options for ultra-highspeed optical modulator-based transmitters, facing multiple challenges precluding a breakthrough in these directions.

3.4. Reconfigurable Photonics

Generally, PICs have been extensively investigated as platforms for optical fiber communications. Over recent decades, the basic driving force behind creating lower-cost and more robust photonic circuits has been the increase in data rates in order to meet the ever-increasing demand of end-users. The main objective of PICs is to process optical signals efficiently and at low latency, over a low-cost and low-power platform. These requirements cannot be simultaneously satisfied by simply considering digital solutions, due to the inevitable severe tradeoffs in terms of energy efficiency and processing speed electronics. This fact, along with observing the track record of electronics re-programmability capabilities, which turned out to be highly valued in practical use-cases, suggests exploring reconfigurability for photonic circuits as well. This concept attracted the attention of researchers and start-ups, and extensive efforts have been invested in reconfigurable and programmable photonic circuits [60–62]. The most promising architectural concept is that of the 2D hexagonal Tunable Base Unit (TBU) mesh. The TBU is basically a tunable coupler constructed by a balanced Mach–Zehnder Interferometer (MZI) [60]. Upon investigating all the parameters and analyzing the TBU in great detail, the functionality of different

topologies based on this basic unit was shown to be realizable. A plethora of photonic functions has been demonstrated through the 2D hexagonal mesh architecture, such as basic tunable Infinite Impulse Response (IIR) and Finite Impulse Response (FIR) filters with feed-forward and feed-backward capabilities and multiple input/output optical linear transformers [60]. Although research on such technology and its applicative benefits is still relatively immature and various drawbacks are still to be addressed, it appears that the successful development of robust, industrial-grade reconfigurable photonics will keep evolving and, as a consequence, pave new ways to streamline design and implementation of an all-optical analog platform supporting a plethora of applications. Automated approaches may enable photonic mesh designs capable of supporting more than just simple photonic functions, e.g., filters. In particular, optical DACs have been proposed in [22], endowed with reconfigurability—which may be traced to the modularity of their design, down to the basic building block level, comprising elements such as “1-bit gates” or the 2:2 Mode Converters as per Figure 15a.

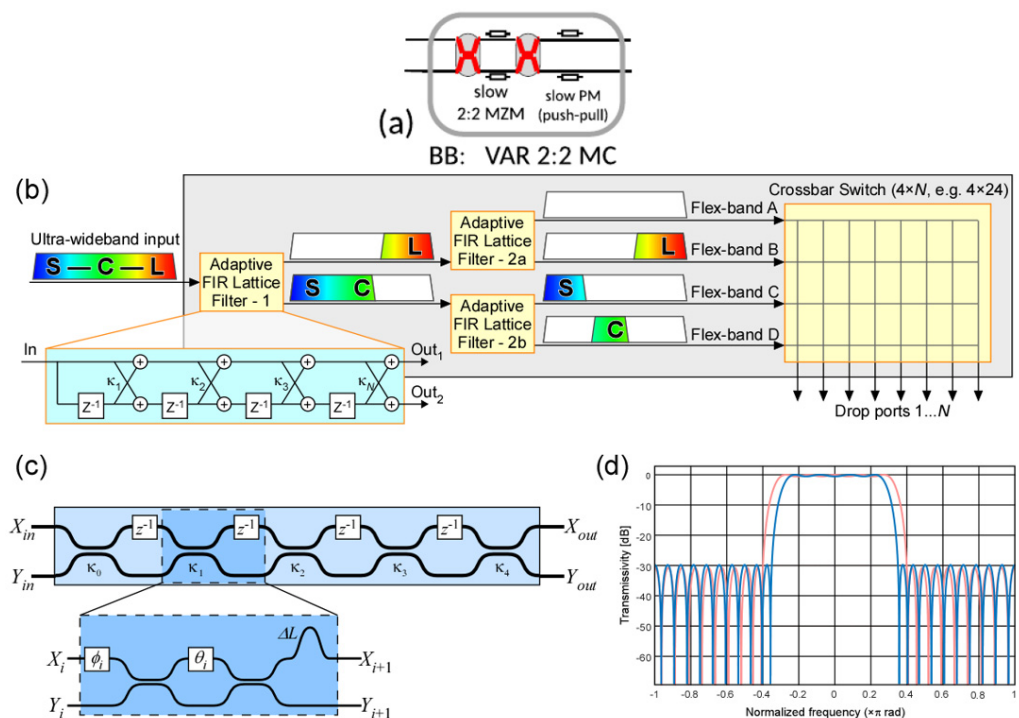


Figure 15. (a) One of the two basic building blocks of the o-DAC [22]; (b) general architecture of the waveband selective switch, consisting of an adaptive filtering stage and an output port switch; (c) structure of photonic lattice filter consisting of repeating blocks of tunable couplers and unit delay. These are implemented by MZI's and prescribed length delay of ΔL (inset); (d) normalized frequency response of an FIR filter having 38 filter taps.

Moreover, even more “exotic” photonic circuits may be implemented over reconfigurable optics, as is the case with waveband selective switches to be discussed in Section 5, to provide processing of optical signal at a very wide bandwidth (over $S + C + L$ amplification bands), routing its spectrum portions in several bands as shown in Figure 15b. Significantly, the reduced waveband count and filter sharpness allow one to meet the filtering requirements with multi-tap FIR optical filters, implemented as adaptive lattice filters on a photonic integrated circuit as opposed to bulkier dispersive free-space optics arrangements with LCoS channel selection. Moreover, the design of direct FIR filters (digital and their optical brethren) based on MZI structures like the TBU is well understood and known to require more stages than IIR filters [61]. Due to the large FSR requirement of the implemented filters (~ 140 nm), IIR filters of low loss would be hard to implement. The spectral resolution (i.e., the transition bandwidth) of an FIR filter would scale with the FSR

divided by the number of taps, such that an implementation comprising a large number of taps (e.g., ≥ 32) be able to attain improved performance. The cascade of FIR filters, as illustrated in Figure 15c, longitudinally increases the chip size, which in essence is a single input-multiple output interferometer, albeit delivering a better-quality spectral response (as shown in Figure 15c). It is worth mentioning that such PIC also requires integrating a large count (~ 100) of fast phase modulators to adapt the filter taps and allow for reconfiguration and better control of the filter response, as is the case with other Reconfigurable PICs. The basic building block will consist of the tunable band drop filter, implemented by photonic FIR filters. As discussed above, the design of reconfigurable FIR filters has already been demonstrated in [62].

In our opinion, reconfigurable photonic circuits may be both the enabling technology for visionary photonic architectures yet to be realized and provide an immense boost for the all-optical processing needed for optical communications. Finally, several other research fields lack the know-how of photonic integration and design, and we believe that they will benefit from the capabilities of reconfigurable photonic technologies.

4. Optical Transmission: Key Challenges and Proposed Directions

4.1. Capacity Scaling: What to Expect in the F6G

According to Cisco, the traffic demands will keep increasing at a rate of approximately 100% every 3 years (Figure 16). The reason for this traffic increase, as mentioned in Section 2, is the need to meet the ever-increasing demand for “fresh” services, which has been accelerated due to the increased tele-working following the COVID-19 pandemic. So, in order to satisfy the requirements of the upcoming F6G services while at the same time avoiding the 100 Tb/s capacity crunch of the Standard Single Mode Fiber (SSMF), network providers and vendors have to investigate and deploy novel techniques aiming at increasing the overall transportation capacity by at least one order of magnitude compared with F5G systems. The general trend of *transportation capacity per single fiber* over time can be seen in Figure 17, according to which during the past five decades, the transportation capacity within an optical fiber started from approximately tens of Mb/s and has now reached approximately 100 Tb/s. This value is the maximum nominal rate of the Single Mode Fiber (SMF) in long-haul transmission. This figure highlights an increase of six orders of magnitude in less than fifty years and clearly underlines the need to find ways to exceed 1 Pb/s by 2030.

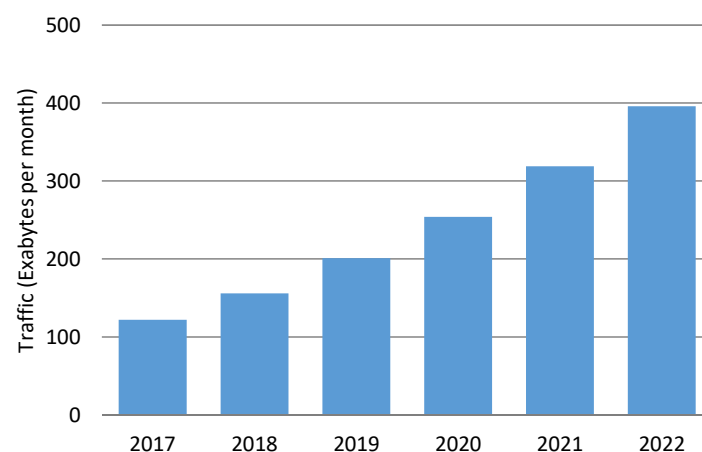


Figure 16. Global IP traffic demands (source: Cisco).

Recently, various ways have been proposed in order to overcome this 100 Tb/s capacity crunch, such as (a) exploiting more spectrally efficient modulation formats, like probabilistic shaping and coded modulation, (b) exploiting the entire low-loss attenuation spectrum of the optical fiber (< 0.4 dB/km), which extends from 1260–1625 nm by transmitting either a higher number of channels or by increasing the bandwidth of each channel (migrating e.g.,

to higher baud rates), and (c) using SDM, mainly by either considering bundles of SMFs or by using multi-core/mode fibers. In all three cases, the overall transportation capacity can be extended beyond 100 Tb/s and eventually satisfy the target of 1 Pb/s for 2030 for commercial systems and the target of 10 Pb/s for research works by 2030, as it is illustrated in Figure 17.

Another observation that can be extracted from this illustration is that the research technology is approximately 8–10 years ahead of commercial systems. This is expected, as the results of the huge effort of researchers around the globe need to be refined and distilled in order to produce the most cost-efficient and, at the same time, performance-efficient methods/technologies/components, which will then proceed to commercialization. In order to attain Pb/s rates, novel optical components need to be introduced, such as band filters, cost-efficient optical amplifiers (especially for O and E-bands), band switches, and new generation pump sharing SDM-based amplifiers, which can provide both increased redundancy and reduced costs [63]. Another key technology, which can aid the F6G networks to transmit data at even larger distances and/or exploit higher cardinality modulation formats, increasing the transported capacity, is ML-based signal processing [64]. For example, Deep Neural Networks (DNNs) using digital backpropagation (DBP) methods can achieve a low-complexity nonlinearity compensation. Their performance is similar to those of conventional DBP modules, but they encounter relaxed computational complexity.

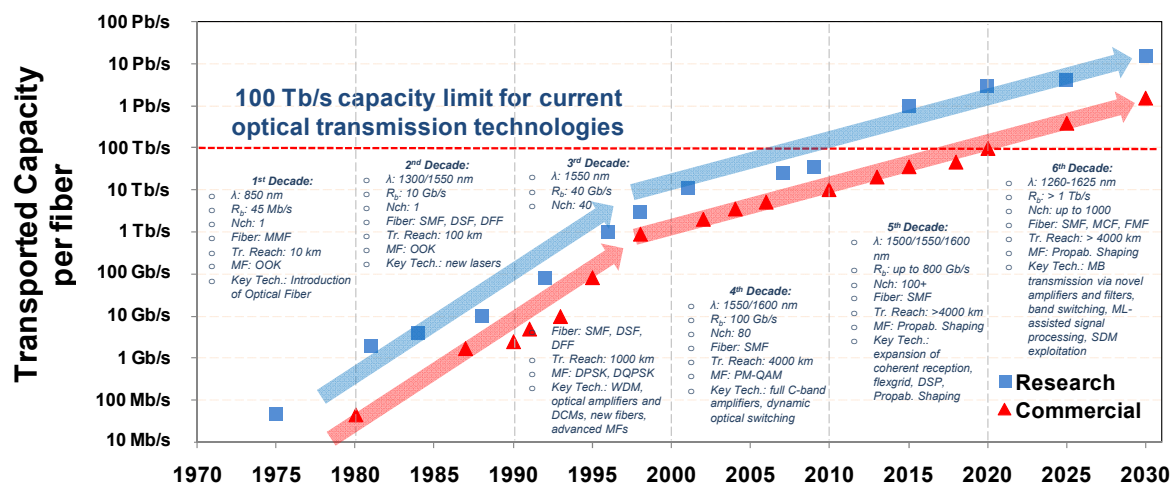


Figure 17. Evolution of transported capacity within a single mode fiber over the last 50 years along with forecasts for up to 2030 [65–67].

Next, we study the evolution of the *capacity per channel* over the time interval of 1970–2020 in order to understand the general trend and elaborate on the capacity needs for the next decade. Figure 18 highlights the need for fresh commercial systems able to reach at least 2 Tb/s per port by the end of the decade, while in [68], the need for up to 6.4 Tb/s by 2031 is also underlined. These rates can be achieved using multiple optical channels packed together forming a super-channel. Today, the highest commercially available rate is 800 Gb/s (Table 4) and can be realized mainly with two options. The first one is to employ a baud rate much larger than those of 100/200G cases, e.g., 90 Gbaud, and the second is to employ more efficient modulation formats, e.g., probabilistic constellation shaping and/or employ a higher cardinality modulation. Each of these alternatives has its own trade-offs, e.g., lower cardinality modulation formats such as 16QAM, require a lower Optical Signal to Noise plus Interference Ratio (OSNIR) in order to attain the same Bit Error Rate (BER) compared with higher cardinality formats, e.g., 64QAM. This eventually leads to a higher reach for the lower cardinality modulation formats; however, this reach is traded for a higher number of channels as the lower cardinality formats consume a wider bandwidth for the same data rate. In this case, capacity is traded for connectivity, and the optimal solution is based solely on the high-level design set by the network engineer.

Another observation that can be derived from Table 4 is that the evolution of the baud rate and modulation format from 100G to 800G clearly indicates that F6G systems need to adopt transceivers with baud rates of 256 Gbaud and even higher in order to exceed 2 Tb/s. The most recent research works demonstrate baud rates of 168 Gbaud with PM-16QAM format [69] and 220 Gbaud with OOK format [70]. Further, the interplay between attainable reach and bit rate is shown in [71]. In particular, in [71] it is shown that when using 130 Gbaud while considering different modulation formats, rates of 930 Gb/s can be transmitted over 1105 km and rates of 1.28 Tb/s can be transmitted over 452.4 km. Finally, rates of 1.6 Tb/s can be transmitted in a link length of 153.4 km [71]. This analysis clearly indicates that in the near future, technology will show significant progress in this direction both by stressing the electronics to exceed 512 Gbaud and by using DSPs, which will be more tailored to system parameters than current DSPs, allowing it to increase the transmission reach (for longer links). However, for short-reach communication, the use of oDAC approaches, as presented in the previous section, seems an excellent option to scale the data rates in a low cost and low power consumption way.

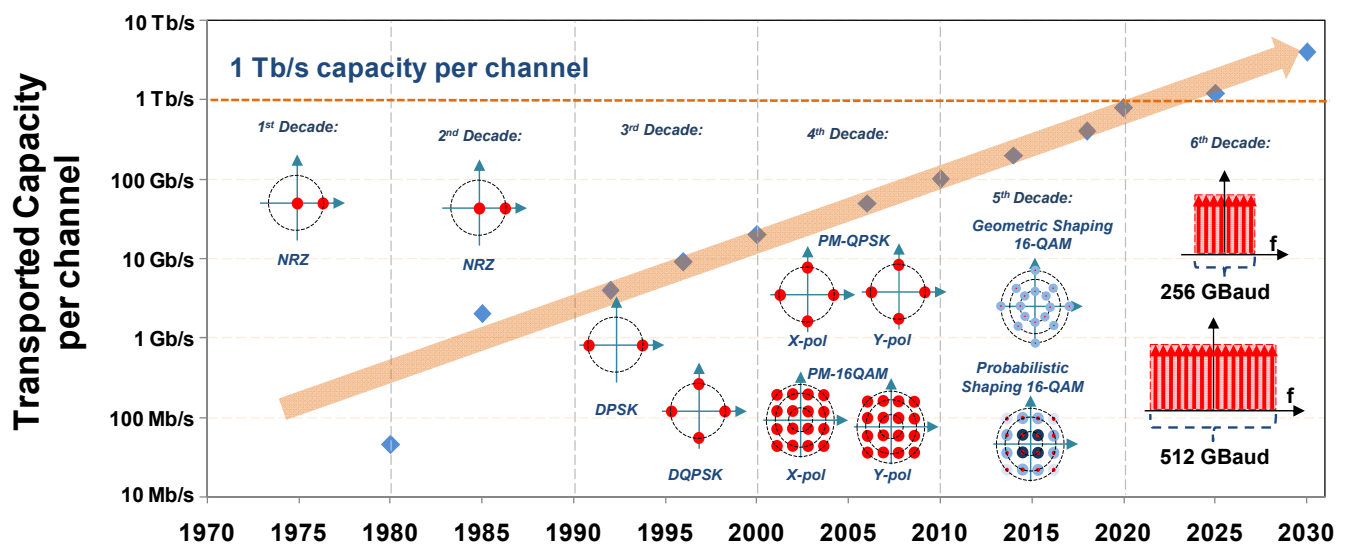


Figure 18. Evolution of transported capacity per single channel for commercially available systems over the last 50 years along with forecasts for up to 2030 [65–67,72,73].

Table 4. Details of commercially available transceivers for regional and long-haul transmission [74].

Type	Modulation Format	Baud Rate	Channel Spacing	Data Rate	Required OSNR (for BER = 10 ^{−3})
100G	PM-QPSK	32 Gbaud	37.5 GHz	100 Gb/s	9.8 dB
200G	PM-16QAM	32 Gbaud	37.5 GHz	200 Gb/s	16.55 dB
400G	PM-16QAM	63 Gbaud	75 GHz	400 Gb/s	16.55 dB
	PM-64QAM	42 Gbaud	50 GHz	400 Gb/s	22.5 dB
	PCS-16QAM	80–95 Gbaud	100 GHz	400 Gb/s	varies
800G	PM-16QAM	128 Gbaud	150 GHz	800 Gb/s	16.55 dB
	PM-32QAM	96 Gbaud	112.5 GHz	800 Gb/s	19.5 dB
	PM-64QAM	80 Gbaud	100 GHz	800 Gb/s	22.5 dB
	PCS-64QAM	90 Gbaud	100 GHz	800 Gb/s	N/A
200–800G	Probabilistic Shaping	60–95 Gbaud	75–100 GHz	200–800 Gb/s	varies

As the rates per channel can reach up to 800 Gb/s with currently available solutions, the attainable rates in the access part of the network are significantly smaller. For example, the most recent PON standard, which is 50G-EPON [75], can provide access to the network with a downstream rate of 50 Gb/s. In the F6G, there is a strong need to advance to the

100G-PON standard or directly to 200G-PON in order to support the various capacity demanding services, which were presented in Section 2. To further understand this need, Figure 19 illustrates the progress over time of the downstream rate for the various PON standards. Figure 19 also designates the main advantages of each PON standard over its predecessor. These advances in bit rate from standard to standard are a result of the advances in the transceiver operational parameters, such as the modulation format, baud rate, operational wavelength, and number of wavelengths. It goes without saying that as the access part of the network is the most sensitive to cost and power consumption, direct detection technology still qualifies to increase the overall rate.

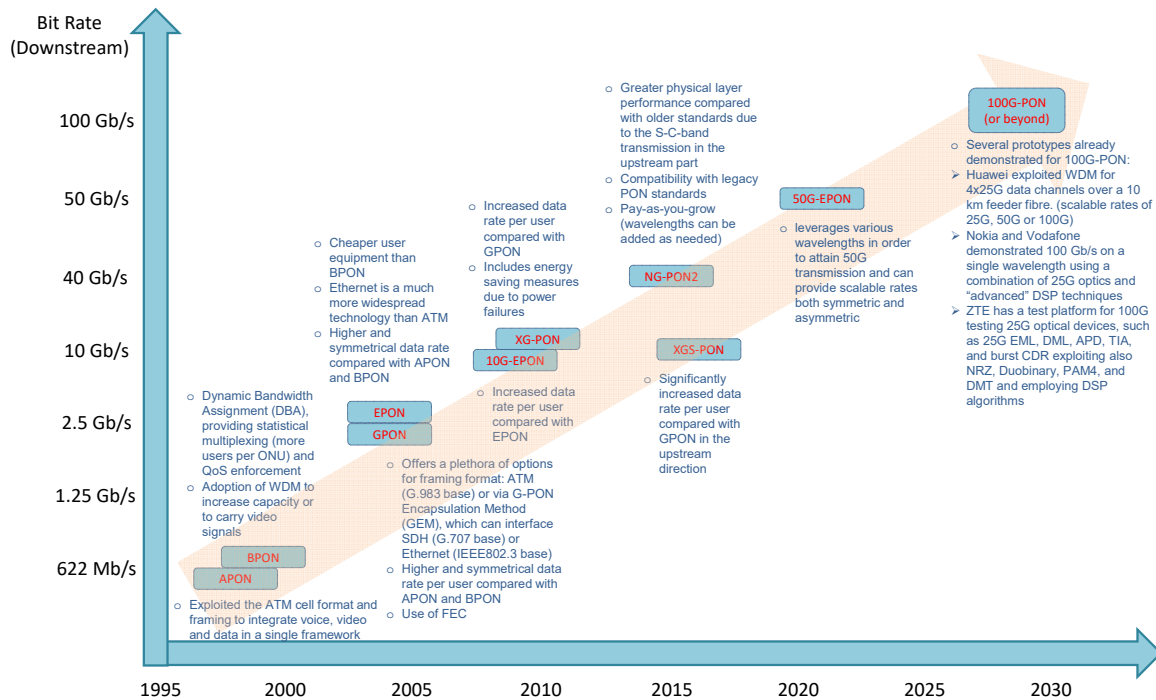


Figure 19. Evolution of bit rate in the downstream direction for various PON standards and the road towards 100G PON (or even beyond 100G).

Regarding the access rate evolution beyond 50 Gb/s, several options for realizing 100G-PON have been demonstrated. In the first option, which was presented by Huawei in BT's Innovation 2017 exhibition, the system exploited a ValkyrieBay chassis equipped with the unique Xena Loki-100G-5S-1P 5-speed dual-media test module in order to generate Ethernet traffic through the 100G PON. The main purpose of this test was the verification of the overall implementation [76]. More specifically, the system exploited WDM, as four wavelengths were employed to carry $4 \times 25\text{G}$ data channels over a 10 km feeder fiber. This implementation is highly scalable as it can support different rates: 25G, 50G, or 100G. The second option is a 100G PON Prototype developed by ZTE [77], which is an integration test platform featuring many capabilities as it can simulate various modulation formats, like Non-Return-to-Zero (NRZ), Duobinary, PAM4, and DMT (Discrete Multitone), whilst various DSP algorithms can be employed. Moreover, it considers four 25G wavelengths supporting the following four combinations: Asymmetric single-wavelength uplink 10G/downlink 25G, symmetric single-wavelength uplink/downlink 25G, asymmetric four-wavelength uplink 40G/downlink 100G, and symmetric four-wavelength uplink/downlink 100G. The feasibility of this prototype was verified at MWC 2017 in Barcelona. The third 100G PON solution was developed by Nokia Bell Labs and validated in Vodafone's Competence Centre in Eschborn, Germany [78]. This option is based on a single wavelength using a combination of 25G optics and advanced DSP techniques to reach 100 Gb/s. As the 100G PON (or even beyond 100G) commercialization is planned for the second half of

the decade, the next PON standard is expected to be the result of a significant amount of work and conveyed knowledge among academia, operators, vendors, and standardization organizations in order to adopt the most cost and energy efficient solution.

One of the main aspects of the adoption of PON technology is the maximization of spectral efficiency. Ideal candidates for achieving this target are Nyquist wavelength division multiplexing PON (Nyquist-WDM-PON) and orthogonal frequency division multiplexing WDM PON (WDM-OFDM-PON). Both solutions can (a) provide a finer granularity compared with Time Division Multiplexing (TDM)-PON schemes, (b) enable the bandwidth assignment on an as-needed basis, and (c) maximize spectral efficiency as they have a rectangular spectrum.

In particular, Orthogonal Frequency Division Multiple Access (OFDMA) PON is a well-established technology in wireless and fixed access systems such as WiMAX, long-term evolution (LTE), Asymmetric Digital Subscriber Line (ADSL), and Wi-Fi, and can be efficiently incorporated into the PON context to provide significant advantages [79–81]. Next, OFDM can be used both for coherent and direct detection schemes. This is important because when the coherent scheme is adopted, the overall performance can be greatly boosted, and on the other hand, when a DD scheme is considered, low-cost components, such as Directly Modulated Laser (DML), Vertical Cavity Surface Emitting Laser (VCSEL), and low-bandwidth electronics along with DMT, can be used, suppressing the overall costs. Finally, OFDMA-PON enables the convergence between wireless and fixed networks, allowing one to manufacture universal components for both uses.

Further, Nyquist-WDM-PON [82] is a capable solution for PON, which aims to minimize the overall number of transceivers by aggregating multiple transceivers onto a single hub transceiver. The hub transceiver uses coherent technology and multiple combined subcarriers based on the Nyquist criterion into a single optical wavelength. In this way, a 100G or a 400G wavelength can be divided into 4×25 Gb/s or 16×25 Gb/s subcarriers, respectively, or even into a combination of different subcarriers and line rates. Using Nyquist-WDM-PON, the network migrates from point-to-point architecture towards point-to-multipoint, decreasing the overall number of optical interfaces from $2N$ to $N + 1$, where N is the number of access nodes. This solution provides significant advantages compared with legacy PON systems. The most important are (a) a decreased number of transceivers due to the use of hub transceivers, (b) better routing efficiency, density, and simplicity, as the overall number of ports is significantly decreased, (c) better alignment of CapEx with actual bandwidth requirements and quick adaptation on changing bandwidth demands and traffic patterns, and (d) lower OpEx in terms of power consumption, footprint, number of aggregation sites, and support. The concept of Nyquist-WDM-PON has been already commercialized in a version with the name “XR-Optics” [83].

Regarding the physical layer performance of Nyquist-WDM-PON and WDM-OFDM-PON, a comparative analysis is illustrated in [84] and shown in Figure 20. This analysis shows that the physical layer performance is highly dependent on the linewidth, resulting in considerable phase noise. In [84], two phase noise compensation methods were considered, namely, common phase error (CPE) and orthogonal basis expansion (OBE). Nyquist-WDM-PON showed a greater performance compared with WDM-OFDM-PON. This happened as the inter-carrier-interference (ICI) in WDM-OFDM-PON cannot be mitigated by CPE. Next, when OBE was used, WDM-OFDM-PON attained a greater performance than Nyquist-WDM-PON under the two cases, especially at small laser-linewidth. WDM-OFDM-PON is vulnerable to phase noise due to the long OFDM symbol period, but with the aid of an effective phase noise suppression method, it can attain a lower BER compared with Nyquist-WDM-PON and eventually qualify as a cost-effective solution for access networks.

4.2. Capacity Increase Using More Spectrally Efficient Modulation Formats

As analyzed above, one option to increase the transportation capacity is to boost the spectral efficiency (SE). SE is a measure of how efficiently the available bandwidth is utilized and equals the data rate divided by the allocated bandwidth. Higher SE, in essence,

means that a higher rate of data can be transmitted using the same spectral width. This can be easily understood, for example, if we consider the 100G and 200G cases of Table 4, where the 200G channels double the data rate by simply tuning the modulation format from QPSK to 16QAM. This increase in the number of “M” states in the M-QAM modulation formats is the most common way to increase the SE in modern coherent optical transmission systems. In addition to this method, there are two other techniques that can aid us in exploiting the available channel capacity closer to its theoretical limit, which are Probabilistic Constellation Shaping (PCS) and Geometric Constellation Shaping (GCS) [85,86]. These methods deviate from uniform square constellations and can provide important gains in terms of the Signal-to-Noise Ratio (SNR). These two methods are pictorially described in Figure 21.

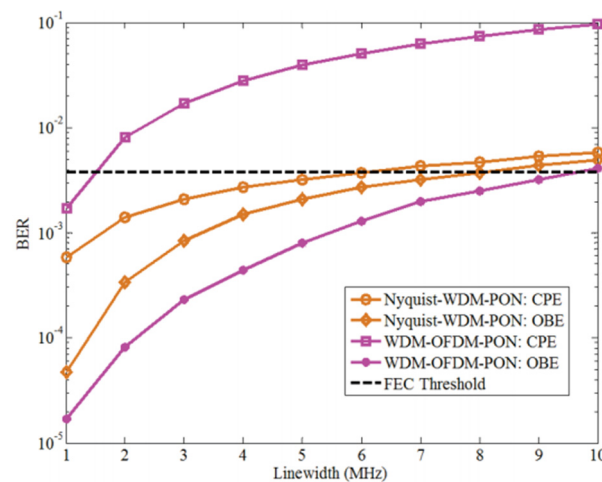


Figure 20. BER performance vs. laser linewidth when QPSK is employed [84]. CPE: Common phase error, OBE: Orthogonal basis expansion.

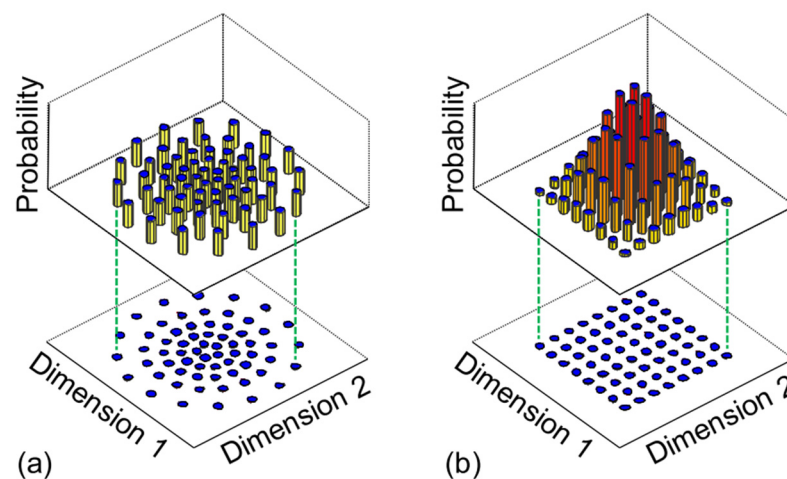


Figure 21. Examples of (a) geometric and (b) probabilistic constellation shaping [86].

In GCS, the location of the constellation points in the complex plane mainly focuses on the areas where the amplitude is small and less on the areas where the amplitude is high, optimizing the signal constellation and allowing it to approach the fundamental Shannon limit. Two methods for realizing GCS are (a) multi-ring constellations, which are used to estimate the Shannon limit of the nonlinear optical fiber channel, and (b) iterative polar modulation (IPM), which is used to achieve experimental SE records [86]. However, the use of GCS comes with the cost of greater complexity, as more computationally “heavy” DSP modules are required compared with uniform constellations. A second disadvantage of this method is that there are no simple solutions for finding locations of the GCS constellation

points for arbitrary channel conditions, and third, Gray mapping increases the complexity of demapping symbols to soft-decision bit metrics [86].

The second shaping method is PCS. This method more frequently exploits the inner constellation points that are less energy/power demanding while the outer points require higher energy and are exploited less frequently. In essence, PCS shapes the probability of occurrence of the constellation points rather than their locations to approximate Gaussian signaling [86]. This method provides significant gains compared with GCS, which are as follows: (a) It is simple to optimize these probabilities through a single parameter, to match any given channel condition, (b) the constellation points are placed on the rectilinear grid of a square QAM template, which facilitates coherent DSP by robust state-of-the-art square-QAM algorithms, and (c) Gray mapping facilitates symbol demapping for subsequent SD FEC. Moreover, PCS shows important advantages compared with uniform M-QAM constellations: (a) There is a much smaller drop in capacity vs. reach relation, allowing for a smoother curve; (b) the impacts of nonlinear effects are reduced, as for the same average power and spectral efficiency, there is a longer Euclidean distance between the constellation points relative to conventional QAM, increasing the overall Optical Signal to Noise Ratio (OSNR); and (c) it allows one to select a baud rate that can guarantee the optimal physical layer performance [87]. It goes with a saying that since PCS is an already commercially deployed technology able to reach 800 Gb/s rates, as shown in Table 4, it will keep advancing in order to become one of the key constellation shaping technologies in F6G long-haul and regional transmission.

4.3. Capacity Increase Employing a Greater Number of Channels

The second way to increase the transported capacity per fiber is to employ a higher number of channels. For this purpose, two options can be envisaged: (a) Populate the low-loss attenuation spectrum of the single mode fiber (around 365 nm) with channels, in this way extending the transmission beyond the C-band, realizing Ultra-Wideband (UWB) transmission (also named Multi-Band transmission; however, throughout the text, we use the term UWB) and/or (b) exploit the space dimension, e.g., populating a bundle of SMFs, or considering transmission within a Multi Core/Multi Mode/Few Mode Fiber, in this way performing SDM. Both UWB and SDM are candidate approaches for F6G and have their own merits, which will be presented in the rest of this sub-section.

4.3.1. Ultra-Wideband Transmission

Ultra-Wideband transmission allows for a ten-fold increase in the number of channels compared with the case of C-band transmission only. However, populating the entire low-loss attenuation spectrum of the SMF with channels is not trivial, as to date, optical components such as amplifiers, filters, and commercially available transceivers are mainly focused on C, L, and parts of the S-band. To further understand the current state, Figure 22 illustrates the attainable gain and noise figure of indicative available doped fiber amplifiers for the five bands of an UWB system. As can be observed, in O and E-bands, the technology at the component level has to be further developed in order to unlock the transmission of these frequencies. We expect that future research will be able to provide components with desirable characteristics, such as amplifiers with sufficient gain, low noise figures, and a significantly wider amplification gain.

To realize UWB transmission, various types of amplifiers can be employed, such as Doped Fiber Amplifiers (DFAs), Semiconductor Optical Amplifiers (SOAs), and Raman amplifiers. The pros and cons of each method are discussed in [74]. According to our opinion, DFAs are currently the dominant amplification schemes, as they (a) are a well-known technology due to the extensive use of EDFAs in the C-band, (b) allow for modular engineering, introducing amplifiers on an as-needed basis, and (c) provide highly desirable characteristics such as low noise figure, gain flatness, and high output power. The full potential of a UWB (when all 365 nm are fully exploited) is to transmit more than 1000 channels (e.g., with 37.5 GHz channel spacing). However, the true number of transmit-

ted channels is expected to be lower, due to the current absence of optical components with desirable characteristics, especially in O and E-bands, as well as the catastrophic impact of nonlinear effects such as Nonlinear Interference (NLI) and Stimulated Raman Scattering (SRS), the impact of which scales nonlinearly with the increase in the total injected power in the fiber. In particular, ref. [88] showed that by using the currently available technology, the transmission of 871 channels in all five bands can be feasible. However, the attainable capacity of a UWB system depends also on the modulation format “carried” by each channel. For example, if PM-16QAM is considered, an overall rate of 174 Tb/s can be envisaged. Next, the estimation of the transparent reach strongly depends on the impact of the physical layer effects, which are a function of various system parameters. In particular, the estimation of transparent reach is a more complex procedure, since each band “sees” different transmission parameters, such as the attenuation parameter, local dispersion parameter, effective area, etc., and for this reason, the attainable reach in each band (even in different channels of the same band) is different, unless an optimization strategy like [89–91] is considered, which can ensure similar physical layer performance in all bands.

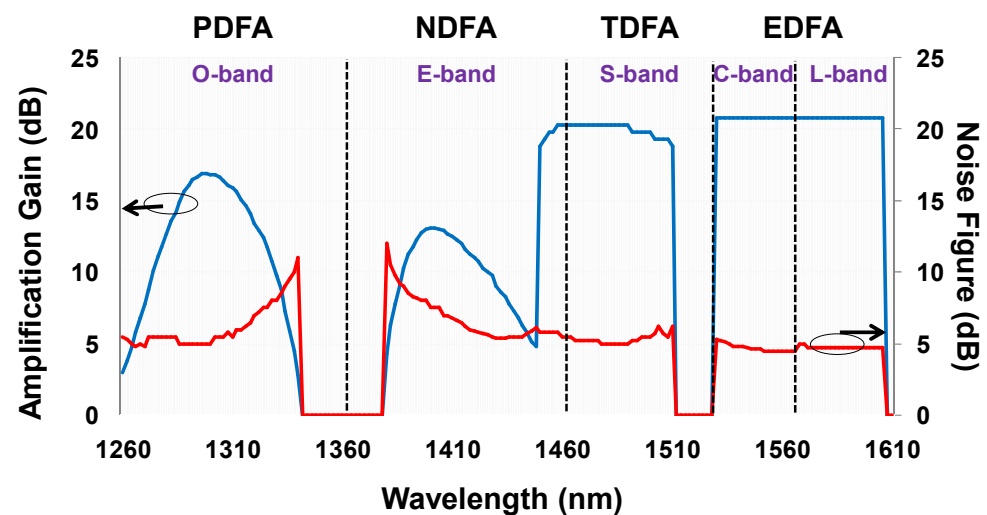


Figure 22. Gain and noise figure of indicative available doped fiber amplifiers assuming a total input power in each amplifier equal to 0 dBm [74].

The attainable reach and bit rate are antagonistic target metrics, as when migrating to a higher modulation format, an increased physical layer performance is required in order to attain the same BER. This eventually leads to a lower transparent reach compared with the case of a lower cardinality format, e.g., PM-QPSK. This means that rates of >250 Tb/s can be theoretically achieved in metro, access, and inter/intra data center networks, while in longer networks, such as submarine and regional, a capacity of up to around 100 Tb/s can be achieved. Figure 23 summarizes the relation between transported capacity and transparent reach up to 10,000 km for experimental works over the past decade [92–116]. As it is evident from this figure, by using either EDFAs alone or in combination with Raman amplifiers, UWB transmission is feasible in long-haul and submarine networks, while for shorter distances, e.g., access/DCI and metro, there is a broader gamut of available options for optical amplification. This allows one to select the most cost-effective technology between DFAs (e.g., Thulium DFA and EDFAs in parallel), hybrid-Raman amplifiers, and SOAs. SOA technology particularly is a very cost-effective option for short distances as it can offer a large amplification bandwidth, e.g., 100 nm, with only one amplifier [100,113].

Hollow-Core Fibers for Further Increasing the Transmission Spectrum

The low-loss attenuation spectrum of SMF spans over approximately 50 THz (O to L bands). However, signal transmission beyond this range, in particular from 1800 to 2350 nm, is possible, allowing an approximately 37 THz additional range using hollow-core fibers [67]. In

the hollow-core fiber, the light propagates within a hollow region, in such a way that only a small portion of the optical signal propagates in the solid fiber material. Hollow-core fibers with proper manufacturing can attain a low fiber loss within a range that spans around 2000 nm. However, the transmission within hollow-core fibers requires the deployment of new fibers, which leads to high installation costs and buying prices. This fiber alternative, as well as the SDM concept, is included in the category of “green-field”, where new fiber types need to be deployed while the UWB transmission is part of the “brown-field” category, where the existing fiber infrastructure is used as the basis for installing new fiber subsystems and elements, such as amplifiers, filters, etc.

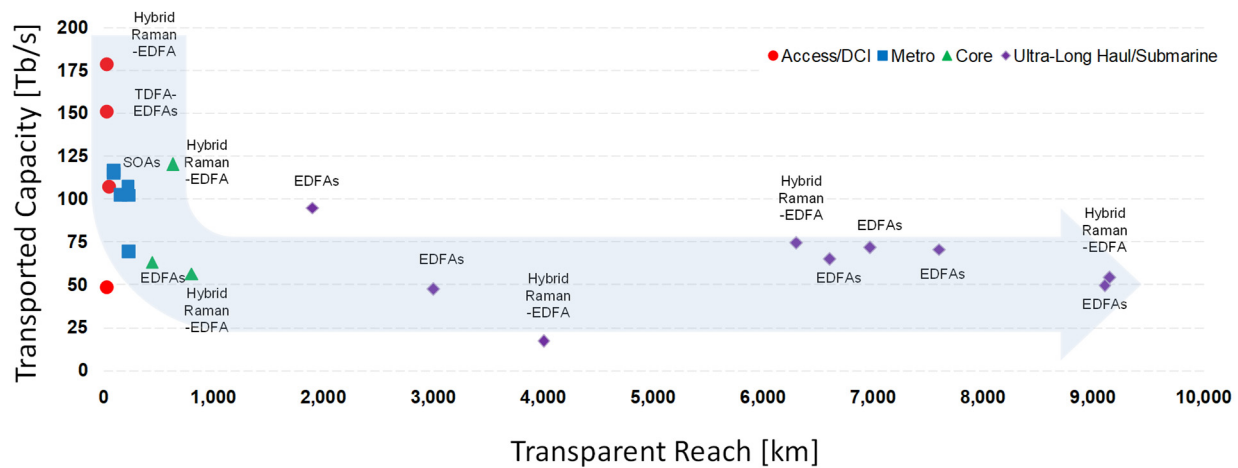


Figure 23. Experimental results on transported capacity vs. transparent reach for UWB transmission based on [92–116].

An important metric that shows the current state of the technological progress in the optical transmission is the “relative bandwidth”, which is equal to the total system bandwidth divided by the central frequency [67]. This metric relates the system bandwidth to its central frequency, and the ultimate target is to approach as close as possible to 100%. For example, a C-band-only system shows a relative bandwidth of less than 3%, while a theoretically fully populated UWB system can attain a relative bandwidth of approximately 25%. Finally, when the transmission spectrum is extended using hollow-core fibers, the relative bandwidth can exceed 65%. As the value of this metric increases, the overall system costs become higher as novel components such as amplifiers, transceivers, band filters, etc., need to be deployed. These components are more costly than those used in C and L-bands because the technology in C and L-bands is more mature, and the economy of scale can lead to reduced costs, compared, e.g., with E and S-bands. This high cost is a significant constraint for network operators that desire to upgrade their infrastructure in order to engage more bands on optical transmission and can steer them towards exploiting SDM techniques, which are analyzed in the next section.

4.3.2. Space Division Multiplexing

Space Division Multiplexing is, in principle, a system that incorporates at least one subsystem (e.g., a transmission fiber, an amplifier, a switching node, or terminal equipment), which implements the concept of “spatial integration of network elements”. SDM is of great interest as it promises to increase the overall transported capacity by multiple times compared with one SSF. In particular, the main options that can be considered to increase the number of spatial channels within the transmission link are [16]:

- Multiplication of the number of conventional fibers (thus implementing parallelism that consists of single-core/single-mode fibers), considering the existence of at least one element that performs spatial integration, e.g., an amplifier with sharing pumps, a switching node, or terminal equipment, named bundles of Single-Mode Fibers (Bu-SMFs).

- Multiplication of the number of cores; within the fiber, multiple cores arranged within the cladding with each supporting a single spatial mode (Multi-Core Fiber—MCF), or multiple cores each supporting multiple modes (Multi-Core-Mode Fiber—MCMF). Coupled Core (CC) fibers. CC can provide strong mode coupling between the different cores, attaining shorter core-to-core distances and higher spatial density compared with the uncoupled MCFs.
- Multiplication of the number of modes in MMF fibers within a single core, supporting a discrete number of spatial modes (Multi-Mode Fiber—MMF, Few-Mode Fiber—FMF).
- A combination of the above categories, e.g., MCF/FMF, is also feasible.

All these combinations are illustrated in Figure 24.

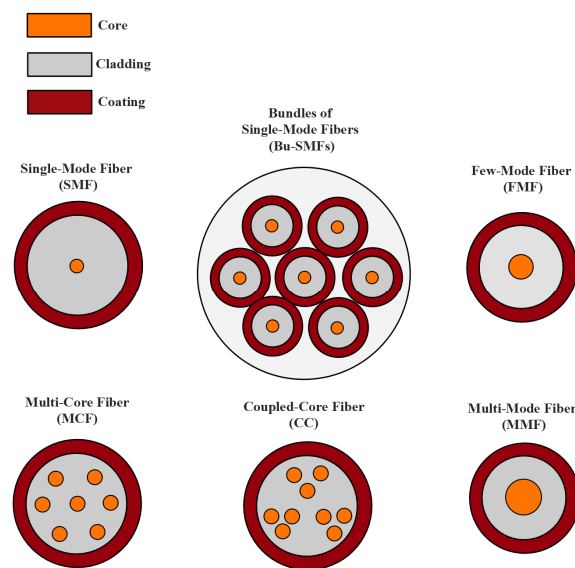


Figure 24. Different SDM options in comparison with standard single mode fiber [16].

As mentioned above, in the case of Bu-SMFs, a Bu-SMF considered an SDM needs to incorporate at least one sharing scheme, e.g., a pump-sharing scheme in the optical amplifiers/repeaters. It is worth mentioning that the main target of SDM, especially in submarine networks, is not to simply increase the number of spatial channels, targeting a higher attainable capacity, but to exploit multiple spatial channels and pump-sharing schemes to achieve a reduction in cost/bit and power/bit quantities while providing obvious modular capacity scaling [16].

The comparison between SDM and UWB can aid in designating three main advantages of SDM; the first is its better physical layer performance. In particular, when SDM transmission utilizing the C-band is compared against lower bands of a UWB system, the SDM system benefits from the (a) negligible impact of SRS, (b) lower attenuation, and (c) higher dispersion, leading to both decreased ASE and nonlinear effects and eventually to an improved physical layer performance. This not only increases the modulation format cardinality (and so the data rate per channel) but also boosts the transparent reach. The latter will lead to a lower number of 3R regenerators in the network (especially in long-haul networks), making SDM systems the ideal candidates for, e.g., long-range terrestrial and submarine networks, when compared with UWB. The second advantage of SDM is the use of “spatial integration of network elements”, such as optical amplifiers, etc., leading to significantly lower OpEx and CapEx. The third advantage of SDM over UWB is the lower-component associated costs, e.g., costs for transceivers, amplifiers, and filters.

However, SDM comes with two significant drawbacks. The first is the need to deploy new fibers in links where there is an insufficiency of available fibers; however, this is not the case in most links, where abundant dark fibers are present. The second is that SDM cannot attain diversity in connectivity compared with UWB. More specifically, UWB systems can

attain diversity in connectivity as the lower bands can employ less costly components employed for shorter links, although these bands result in a shorter reach when they are compared with SDM. On the other hand, in UWB, only the C and L-bands can be exploited for the more distant links of a network, which cannot be the case in C-band SDM systems where the entire available spectrum is considered “premium” due to its high-quality transmission.

Certainly, a combination of SDM/UWB is possible, e.g., by considering a multiple fiber transmission, e.g., Bu-SMFs, exploiting both C and L-bands. However, in order to select the optimal solution between (a) the various SDM variants, (b) the exploited amplification bands of a UWB system, and (c) a combination of them, we need to take into account a number of different factors, where many of them are antagonistic, such as the attainable capacity, node connectivity, cost/energy-effectiveness, transparent reach, node scalability, system upgradeability, and node/spectrum flexibility.

Cost-effectiveness is obviously one of the most important factors when designing an optical network. SDM can reduce the overall component-associated costs by exploiting “spatial integration of network elements”, e.g., amplifiers. Considering transmission within multiple modes and/or cores, the most important concern is if these modes/cores intermix. This is an important issue, as a possible energy transfer between them will result in a lower physical layer performance, increasing the BER of the transmitted channels. For example, in multi-mode fibers, degenerate spatial modes exhibit mixing during fiber propagation while bundles of SMF do not. Proper system design may suppress the impact of this mixing. Further, MCFs’ coupling can be reduced by considering different neighboring core properties and increasing the pitch [117]. Note also that the placement of identical cores in proximity leads to mutual coupling [118], allowing more precise control. Mixing between the modes in an MMF can be reduced by breaking the mode group degeneracy [119]. Optical amplification in UWB systems, when DFA technology is adopted, can be achieved with the use of multiple amplifiers. More specifically, a single amplifier could be employed for each band, which is placed either in parallel or serial [90]. On the other hand, power feeding in SDM systems utilizing the C-band can be implemented by groups of EDFAs, e.g., one per guided mode, core, or fiber [120,121]. A significant benefit of SDM over UWB here is the ability to share common pumping lasers [122], in this way reducing the number of laser pumps. SDM is also advantageous when compared with UWB as it possesses the ability to share the lasers in the transmitter and receiver parts [123]. In particular, if mode mixing exists, a common laser source leverages the post-detection signal processing required to unravel the original information, as the phase relationship is fixed. However, SDM shows higher costs than UWB in cases of limited fiber availability or in cases where, due to regulatory aspects, network operators are forced to pay rent to a government body/agency for any occupied fiber resources. For example, CAPEX aimed to roll-out a new fiber is ~25 keuro/km in rural areas, and up to ~500 keuro/km in metropolitan areas [124]. In particular, for a European country, the lease cost is approximately $0.33 \times (\sim \$1308)$ per fiber/km/year for five years leasing package; but the lease cost in an Indian network is approximately $0.007 \times (\sim \$29)$ per fiber/km/year [125]. These leasing costs need to be quantified during the selection of the optimal solution between UWB and SDM.

The exploitation of SDM in terrestrial networks will not only aid in attaining the target of 10 Pb/s by 2030 (Figure 17) but will also significantly boost node connectivity through the introduction of additional channels, which are transmitted through the additional cores and fibers. In particular, the number of parallel cores can reach up to 32 for fiber diameters of $\leq 250 \mu\text{m}$, where glass remains flexible, transporting a capacity of 1 Pb/s over more than 200 km [126]. Moreover, with the use of the 8D-16QAM format, the transmission distance can exceed 1200 km with a capacity of 0.75 Pbit/s. Further, in [127], it is demonstrated that the efficient operation of an SDM network is feasible, as the channels are adaptively (re)configured, taking into account the inter-core crosstalk with the aid of a software-defined network (SDN) controller. Regarding the introduction of SDM in terrestrial networks, the availability of multi-/core/fiber/mode amplifiers is a prerequi-

site. In particular, a Multi-Core Erbium/Ytterbium-Doped Fiber Amplifier (MC-EYDFA) can be a promising solution for the power restoration of the channels in multiple cores; however, some challenges need to be addressed, such as the reduction of its size and power consumption. Authors in [120] showed that a 32-core EYDFA can reduce the overall power consumption when benchmarked against a multiple EDFA scheme. This efficiency improvement for cladding pumping originates from increasing the effective area of active cores. Authors in [128] showed increased cladding pump efficiency for 19-core EDFA in C or L-bands while a cost analysis designates that the common amplifier brings long-term cost savings of 33% and up to 55% power savings [129]. In order to realize SDM within the limits of a terrestrial network, the existence of Optical Cross Connects (OXC) with SDM capabilities is a prerequisite. Scalability is the most important issue in order to accommodate several types of switching granularity demands, and a layered switching architecture is mandated. In future SDM networks, when the capacity per path will exceed several Tb/s, the introduction of spatial OXC-based architectures [130,131] will be a must. The successful migration from current Wavelength Selective Switches (WSS)-based networks towards layered and scalable SDM switches [132,133] will be key to the success of SDM-based networks.

The era of SDM deployments in submarine networks has already started. The first generation of SDM-based submarine systems was announced and started its deployment phase in 2020, before any terrestrial SDM network of any kind had been deployed. It is characterized by early technology advancements that implement the concept of “spatial integration of network elements” with optical amplifiers. The spatial integration/sharing of resources is implemented in the submarine optical amplifiers via the so-called “Repeater Pump Farming” (RPF) technique. RPF consists of a group (named “farm”) of repeaters, which are cross-connected to each other. Each RPF farm supports a certain group of Fiber Pairs (FPs) and utilizes a group of optical pumps that are shared among groups of FPs [134,135]. A significant advantage of RPFs is that they can continue pumping FPs even in cases in which one or more pumps fail, offering a promising solution for network survivability by assuring redundancy. A schematic of an RPF system is illustrated in Figure 25.

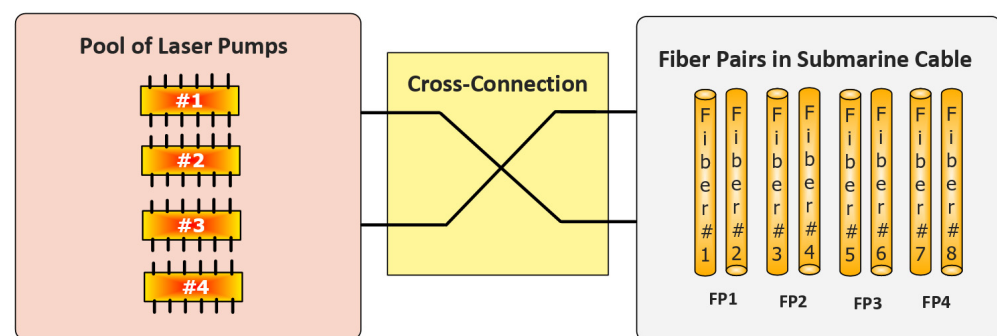


Figure 25. RPF systems that are expected to be in use in all future subsea cable systems [136].

SDM in Terrestrial and Submarine Networks

For the realization of SDM, several networking components do exist, such as WSSs and Reconfigurable Optical Add Drop Multiplexers (ROADMs), which, when compared with UWB, the WSS and ROADMs that can incorporate O, E, or S-bands are not generally commercially available. Usually, a submarine OADM node comprises both a Branch Unit (BU) and a Wavelength Management Unit (Figure 26). Fiber pairs may bypass the node (through the BU) if they are routed directly to other destinations or may enter the node to be switched through the WMU BU to their destination. Although flexibility may lead to higher cable utilization in the case of a reconfigurable OADM, strict security protocols must be run to prevent unwanted or faulty node configurations and possible unauthorized access. A comparative analysis between UWB and SDM for the submarine cables is

tabulated in Table 5. As it is evident, the SDM can support a significantly larger number of fiber pairs along with very high-power repeaters to rectify the power of the optical signals, which are expected to be significantly larger in number compared with traditional cables. Moreover, the transmission within SDM cables is restricted in the C-band, while PCS can be employed to enhance the channel performance.

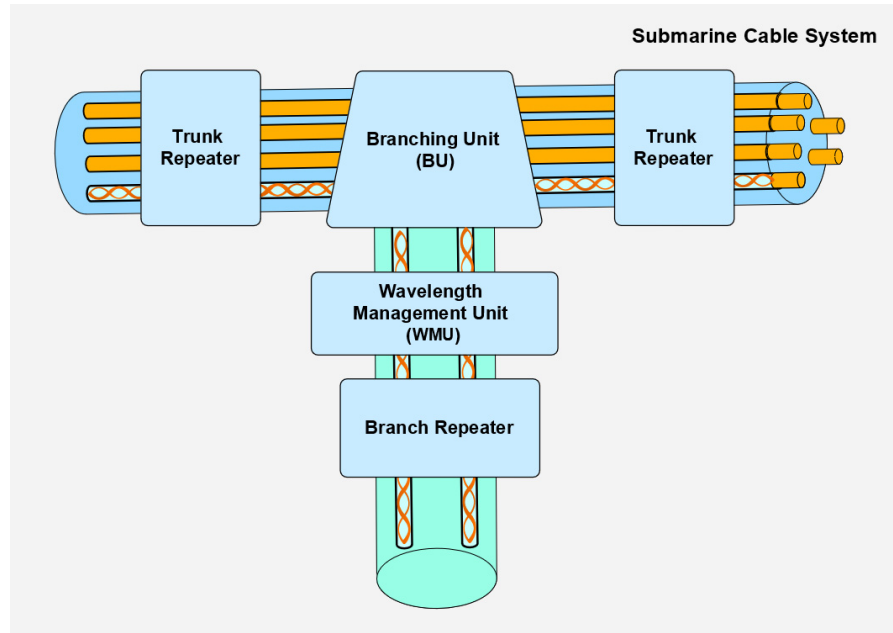


Figure 26. Schematic illustration of a Submarine OADM node [136].

Table 5. Traditional vs. SDM Submarine Cables for various metrics [136].

	SDM Cable	Traditional Cable
Submarine Cable	More fibers (12, 16, 24 FPPs and more in the future)	6 FPPs and maximum 8 FPPs
Fiber Effective Area (A_{eff})	Low effective area. $A_{eff} = 80\text{--}110\text{ }\mu\text{m}^2$, $a = 0.15\text{--}0.16\text{ dB/km}$	High effective area, $A_{eff} = 125\text{--}150\text{ }\mu\text{m}^2$, $a = 0.15\text{ dB/km}$
Repeater Type	Repeater pump farming	Each fiber has its own laser pumps
Branching Unit ROADMs	Fiber pair switching in branch units	No fiber pair switching in Branching unit ROADMs
OSNR	Lower OSNR	High OSNR
Modulation Formats	PCS (Probabilistic Constellation Shaping)	BPSK, QPSK, 8-QAM and 16-QAM
C + L Band Technology	Currently restricted in C-Band	C + L Band supported up to 144 channels fiber/pair
PFE	Same PFE, capacity (Maximum 15 kV)	Same PFE

To understand the potential of SDM systems in increasing the transportation capacity deeper, Figure 27 illustrates the total capacity of deployed submarine cables with and without the use of SDM. From this figure, we can observe the trend to migrate to SDM in order to overcome the 100 Tb/s capacity crunch, showing the potential to reach 1 Pb/s by 2030, satisfying the challenging demands of F6G services as they were presented in Section 2.

SDM in Wireless Fronthaul/Backhaul

It should also be emphasized that SDM is an excellent option to support the ever-increasing demands of traffic in the wireless part of the network by offering enhanced fronthaul/backhaul capabilities, as the antenna cell sites (or remote units) are attached via an optical distribution network (ODN), which can exploit SDM [137] (Figure 28). As a consequence, the deployed infrastructure can concurrently support multiple heterogeneous streams of digital and/or analog radio over fiber (DRoF/AroF, respectively), which can distribute heterogeneous traffic in a coordinated fashion through a converged infrastructure. The Central Office (CO) has the capability to exploit space and spectrum resources in an automated way, allowing channel establishment between the CO and cell sites in a 2D space (WDM + SDM), pairing baseband units (BBU) with remote radio units (RRU). As

the access requires cost- and energy-efficient solutions, it will significantly benefit from SDM, mainly using passive components, such as couplers and AWGs. However, the use of active components, such as WSSs, can be considered if the cost needs to be traded with flexible resource allocation.

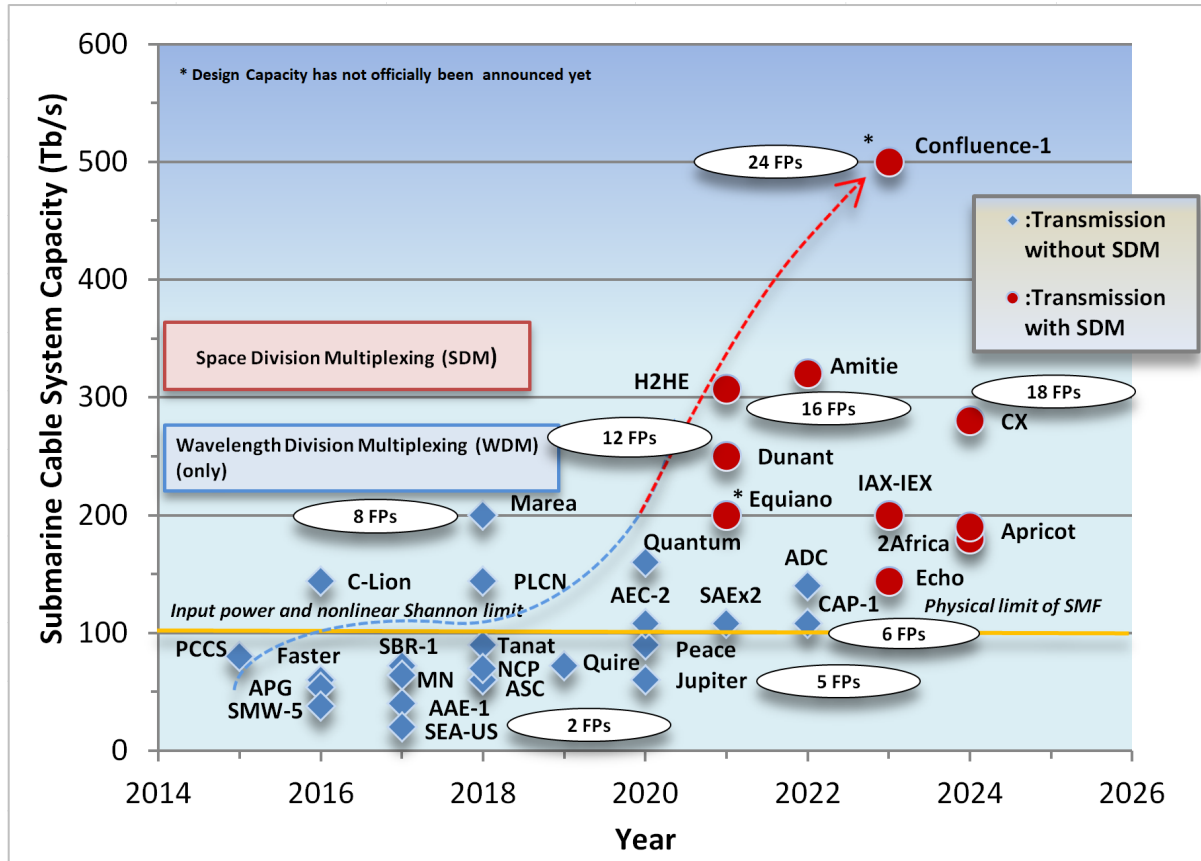


Figure 27. Transportation capacity of submarine cables with and without SDM over the years.

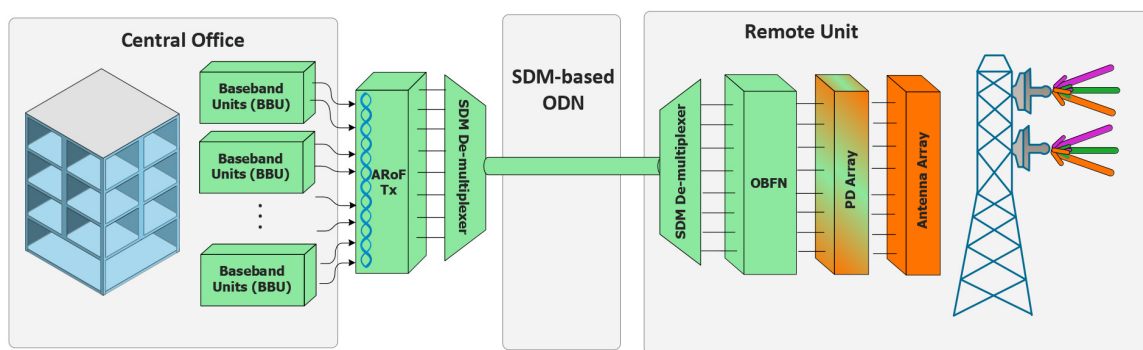


Figure 28. SDM-based Optical Distribution Network (ODN). OBFN: Optical Beamforming Network, PD: Photodiode, BBU: Baseband Unit, ARoF: Analog Radio over Fiber [137].

SDM in Inter/Intra Data Center Networks

Intra and inter data center communication can greatly benefit from the exploitation of the spatial dimension. The data rates in these two types of networks are usually low, such as 25 Gb/s and up to 100 Gb/s per fiber, mainly exploiting direct detection methods such as NRZ and PAM-4. However, they can be further boosted up to 220 Gb/s OOK and 408 Gb/s 8-PAM, as shown in [70], increasing the transported capacity (per channel) when needed. Based on the characteristics of currently deployed intra and inter data center

networks, a very large number of parallel single mode fibers ($>10,000$ s) are exploited in order to attain Pb/s rates. As a consequence, SDM is an already adopted solution here, where each fiber is populated with only a limited number of channels, e.g., four or eight, giving the opportunity to increase the overall transported capacity by one or two orders of magnitude both through the use of a larger number of channels and by increasing the data rate per channel, e.g., by scaling the baud rate.

4.3.3. Summarizing the Benefits of UWB and SDM-Based Systems

Before we conclude this sub-section, we wish to highlight the need to exploit all available capacity scaling dimensions (polarization, amplitude, phase, and number of spectral and spatial channels) and tailor them to specific applications and network domains. On one hand, SDM systems based on bundles of SSMFs are an already-adopted solution in submarine networks and intra-datacenter networks. However, the need for their deployment in terrestrial network segments is yet unclear. SDM also has very good potential to support the capacity and connectivity demands of the fronthaul. On the other hand, UWB (i.e., with mainly C and L-band transmission) systems have been a reality for over a decade now. The main question is if UWB is more economically feasible than, e.g., a 3-fiber SDM system that achieves the same capacity. To answer this question, one needs to delineate the most cost-effective solutions between SDM, UWD, and their combination, accounting for fiber availability, maturity—both at the component and system levels—the target total capacity, capacity per lane/channel, transmission reach, and the targeted specifications for cost/power consumption per transmitted bit. To reach this target, a technoeconomic analysis on the basis of a network planning study is missing from the literature and needs to be performed for indicative network types, e.g., submarine, access, etc.

Regarding fiber availability, UWB can reach up to 100% availability as there is at least one fiber present in all network links. On the other hand, SDM in terrestrial links shows a lower fiber availability as the existence of bunches of dark fibers is not always guaranteed. Next, SDM is advantageous over UWB, as it exploits a well-operated and mature technology for various components, such as transceivers, amplifiers, filters, etc., since it focuses on the third transmission window. Moreover, the physical layer performance of Bu-SMF is significantly higher when it is compared with UWB systems (beyond C and L-bands), allowing to attain a longer transmission reach, prohibiting the use of UWB applicability in submarine and long-haul transmission systems as they require a large number of regenerators, especially for the channels in the lower bands. However, in the core domain, as shown in [88], four out of five bands of an UWB system can interconnect even the most distant nodes of a core network, while the O-band can be used to interconnect less distant nodes (e.g., up to 600 km), showing that UWB is a very good candidate for the terrestrial domain. This diversity of UWB systems is highly plausible, as different bands can be assigned to different network paths and/or carry different data rates, in this way balancing the cost/transparent reach ratio. Merging the advantages of both worlds, we can say that a combination of UWB and SDM systems seems to be the most efficient solution to maximize the terrestrial network connectivity, allowing it to transport a multi-thousand number of channels through each optical link.

Next, both UWB and SDM systems have excellent upgradeability capabilities, as a new band or fiber can be engaged when the already active bands or fibers reach a utilization threshold, e.g., 60 or 70%, allowing it to follow a pay-as-you-grow policy, reducing the first-day capital expenditure. Another important advantage of SDM systems compared with UWB ones is the possibility of using common components for a large number of cores/fibers/modes, reducing the overall costs and power consumption. On the other hand, UWB can exploit amplifiers in multiple bands, such as C + L bands EDFA, UWB SOAs, and Raman amplifiers; however, these components are confined to two or three bands at most. A comparative study between UWB and bundles of C-band SMFs for their most important qualitative features is tabulated in Table 6.

Table 6. Qualitative Comparison of UWB and C-band SDM systems.

	Ultra-Wideband (UWB)	Space Division Multiplexing Based on Fiber Bundles (Bu-MF)
Cost	Significantly lower costs than SDM in cases of limited fiber availability	Lower component associated costs when mainly C-band is exploited
Connectivity and reach	Increased connectivity and flexibility as each band can be exploited for different transmission length	Higher transparent length as C-band shows the best physical layer performance and the fibers/components have optimized performance
Upgradeability	Very high considering a pay as you grow policy	Very high considering a pay as you grow policy
Diversity	Diversity in data rate per channel and reach can be attained by tailoring each band to specific requests (e.g., lower bands to shorter links and higher bands to longer ones)	All channels are considered “premium”, so diversification in terms of data rate per channel and reach cannot be considered
Commercialization	Mainly C and L bands	Well established commercially available technology in C-band
Spatially integrated network elements	Only when UWB amplifiers are used, e.g., Raman, SOA > 100 nm, C + L EDFA	Possible, e.g., shared amplification pumps among the various fibers and lasers at the transceiver sides
Best solution for	terrestrial networks	access/DCI, submarine networks

Concluding this sub-section, we wish to underline that using the currently available commercial components, it is possible to use UWB alongside SDM systems in a complementary way based on bundles of SMFs. SDM systems based on new fiber types (e.g., MCFs or FMFs) are expected to be further commercialized in the future, due to the immaturity of the technology, performance limitations, and the requirement for new fiber deployments that are very costly compared to their alternative solutions. In addition, UWB systems alone can be readily employed, extending the capacity of already deployed SMFs and providing a short- to medium-term cost-effective solution for network operators. However, there is a strong need to migrate to the spatial dimension at a rapid pace as it offers a theoretically unbounded capacity multiplier potential, allowing it to exceed 1 Pb/s rates, and can efficiently underpin the upcoming network transformation in order to support 6G and F6G services.

4.3.4. Combining the Benefits of UWB and SDM

In this section, we demonstrate how a multi-PB/s TRx block can be formed using UWB- and SDM-based systems along with the use of oDAC as it was described in Section 3. The oDAC, as a building block (BB), can be aggregated using several forms of multiplexing, namely spectral (WDM), spatial (SDM), polarization, and quadrature multiplexing, as depicted in Figure 29. The oDAC will be the key component of the transceivers, which will enable the aggregation of higher-capacity lanes in terms of spectral efficiency. TRxs incorporating single oDACs may suffice to serve low-to-moderate capacity 6G photonics interconnecting fiber links without additional degradation using DD. To achieve higher data rates for the highest UWB capacity, spectral and/or spatial multiplexing can be applied to the outputs of an array of unipolar or bipolar PAM oDAC outputs.

With the programmable oDAC, we can obtain a key building block to spur higher-level flexible multiplexing of lanes, combining UWB WDM and SDM to scale the overall transmission capacity up to Pb/s, as depicted in Figure 29. UWB/SDM optical links are then aggregated from per-wavelength BBs of up to 2 Tb/s. The envisioned optical link using compact oDAC arrays would support L spectral lanes and N spatial lanes over a single SDM fiber. Having $N \geq 20$ and $L \approx 100$ (over the S, C, and/or L bands), thus

$L \times N = 2000$, carrying 128 GBaud optical signals and bringing the raw per-link capacity to >1 Pb/s for DD and >4 Pb/s for COH links.

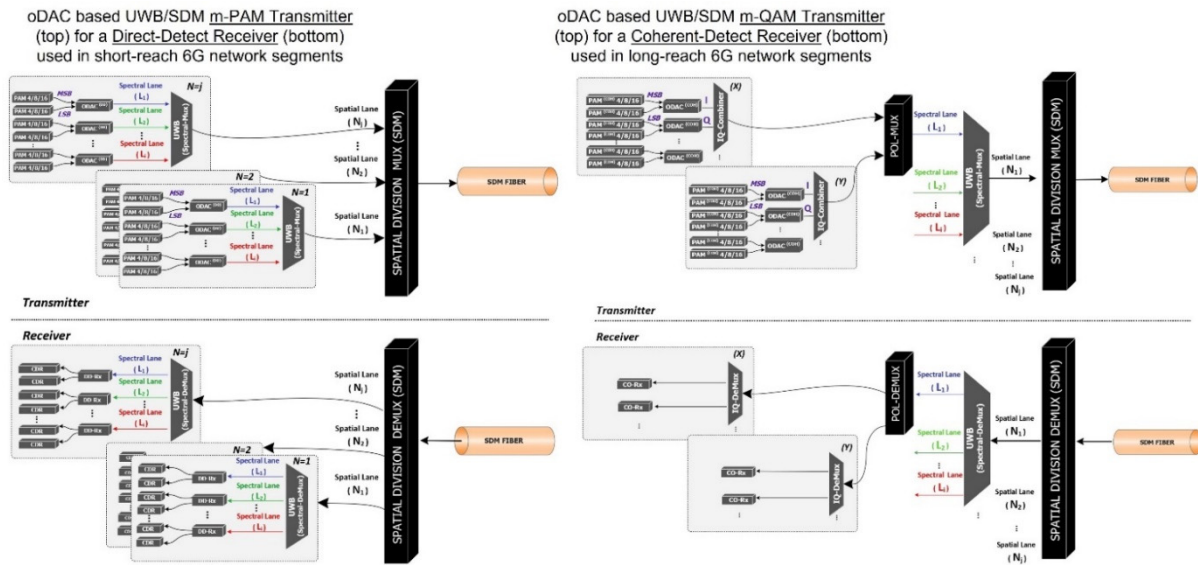


Figure 29. Multi-Pb/s TRx block diagram in an UWB-SDM scenario for future 6G networks.

The oDAC aggregation methodology enables one to port and proliferate, at the 6G TRx level, the full benefits of the underlying oDAC BBs, namely the improved tradeoffs in data-rate vs. power dissipation vs. footprint, and the flexibly reprogrammable capacity from relatively slow rates up to UWB capacity. Thus, an oDAC PIC design is classified as “future-proof” as shown in Figure 30.

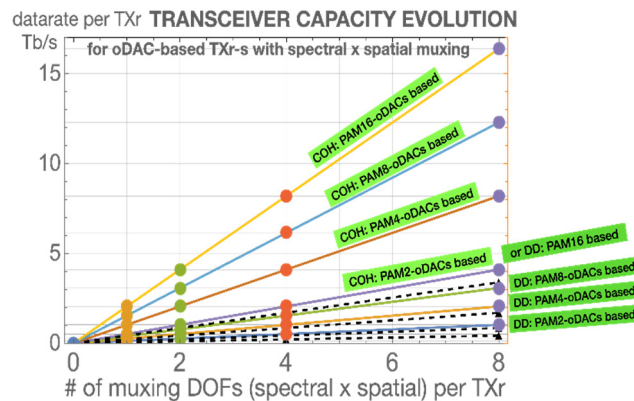


Figure 30. Data rate per TRx vs. number of multiplexing Degrees of Freedom.

4.3.5. Towards the Ultimate Capacity Limits of Optical Transmission

In this sub-section, we briefly elaborate on the main factors that can stress optical transmission toward its practical capacity limits. In order to achieve this, we need to maximize the following three quantities: (a) The bit rate per channel, (b) the number of employed channels per spatial element, e.g., fiber/core/mode, and (c) the number of spatial elements. Given that each channel has a specific bandwidth, the bit rate per channel is maximized by selecting a more spectrally efficient modulation format, e.g., 16 or 32QAM instead of QPSK. However, there is a clear tradeoff between the spectral efficiency and the physical layer performance, as the higher cardinality modulation formats require a significantly larger SNR in order to attain the same BER. This is clearer when the Shannon–

Hartley theorem is considered, which calculates the spectral efficiency (SE) in the presence of noise as follows:

$$SE = \frac{C}{B} = \log_2 \left(1 + \frac{S}{N} \right) \quad (1)$$

where C is the channel capacity in Gb/s, B is the bandwidth of the channel in GHz, and S/N is the signal-to-noise ratio. From Equation (1), it is clear that a high SNR is required to transmit multiple b/s/Hz, which cannot be attained within, e.g., a core network, via PM-32QAM, PM-64QAM, or even higher-cardinality formats for long distances more than a few hundreds of kilometers [91], mainly due to the accumulation of ASE noise and fiber nonlinearity. In a core network, PM-QPSK or even PM-16QAM can be exploited to interconnect distant nodes [90], as these modulation formats have relaxed SNR requirements compared with higher-cardinality formats, in order to attain the same BER. Certainly, the spectral efficiency can be boosted using (a) sophisticated DSP modules, which can significantly improve the signal's quality, however with additional computational complexity and added cost/power consumption, and (b) using more sophisticated forward error correction codes, but at the cost of an increased number of redundant bits. Next, increasing the number of transmitted channels within the same spatial element, e.g., fiber, will directly result in an N_{ch} multiplier. This can be realized by exploiting the low-loss attenuation spectrum of the optical fiber as analyzed in Section 4.3.1. The ultimate limit of UWB is the 365 nm spectrum, which is obviously finite, and after its exploitation, only the third method can be used, which is the space division multiplexing. This method can pack a very large number of spatial elements, in practice much larger than 24, which is the number of the largest SDM system up to now, offering another capacity multiplier, allowing one to attain multi-Pb/s rates within a single transmission link. The aforementioned analysis is summarized in Figure 31, where the three methods are combined to maximize the number of transmitted data in an optical system.

Predictions on the Attainable Capacity

Based on the announced capabilities of submarine cables, we can perform predictions about the transported capacity for the coming years based on data taken from previous decades. For this purpose, Figure 32 illustrates the announced transported capacity of various submarine fiber cables [16] with and without SDM. As is evident, SDM is the key technology that can assist in exceeding the limit of 100 Tb/s and reach 1 Pb/s by 2030. These predictions are fully aligned with the predictions of various research works summarized in Figure 17, where it was also highlighted that the capacity of commercially available systems will reach 1 Pb/s in 2030.

Predictions on the attainable capacity times length product can be also performed using the Optical Moor's Law (OML) formula introduced in [138] for submarine networks as follows:

$$C \cdot B_{[Pb/s.km]} = 10 \cdot 2^{(Year-2000)/F} \quad (2)$$

where the parameter *Year* denotes the year selected to estimate the predicted $C \cdot B$ product and F is a parameter that characterizes how fast in time the $C \cdot B$ product is scaled. In the original work of [138], F is equal to 3.75, which means doubling every 3.75 years or every 45 months. In this work, we exploit this formula, and based on recent experimental results for ultra-long haul and/or submarine transmission (taken from Figure 23), we slightly modify the value of F . In particular, from Figure 33 we can observe that by setting an F value equal to 3.125 in Equation (2), the fitting error is smaller. This is translated into doubling of the $C \cdot B$ product approximately every 37.5 months, which designates faster scaling compared to the value of F equal to 3.75. According to our opinion, this can be mainly attributed to the unlocking of new amplification bands, which allowed an increase in the transported capacity C .

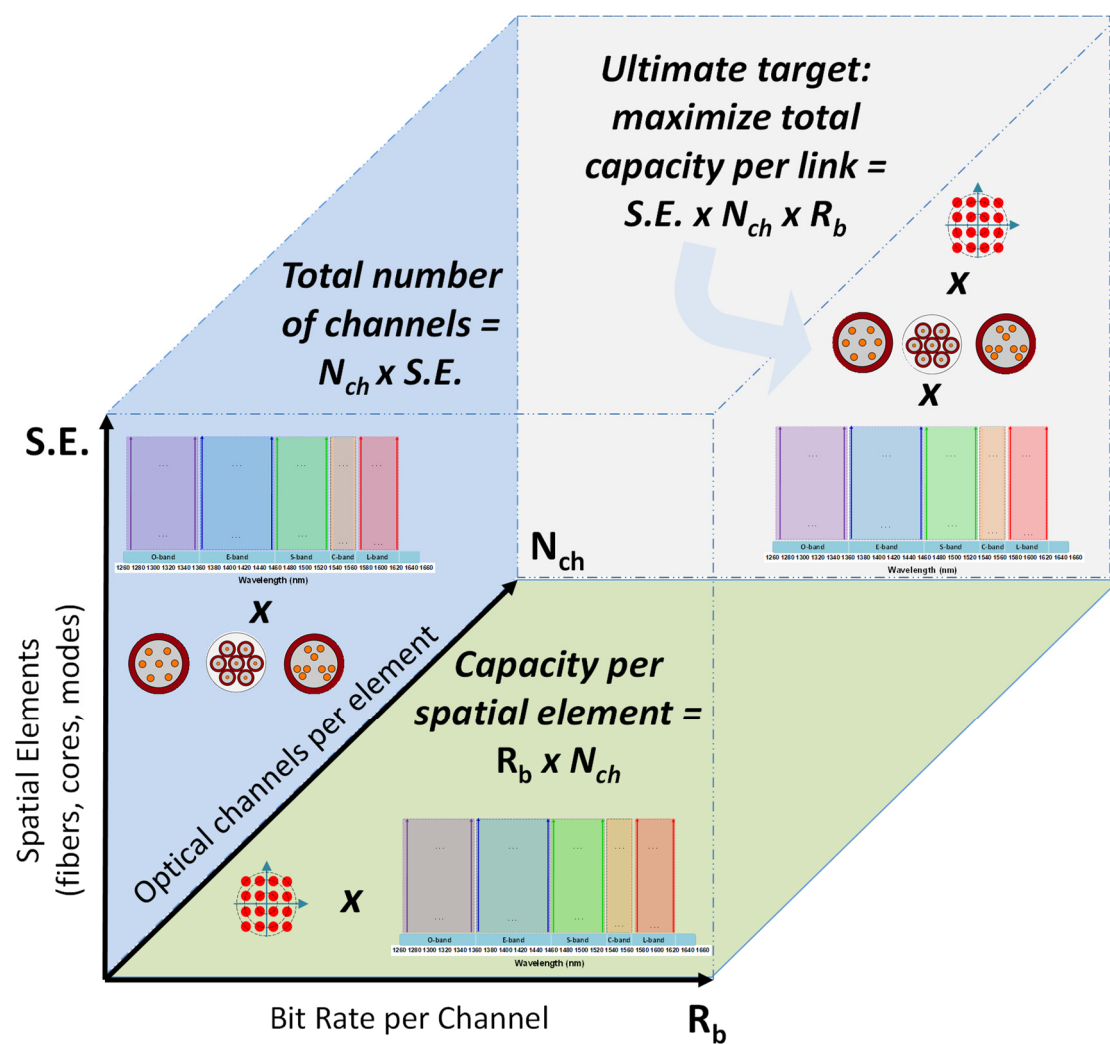


Figure 31. Illustration of the three ways to increase the number of transmitted data in an optical system: by increasing the number of spatial elements, by migrating to a higher cardinality modulation format, and by transmitting a higher number of channels.

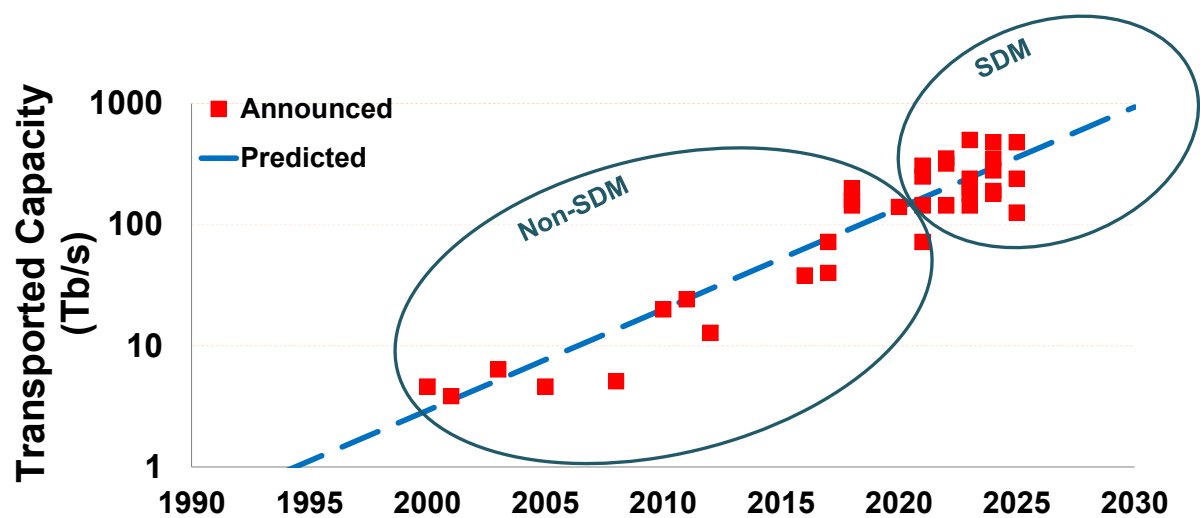


Figure 32. Prediction of transportation capacity (in Tb/s) based on currently deployed and planned submarine cables [16].

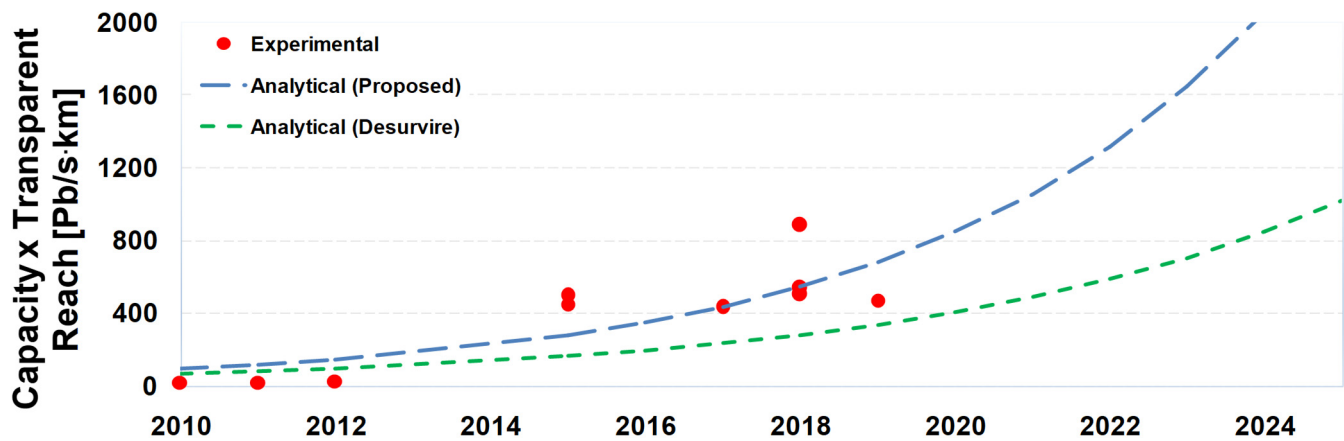


Figure 33. Predictions of capacity times length product (in Pb/s·km) based on experimental studies.

5. Optical Switching: Key Challenges and Proposed Directions

5.1. Need for More Sophisticated Switches to Support the F6G Ecosystem

Today's industrial networks are not capable of handling the requirements of the growing IoT ecosystem, which incorporates the communication between machines, robots and sensors, especially in the industrial sector. Low data rates, high latency, and limited connectivity are the main characteristics of currently deployed networks, and they have become bottlenecks as they limit industrial manufacturing quality and efficiency. Therefore, there is an urgent demand to provide more bandwidth, ultra-low latency, and higher connectivity in order to handle the industry's time-sensitive traffic flow for automated manufacturing and industrial practices [13]. To further understand the optical switching required for the F6G ecosystem, we summarize some key quantities as they were stated in the previous EU-funded HORIZON-CL4-2021-DIGITAL-EMERGING-01-06 call:

- Reliable and low latency communication with guaranteed service quality for the digital transformation of industrial processes.
- Reduced congestion in data communication when a multiplicity of applications competes for simultaneous delivery, thereby causing data loss or a delay in data delivery.
- Reduced power consumption to some pico-Joule per bit through the broader use of optical networking technologies, interconnects, and integrated optical communication components.
- Lowered barrier for the uptake of higher-performance communication technologies by reducing the cost of transmission interfaces to around 50 cents per Gigabit per second.

These requirements are critical for the operation of F6G networks and services and, in our opinion, a large amount of research work needs to be performed in order to offer the targeted switching components. The currently available solutions for switching, especially for services of the industrial sector, are almost entirely based on electrical interconnects, using expensive copper cables, and electronic switches for the aggregation of non-time-sensitive traffic and point-to-point links for the time-sensitive traffic. In the following paragraph, we present the main switching challenges that need to be efficiently addressed in order to satisfy the aforementioned requirements.

One technical challenge for the F6G ecosystem is to provide a unified solution that can meet the stringent latency requirements utilizing a P2MP architecture for both time-sensitive and non-time-sensitive traffic. A second challenge from an economical point of view is to provide a networking solution that can satisfy the cost and power consumption requirements mentioned above, as the traffic demands are scaling with time and are becoming larger. A third challenge is to create consensus around this solution with other system vendors and I4.0 system operators and be able to enter the very competitive, and somewhat closed, market of optical communication for industrial networks. Finally, the last challenge is to handle the very high capacity, which ends up in an optical node and needs to be switched efficiently at its egress. A schematical illustration of the switching concept,

which can be developed to interconnect both the “Things” within a factory and between the different factories is shown in Figure 34. In this schematic, two different switches are considered, one that is employed to interconnect the various “things” among the various factory floors (OXC-IF) and another one that can switch the traffic to and from the different interconnected factories (OXC-XC). Of course, depending on the factory characteristics and its dimensions, e.g., number of floors and number of interconnected items, it is possible to consider only a single optical switch per factory unit.

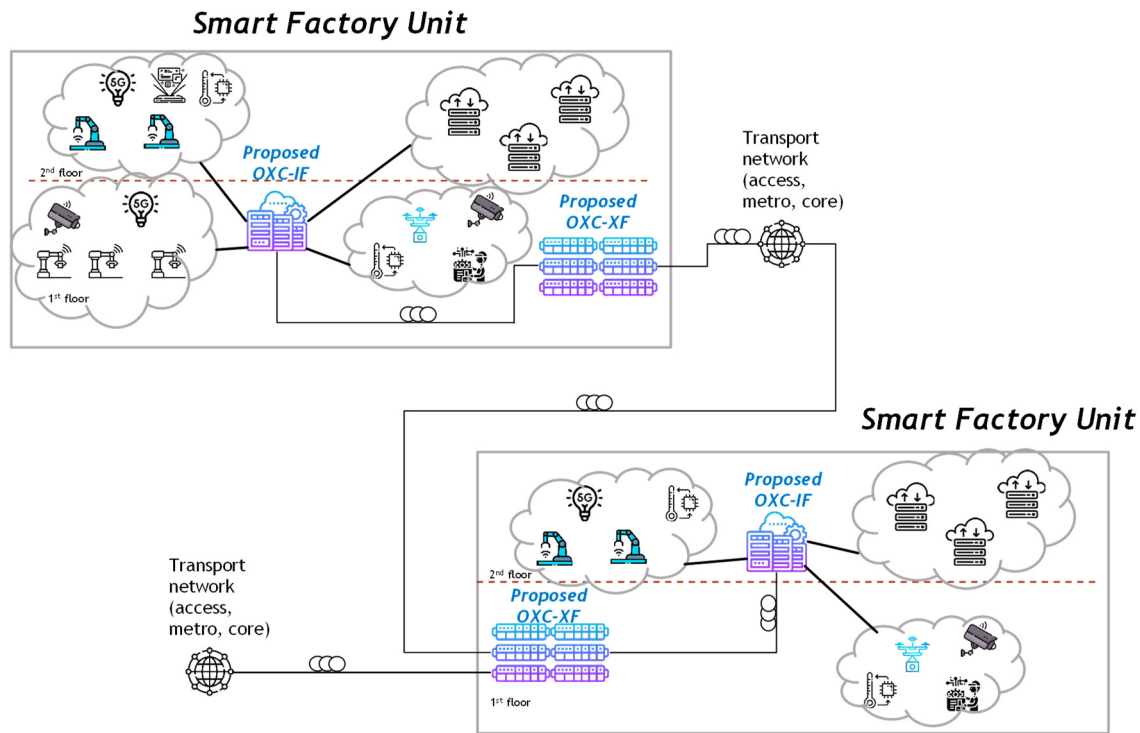


Figure 34. High-level representation of the industrial switching network for inter-(OXC-XF) and intra-factory (OXC-IF) connectivity.

In general, the optical switches can be categorized based on their supported services, as defined in Section 2, into (a) ultra-fast, dedicated to Time-Sensitive Networks (TSN), and (b) ultra-high capacity, dedicated to use-cases that require switching very high-volume traffic. In the next sub-sections, we discuss the challenges and potential solutions for these two discrete cases of switching.

5.2. Ultra-High Capacity Switching

To further understand the current needs for ultra-high-capacity switching, we pictorially describe the evolution of switching over time in Figure 35. As it is evident, in the early years (before 2000), it was the Synchronous Digital Hierarchy Digital Cross-Connect (SDH DXC) architecture that was first used to switch SDH-based signals. Electronic switches (SDH DXC) were mainly used in backbone networks operating with WDM technology. During these years, the network topology was entirely fixed with preassigned wavelengths being dropped/added at certain sites with the assistance of OADMs (optical add/drop multiplexers). Later on, OADMs were replaced by ROADMs that brought a level of flexibility and adaptability to the network, as a response to changing needs. Afterward, Planar lightwave circuit (PLC)-based ROADM node architecture was initially used to support the Add/Drop function of wavelength channels to colored ports (fixed port/wavelength assignment) for delivering traffic from/to local premises. This Add/Drop ROADM part used a thermo-optic switch (TO-SW), which was implemented in a PLC. PLC TO-SWs (made from SiO₂, which is a rather stable material) have no moving parts and, therefore

provide enhanced reliability to the ROADM architecture. Another approach comprising the same architecture is the wavelength blocker (WB)-based ROADM node architecture. In this method, the Add/Drop traffic is switched using a liquid crystal or micro electromechanical system (MEMS). This approach has good filtering characteristics, yet the dropped (and through) wavelength channels remain wavelength multiplexed. However, the filtering spectrum is broader and sharper than that of a PLC-based ROADM, which is based on wavelength demultiplexing.

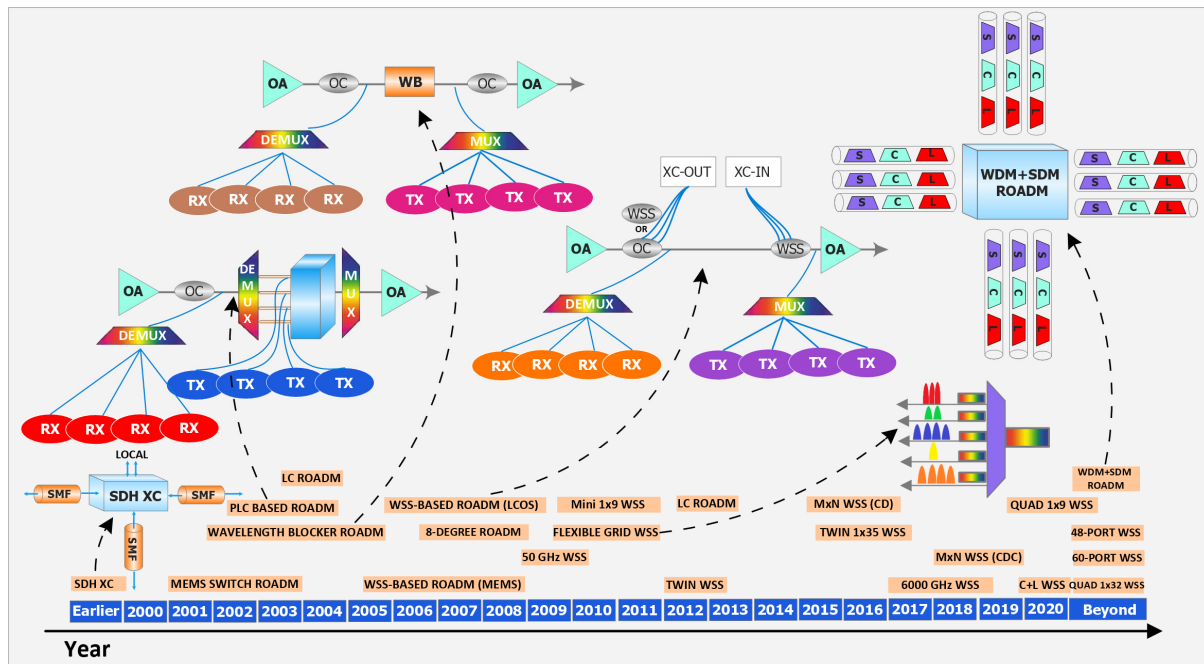


Figure 35. Evolution of optical switching over time (from SDH to SDM/ROADM switching functionality).

The Add/Drop switching part (in a WSS-based ROADM) is implemented using MEMS, a liquid crystal, or a liquid crystal on silicon (LCOS). Advanced filtering (as in WB-based ROADM) and excellent multi-degree capability (using multi-port WSSs) are now feasible. The size and complexity of the WSS scale are associated with the number of addressable spectral points (=operating bandwidth/optical resolution) and the number of output fiber ports. Increases in these factors lead to more capable ROADMs but with larger and more expensive WSSs. Therefore, we will likely need new optical node-switching architectures to support the needs for UWB/SDM switching.

A few years later, the flex grid concept was introduced as a revolutionary technology that allowed network and service providers to maximize the capacity of their premises by tailoring the channel bandwidth to user demands. Flex grid is a flexible solution that can support channel spacing from 50 to 200 GHz. A key feature is its software configurability, which means that the channel spacing can be dynamically tuned according to specific user demands, offering 6.25 GHz or 12.5 GHz granularity.

Figure 36 depicts a proposed next-generation optical switching node architecture, which can cross-connect communication channels among spatially parallel links that support UWB/WDM transmission (covering, e.g., at first the three distinct bands: S, C, L) and can serve as a part of a Multi-Granular (MG) switch. This architecture will be able to switch traffic from single channels, super-channels, bands, and entire fibers. Therefore, it will be a promising candidate for the future optical switching era.

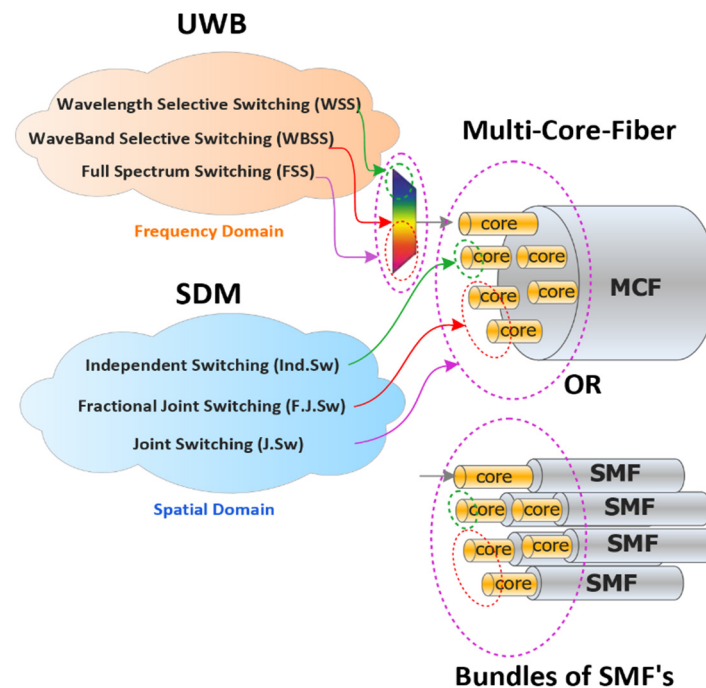


Figure 36. Multi-Granular Wave Band Selective Switch.

This switch is usually placed on intermediate nodes (OADMs/ROADMs) in a backbone optical network in order to switch traffic from/to the node. At first, the introduction of WDM in optical transmission required switches with wavelength switching capability. Nowadays, optical switches have super-channel switching capabilities in order to provide the required traffic from/to different nodes using super-channels, which can provide flexible data rates as the exploited bandwidth is in multiples of 12.5 GHz or even 6.25 GHz. In the coming decades, SDM is expected to be a strong candidate to increase capacity and connectivity, as was analyzed in Section 4, and as a consequence, the development and introduction of full-fiber switches will be a must. However, there will be a strong need for this switch to be MG in order to provide all capabilities between wavelength switching and full-fiber switching. This switch needs to incorporate both WSSs, which can distinguish every wavelength of each incoming fiber and then switch it to the appropriate output port, and WaveBand Selective Switches (WBSSs), which can switch entire amplification bands to the appropriate output ports. The MG-switch will be able to perform switching at the level of (i) wavelength, (ii) super-channel, (iii) band, and (iv) fully populated with channels fiber, alongside spatial lane switching of (i) independent switched, (ii) fractionally joint switched, and (iii) joint switched spatial super-channels. The development of an WBSS is an important intermediate step between current super-channel switches and future full-fiber switches.

Several subsystems and technologies are available to implement such a novel optical switching node, but the “missing-link” is a subsystem that can support flexible reconfigurable switching of UWB, bridging the gap from today’s super-channel switching to tomorrow’s full-spectrum fiber switching. Also, since F6G network nodes will become denser, more plentiful, and located in more space-limited sites, the switching technology must move away from bulk optics towards more compact, planar technologies. Therefore, the development of a WBSS in PIC format is a must, being able to complement the vital WSSs of today’s state-of-the-art network architectures (thus providing the “missing-link” to the evolution of optical networks). The general concept of the WBSS is pictorially described in Figure 36.

The need for a WBSS switch is further highlighted by Bell Labs, which predicted that by 2040, we may need a 250 spatial channels-based network operating over the full

(C + L + S)-bands bandwidth, supporting 66 wavelengths with a possible symbol rate of 300 Gbaud and a spectral efficiency of 20 b/s/Hz. This system must realize a capacity per spatial channel of 400 Tb/s and a total throughput of 100 Pb/s. In this scenario, UWB and SDM need to be combined to transport such amounts of traffic. However, as both techniques introduce new switching challenges at network nodes, the switching scalability is much greater, and operation without blocking and contention needs to be ensured. While the available optical fiber switches can be modified to support wider operating wavelength ranges and larger wavelength channel counts, there is no elegant, cost-effective way to do so. Currently, available WSSs can be modified to support multi-band transmission but become physically large and costly [139]. Further, OXC can support wideband operation, but access to wavelength channels necessitates the introduction of demultiplexers, making this option cumbersome with the need for large up-front investments. Moreover, both available WSSs and OXCs utilize slow switching mechanisms based on beam-steering to transit from one state to the other, and the induced delays are significant. This makes them less suitable for F6G applications, which have very stringent latency requirements and need significantly denser networks compared with F5G ones.

In parallel, continuous progress in optical transceivers by way of greater integration of novel photonics and optoelectronic devices and advancements in DSP are leading to higher-capacity optical interfaces (at the desired lower cost/bit and energy/bit metrics). As such, optical channel bandwidths are increasing and, concurrently, the number of wavelength multiplexed channels over a given spectral window is decreasing. This trend suggests that full-band transceivers (having integrated frequency comb sources with dedicated modulators and detectors per spectral line) may become commoditized by the decade's end and optical bandwidth will be resourced by full fiber bandwidth and routed throughout the network using space switches, i.e., OXC. This optical networking scenario lacks the efficiencies associated with resource sharing (of fibers, optical amplifiers, switches, etc.) and flexibility to adapt the optical bandwidth utilization to the per-connection capacity needs. Furthermore, the optical fiber infrastructure for full fiber allocation per connection will necessarily be massively fiber-parallel and require very large OXC to be deployed at network nodes from the onset to support full connectivity [140].

The proposed novel switching paradigm, which can address the aforementioned challenges posed by optical switching, is pictorially described in Figure 37. This node can cross-connect communication channels among spatially parallel links that support UWB/WDM operation (covering, e.g., at first three distinct bands: S, C, and L) and can serve as a part of a MG switch, which will be able to switch traffic from single channels, super-channels, bands, and entire fibers concurrently.

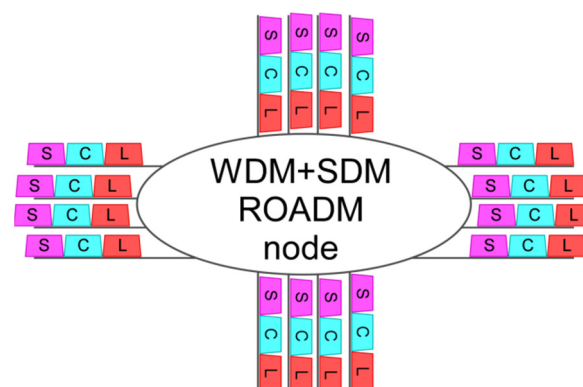


Figure 37. Generalized architecture of a node with SDM/UWB functionality.

Fundamentally, there is a strong need for a new WBSS module, such as the one pictorially described in Figure 38, that has the following characteristics: (a) It is efficiently implemented in a PIC platform, (b) it can be adaptively tuned in wavelength and optical bandwidth, (c) it can be scalable to large port counts, and (d) it can operate at mi-

crosecond switching rates. Network nodes utilizing the WBSS can be structured in a route-and-select topology, with individual switches placed on each I/O fiber port and expressing band-spanning fiber traffic towards its ultimate destination. The network node architecture supports legacy traffic by conventional WSS at a hierarchy below the WBSS, offering routing to DWDM traffic channels, before being re-multiplexed to the multi-band network (Figure 38). Connectivity between the network hierarchy elements is implemented by an OXC that further assists in transceiver sharing for handling add/drop channels in a colorless/directionless/contentionless (C/D/C) manner. The node can be reconfigured per accepted request in a centralized fashion, as done in today's networks, which lack significant dynamicity, yet accelerated due to a combination of faster processing power for requests and faster response times of the WBSS. An alternative operation mode of cycling through predetermined time-slotted connectivity patterns can allow direct connections between communicating pairs at target switch epochs, with data buffering at the transmitter, thereby guaranteeing time-of-flight latencies across the network and no loss of information due to buffer overflows.

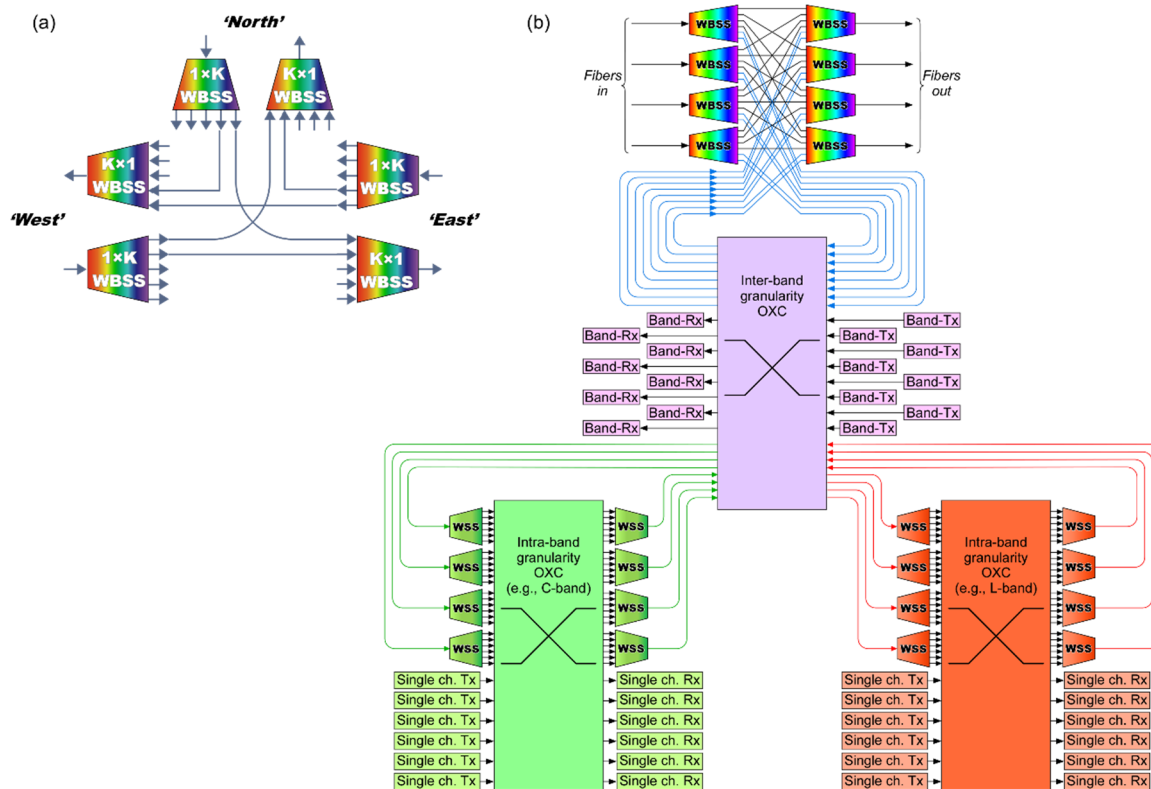


Figure 38. (a) Route and select topology implemented with WBSS between ingress and egress fiber ports. (b) Multi-granular optical node enabled with interconnecting OXC for access to emerging full-band add and drop transceivers, as well as WDM level granularity with existing WSS technology in support of legacy transmission.

5.2.1. On the Road towards Realizing a WBSS

Our vision in this direction for not-too-distant future networks is based on switches routing entire communication bands (S, C, or L). Multi-band transmission alone will not provide sufficient capacity, and links will incorporate SDM solutions as well, as already mentioned in the previous section. Under this upcoming scenario, a new switching paradigm allows one to switch entire bands and can offer high output port counts. A new switching architecture needs to be designed and implemented on a chip that combines adaptive filtering for band selection and adaptation as well as crossbar switches for scalable output port counts. The switch needs to be implemented on a PIC platform, on account of its low losses and thermal stability to utilize fast phase modulators that can operate

under 1 μ s, draw very little power per switching event, and be honed to operate with low polarization dependencies.

Moreover, the envisaged hierarchical network node aims to offer fast, route-and-select architecture at the band level implemented at the top tier, with a secondary route-and-select architecture implemented with today's per-band WSS for backward compatibility with legacy transmission schemes. An OXC disposed in between the two tiers offers C/D/C access to add/drop channels. The network node can be assembled and chassis-integrated, sharing a common control plane and communication port, with enhancements for faster network reconfiguration times. Regarding the performance characterization of mixed optical circuits flowing through the node, some bands rapidly switched at the top tier and others flowed through the bottom tier (mimicking legacy DWDM traffic), targeting low crosstalk (≤ -20 dB) and spurious transient strength (≤ 1 dB) and duration (≤ 1 μ s) on quasi-static, bottom tier flows. These are important technical metrics that can enable the seamless operation of F6G services during their entire life-cycle.

5.2.2. Optical Node Switching Architectures

In currently deployed backbone networks, intermediate nodes (OADMs/ ROADMs) have to switch traffic to their successor nodes in an efficient way. A common practice is to use network elements such as WSSs, which can distinguish every wavelength of each incoming fiber and then can switch it to the appropriate output port. So, in this way, there are two main approaches: (a) The spatial domain and (b) the frequency domain. The spatial domain consists of three main switching strategies: Independent Switching (Ind-Sw), Fractional Joint Switching (Fr-J-Sw) and Joint Switching (J-Sw). The Independent Switching (Ind-Sw) strategy uses wavelengths that can be switched independently in a non-blocking way. The Joint Switching (J-Sw) and Fractional Joint Switching (Fr-J-Sw) strategies switch wavelengths either altogether or in small groups, respectively. However, if the number of fibers and, consequently, the total number of wavelengths is increased, a ROADM must deploy many WSSs, resulting in large size and cost. On the other hand, the frequency domain consists of WSS, WBSS, and, finally, Full Spectrum Spatial Switching (FSSS). The Wavelength Switching (WS) of the uncoupled spatial super-channels approach in [140] switches specific wavelengths of all incoming spatial channels together, an approach similar to J-Sw. The trade-offs are obvious: The Ind-Sw strategy switches all data carriers with no limits but with large sizes and costs. J-Sw, Fr-J-Sw, and WS strategies do not provide a high degree of switching freedom (as Ind-Sw does) but can save money and complexity. In the FSSS approach [140], some pre-selected fibers or cores are committed to serving specific source–destination pairs. In FSSS, no wavelength distinction is required in the intermediate nodes, resulting in simpler backbone network architectures. On the other hand, if the traffic demands are much lower than the dedicated fibers' capacity, the total capacity can be under-utilized. Of course, depending on traffic conditions, hybrid approaches can be deployed.

There has been a lot of scientific research on the above switching architectures so far. A. Neto, et al. in [140] proposed using the Ind-Sw. strategy when dealing with light loads and diverting to FSSS when heavy loads arise. This happens because high loads ensure that the capacity of the pre-selected fibers/cores will be fully used. Moreover, the authors reviewed several node architectures that can support the Ind-Sw, WS of uncoupled spatial super-channels, and FSSS switching strategies.

As mentioned above, a fundamental element in optical network nodes is the OXC, which handles WDM signals without costly optical-to-electrical and electrical-to-optical conversion. It employs integrated interconnections to build an all-optical switching device, achieving high-level, integrated, fiber patching-free, and all-optical cross-connections, and manages to improve the switching efficiency, especially on large-granularity services.

K. Chen et al. and H. Hasegawa et al. in [141,142], respectively, studied the scalability problems of large ROADMs/OXCs due to the rising number of required WSSs. More specifically, the authors in [141] proposed a two-level architecture approach to construct a

modular large-scale OXC. Several small-scale OXCs are designed and then interconnected to each other in an effort to both ensure full-scale connectivity and reduce the number of devices and intra-node optical links. It is found that this modular OXC design achieves low insertion loss and does not become “big and fat” when input fiber numbers increase.

A proposal for relaxing the full-mesh connectivity to resolve the issue of the large number of required WSSs was presented in [142]. The authors studied the trade-off between full-mesh connectivity and routing performance. They showed that this trade-off can be faced by splitting the inter-connection parts into small regular sub-systems. Therefore, they tried to save space and costs by adding a little more complexity. They finally studied a fiber granular routing as an alternative scheme for cost-effective switching.

In [143] T. Kuno, et al. experimentally demonstrated a high-throughput OXC architecture that employs spatially jointed flexible waveband routing. Their results confirmed a net OXC throughput of 2.15 Pb/s, an OXC port count of 84, and a hop count of 7 at a transmission distance of 700 km. Their structure employed 64-channel 400-Gb/s dual-carrier DP-16QAM signals with 75 GHz spacing in 4.8 THz of the full C-band. Finally, the authors concluded that this OXC architecture can be applied efficiently to metro networks.

Another way to speed up optical switching is by considering an OXC architecture that deploys spatially jointed flexible-waveband routing using a 37.5 GHz grid, for transmission distances over 1600 km, 700 km, and 600 km using 32 GBaud DP-QPSK, DP-8QAM, and DP-16QAM, respectively. This architecture was presented in [144] and follows a Joint Switching (J-Sw) strategy by deploying special switches (named Delivery and Coupling (DC) switches), which are inserted between J-Sw WSSs to face possible routing restrictions. Simulations of the proposed architecture showed similar performances to the non-restricted OXC architecture while, at the same time, complexity and costs were lower. The authors concluded that this architecture could suit metro networks and would be a cost-effective architecture that could overcome the barriers to the realization of SDM networks.

A very Interesting two-layered architecture for ROADMs was presented by J. Zhang et al. in [145]. The two available layers provide a flexible and efficient management of MCF switching and, at the same time, support traffic grooming and the node’s add/drop modules. This two-layer architecture achieved low values in average transmission loss, crosstalk, and BER, anticipating the somewhat higher construction complexity. Their findings showed that a multi-layer design can efficiently deal with the scalability issues of single-layered ROADMs, and also seems to be a promising architecture for future ROADM designs.

The last alternative for higher bandwidth usage is the utilization of extra amplification bands, as analyzed in the previous section. Several recent proposals dictate the concurrent use of S, E, and C bands. Theoretically, UWB can use approximately 50 THz of optical bandwidth from 1260 nm to 1650 nm, thus providing the desired extra capacities. The price to be paid will be mainly the greater impact of fiber nonlinear effects in the smaller wavelengths. UWB switching can be built on multiple WSSs and a series of optical amplifiers. Therefore, UWB technology is a promising candidate in an effort to avoid higher sizes and costs and, therefore, to reduce complexity.

N. Fontaine et al. in [139] demonstrated a high port count (47 ports) Ultra-Wideband WSS that can support switching from 1300 nm to 1565 nm with low insertion loss. The switch provides a range of 36 THz (or 250 nm) and covers parts of the O band and S, E, and C bands.

S. Ding, et al. in [146] proposed a flexibility measurement approach in SDM Elastic Optical Networks (EONs) to quantitatively evaluate the switching flexibility of node architectures. Their results showed that an architecture introducing lane changes (LCs), employing the Ind-Sw strategy, and maximizing the number of A/D ports and the spectral granularity can achieve the best switching flexibility performance.

A new OXC structure ([147]), which can effectively reduce the hardware cost by saving the switch scale, was presented in [147]. Experimental results showed that the proposed layered m-OXC scheme can achieve similar blocking performance to fully connected OXCs with up to 76.1% hardware scale reductions and 93% searching time reductions.

A new optical network architecture named the Spatial Channel Network (SCN) was presented by M. Jinno in [20]. In SCNs, the optical layer “is explicitly decoupled from the hierarchical SDM and WDM layers, and an optical node evolves into a Spatial Cross Connect (SXC) and a Wavelength Cross Connect (WXC) to achieve a Hierarchical Optical Cross Connect (HOXC)”, in an effort to simplify optical switching procedures and protocols.

Moreover, the author presented a Routing and SDM/WDM Multilayer Resource Assignment (RSWA) heuristic protocol in order to minimize the number of needed Spatial Lanes (SLs). An interesting and useful characteristic of SCNs is that they separate traffic demands and network nodes into two kinds. Traffic demands are classified as express and local ones. Express traffic has an SL filling ratio higher than a relatively high threshold. This means that this demand can almost fulfill an SL, and as so, an entire SL is dedicated to it. Although this technique may not use the whole SL’s bandwidth in some cases, it does, however, result in simpler and faster RSWA protocols. Local traffic demands, as they cannot fill an SL, are directed to adjacent specific nodes and multiplexed with other similar traffic. So, SCNs are another way to relax switching demands from the physical layer and thus the need for large OXCs and move them to an upper layer. In this way, SCNs seem to be able to face ROADMs’ scalability issues.

We predict that SCNs will be widely used in future optical networks as they combine significantly less hardware in ROADMs (less WSSs) and faster switching for the express traffic class at the small cost of handling two types of traffic and a different (but not necessarily slower) Routing and Wavelength Assignment (RWA) algorithm. We are currently working on deploying the SCN architecture in a recently proposed submarine optical network for the Mediterranean Sea [148] to analytically exploit their potential.

A recent EU-funded project that aims to develop optical switches with UWB capabilities is the “Flexible Scalable Energy Efficient networking” [149]. FLEX-SCALE has the ambition of developing an UWB+SDM optical node (ON) supporting capacities ≥ 10 Pb/s, facing the scaling challenges and requirements posed by 6G applications on the backbone and x-haul networks. This node is based on innovative optical switching technologies such as the novel WBSS and state-of-the-art energy efficient optical transceivers, the oDACs. The main aim of the WBSS is to switch traffic by flexibly defining distinct bands carved from the UWB window of operation (spanning the wavelength range of 1460–1625 nm, designated today as the S, C, and L bands) and switching the information-bearing flexible bands (wide spectral super-channels) about ingress–egress fibers using the proven R&S topology. Introducing OXCs and WSS beneath the WBSS completes the MG-ON, which can then switch communication traffic at full-fiber, flexible-band, or individual wavelength channel granularity, whilst supporting reconfigurable add-drop in color-/direction-/contention-less (C/D/C) fashion.

We predict that architectures overcoming the scalability limitations of ROADMs will be more than essential in the near future. The first future direction is the multi-layered OXC architectures (two-layered or even three-layered), as these architectures will need fewer optical components and fibers, relax the full connectivity OXC demands, and provide acceptable fiber/wavelength routing performance. A second direction will be the use of specialized routing and wavelength assignment algorithms, which will meet the upcoming excessive routing/switching needs in the OXCs and, at the same time, allow for the use of a more efficient J-Sw strategy. Last, but not least, a third future direction will be the use of both WBSSs and WSSs, preferably within the same node in order to efficiently support Multi-Band switching.

5.3. Ultra-Fast Switching

Switches that are able to provide very low latency are indispensable components within an Industrial 4.0 and or/a Data Center (DC) environment. In particular, these switches need to:

- (a) Offer seamless optical connectivity between factory buildings, micro-data centers, or edge cloud computing.

- (b) Ensure low congestion, latency, and jitter when routing the traffic flows in the optical domain from the various end-points of the industrial network.
- (c) Provide high scalability and cascadeability, allowing the seamless operation of a highly densified industrial environment, consisting of a large number of inter-connected “things” such as robots, machines, etc.
- (d) Provide a sufficient physical layer performance even for demanding industrial environments, which comprise a large number of inter-connected buildings and “things”, such as robots, machines, etc., ensuring a very low BER even after a large number of traversed nodes in a densified environment.
- (e) Provide a cost- and energy-efficient switching solution, which comprises low-cost and zero/low-power consumption components (e.g., power splitters, combiners, arrayed waveguide gratings, and wavelength blockers).

The switches with these characteristics need to be able to satisfy various KPIs concurrently, as the Industrial services are both latency- and jitter-critical, while a high connectivity along with a very low packet loss ratio is required. The main KPIs for both intra and inter-factory connectivity are illustrated in Table 7.

Table 7. Main KPIs for intra and inter factory switches.

KPI	Inter-Factory	Intra-Factory
Capacity	Fronthaul: up to hundreds of Gb/s Tb/s scale	End point data rate up to 2 Gb/s; P2MP with 64 or higher end points
Latency	End-to-end latency: <100 μ s	End to end latency: 10 μ s (excluding fibre propagation)
Reliability	Very high	99.999% (of packets)
Power Consumption	few Watts per Tb/s	few Watts per Tb/s
Cost	50 cents per Gb/s	50 cents per Gb/s
Electromagnetic interference resiliency	Required	Required
Jitter	End-to-end jitter: 30 ns to a few μ s depending on the application	30 ns to 50 ns
Dynamics	ms-timescale	P2MP can be with fixed BW allocation
Guaranteed Delivery	End-to-end Packet loss rate: <10 ⁻¹⁰	BER: <10 ⁻⁵ (FEC with optimized latency)
Densification/Scalability	Number of competing time sensitive flows: >100 Number of machines in each edge cloud: ~200	P2MP aggregates the traffic of 64 end points into a single head end—increase density Scalability could be provided by the use of WDM

Currently available solutions are not able to support TSN as they cannot provide the required levels of flexibility (e.g., traffic dynamics) and determinism (e.g., jitter) concurrently [11]. In particular, Ethernet can effectively support the traffic dynamics; however, it cannot offer the required determinism. This is a result of multiple flows, which contend for the same output port experiencing random latency, and hence, jitter. To solve this issue, synchronous arrivals of packets and regular interleaving are needed, which would require client synchronization to the network. Another potential available solution is Industrial Ethernet, which provides determinism through its protocols (with sub- μ s jitter); however, static scheduling hinders the dynamics and flexibility. The next solution according to [11] is an Optical Transport Network (OTN), which is deterministic but inflexible. In general, an OTN or its variation (FlexE) can meet the current fronthaul requirement; however, they lack standardization to carry CPRI traffic and limited dynamics, and the relatively high cost makes them unsuitable for local networks, such as the ones on factory floors. Next, various PON standards can be potential solutions; however, they can address either flexibility or determinism but not both at the same time. For example, TWDM-PON, through the use of a Fixed Bandwidth Assignment (FBA) scheduler, can counterbalance jitter; however, it removes the benefits of statistical multiplexing while reducing the network dynamics, which is static in essence. Finally, the introduction of TSN maintains the trade-off between flexibility and determinism; however, it is a very

capable solution that offers low latency, low jitter, high speed, and guaranteed delivery use cases [11].

The switching architectures of [10,17] aim to satisfy the requirements of TSN networks. In [10], an optical wavelength, space, and time WDM cross-connect switch is employed to realize the optical metro node architecture and the Data Center Networks (DCN) architecture and consists of express and add/drop ports, photonicallly integrated WSS aggregation/disaggregation functions for merging/dropping the network traffic, and photonicallly integrated multi-cast switch (MCS). The modular approach enables one to scale the architecture in a pay-as-you-grow approach by using photonicallly integrated devices for wavelength and space switching. This photonic WDM switch employs SOA as an on-chip gain element for lossless operation. A significant advantage of this switch is the fast-switching time of the SOA and the high contrast ratio that make the SOA a very good candidate for fast packet-based switching operation. Next, [17] developed a novel DCN architecture utilizing OFDM and parallel signal detection technologies. The candidate architecture offers fine-grain bandwidth allocation, high switching speed, and low and uniform latency, which are vital for ultra-fast switches. This implementation has been experimentally demonstrated and verified successfully for the MIMO OFDM switching and fine-granularity flexible bandwidth sharing features. Moreover, efficient sub-carrier allocation algorithms have been developed for the fine-grain bandwidth allocation. The simulation results showed that the MIMO OFDM-based architecture provides low latency and high-throughput switching. Furthermore, the implementation of the scheduler shows that it can support a high number of nodes and subcarriers offering excellent scalability capabilities.

Figure 39 shows the high-level architecture of our vision on the Industry 4.0 switching architecture that aims to support both inter- and intra-factory communication. This architecture aims to connect the variety of end-points that can be found in a modern and future factory environment (including various “things”, such as machines, sensors, robots, etc.) with a centralized control that can be seen as a micro-data center (microDC), which can be located either within the factory or at a different site. The microDC has the flexibility to host a variety of different services such as the centralized control of the machine and robots on the factory floor, centralized logistic management, digital twin functionalities, and predictive maintenance. One of the main advantages of this flexible solution is that services can be migrated seamlessly to micro-DC located in a different location, increasing the reliability and availability of the services and allowing for the smooth growth and upgrade of the processing capabilities.

The key element of this network is the Flexible Optical Add/Drop Multiplexing (FOADM) node. This new design will incorporate software-programmable photonicallly integrated-circuit-based subsystems, controlled by an intelligent software management system, capable of simplifying and optimizing network operations. More specifically, novel photonic switching schemes (optical switches), which are fast-reconfigurable (sub-ms) and optimize the utilization of resources across different kinds of traffic (non/-time-sensitive) using an intelligent control plane, need to be implemented. These optical switches allow for fast routing of traffic on individual wavelengths that can be dynamically added, forwarded, or dropped at any network point. While the optical switch itself is going to operate at high speeds in the order of 10 ns, a key element of this network is the scheduling of the traffic in the FOADM nodes. The scheduling with the assistance of an intelligent software management system will ensure the ultra-low latency and jitter required for traffic delivery in Industry 4.0 use cases.

In the intra-factory network, the candidate architecture aims to provide a solution that will replace the current options for Industrial Ethernet and several other proprietary communications buses. These options are almost entirely based on electrical interconnects, using expensive copper cables and electronic switches for the aggregation of the non-time sensitive traffic and point-to-point links for the time-sensitive traffic. The most advanced demonstration of time-sensitive networks over packet-switched networks can achieve a

latency of $<100 \mu\text{s}$ with $<100 \text{ ns}$ jitter, making use of proprietary hardware that essentially creates a point-to-point link between the switches, with a very inefficient use of the network resources [150]. This will aid in developing a solution using a low-cost P2MP fiber network that will replace the copper-based electrical interconnects with an optical fiber and passive splitters/combiners. The proposed network aims to support both time-sensitive and time-insensitive connectivity. While the time-insensitive traffic can be easily supported by terminating and aggregating the connections from the end points at the input of the optical switch, the time-sensitive traffic and connections will be forwarded directly to the network by the FOADM node.

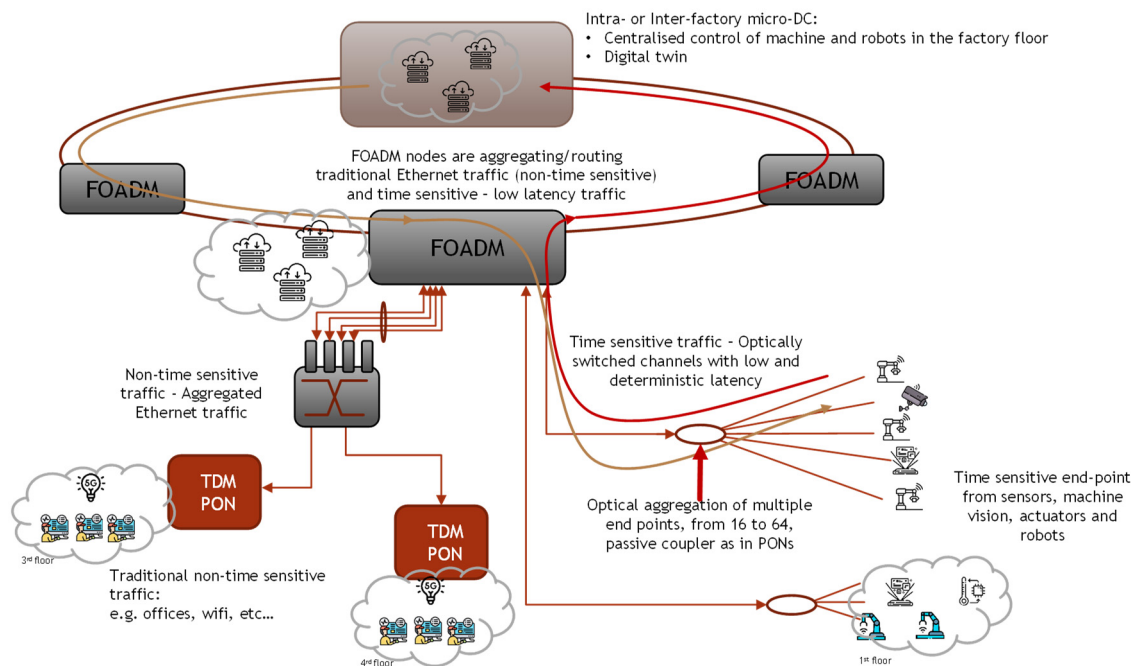


Figure 39. High-level representation of our vision on the I4.0 inter- and intra-factory connectivity.

The Intra-factory solution can support the optical aggregation of up to 64 end-points with data rates up to around 1 Gb/s per end-point and distances of a few kilometers. The solutions will use PON interfaces and technologies developed for residential optical access networks, such as XGS-PON and NG-PON2. In order to interface with the proposed optically switched network and meet the required latency and reliability performances, scheduling of the traffic in the PON systems will need to be integrated with new designs of the overall architecture. The design of the PON scheduler can be based on the work performed in utilizing TDM-PON for fronthaul applications [151].

The proposed solution can effectively address all the KPIs in Table 7 set for ultra-fast switches, whilst, in addition, it will allow one to: (i) reduce the congestion since optical networks can support high capacity; (ii) reduce the power consumption, due to the lower consumption of optical components in comparison with electronic ones; and (iii) reduce the cost of transmission interfaces thanks to the use of end-to-end optics, avoiding intermediate conversions to the electrical domain, thus collectively improving performance while, at the same time, minimizing the environmental impact. The fact that control can only be performed at the edges of the network makes the above solution an ideal candidate for the F6G ecosystem.

6. Conclusions

The 6th generation of fixed networks is about to offer humankind new services and exert a profound impact on all aspects of human activity. In this vision article, we first categorized key F6G services and shed light on their main requirements, to be met concurrently:

Low latency, a high bit rate, and ample connectivity. Next, we examined the main building blocks of the network to be developed using low-cost and low-power-consumption techniques. In particular, acknowledging that electronics is approaching its limits and that all-optical techniques will be increasingly called ‘to the rescue’, we explained how our proposed direction for adopting an optical-DAC is fully aligned with and supports the trend of improved energy efficiency and enhanced performance. Moreover, we proposed directions including three strategies to increase the rate of transmitted data in an optical system: The use of more spectrally efficient modulation formats, full exploitation of the physically available amplification bands of SMF, and the adoption of SDM. The implementations of each of these strategies, or a combination thereof, depend on the network domain—e.g., metro vs. core—and target constraints on cost, footprint, and power dissipation. Further, we discussed the two classes of optical switches featuring ultra-fast (enabling Time-Sensitive services) vs. ultra-high capacity (enabling use-cases that require switching very high-volume traffic) along with their requirements. Finally, we proposed potential solutions and directions based on the development of multi-granular waveband-selective flexibly switched optical add/drop multiplexing nodes, respectively.

Author Contributions: Conceptualization, methodology approach development, editing, writing, and reviewing: M.N., D.M.M., R.M., K.P., D.U., K.M., C.P. and I.T. All authors have read and agreed to the published version of the manuscript.

Funding: This research received no external funding.

Data Availability Statement: The data discussed in this article have been referenced at the corresponding points.

Conflicts of Interest: The authors declare no conflict of interest.

References

1. Wild, T.; Braun, V.; Viswanathan, H. Joint Design of Communication and Sensing for Beyond 5G and 6G Systems. *IEEE Access* **2021**, *9*, 30845–30857. [\[CrossRef\]](#)
2. Stavdas, A. 5G as a Catalyst for a Wider Technological Fusion that Enables the Fourth Industrial Revolution. In Proceedings of the IET Conference Proceedings, Online, 2–3 June 2021; pp. 39–49. [\[CrossRef\]](#)
3. Stavdas, A. Networked Intelligence: A Wider Fusion of Technologies that Spurs the Fourth Industrial Revolution. Part II: The Transformation of Production Systems. *World Rev. Political Econ.* **2021**, *12*, 236–254. [\[CrossRef\]](#)
4. Stavdas, A. Networked Intelligence: A Wider Fusion of Technologies that Spurs the Fourth Industrial Revolution. Part I: Foundations. *World Rev. Political Econ.* **2021**, *12*, 220–235. [\[CrossRef\]](#)
5. Uzunidis, D.; Logothetis, M.; Stavdas, A.; Hillerkuss, D.; Tomkos, I. Fifty Years of Fixed Optical Networks Evolution: A Survey of Architectural and Technological Developments in a Layered Approach. *Telecom* **2022**, *3*, 619–674. [\[CrossRef\]](#)
6. European Technology Platform NetWorld2020. Smart Networks in the context of NGI. Strategic Research and Innovation Agenda. *Eur. Technol. Platf.* **2021**, *27*, 1–240.
7. Fifth Generation Fixed Network (F5G); F5G Generation Definition Release #1. Available online: <https://www.etsi.org/technologies/fifth-generation-fixed-network-f5g> (accessed on 8 October 2023).
8. *The Fifth Generation Fixed Network (F5G): Bringing Fiber to Everywhere and Everything*; ETSI White Paper No. #41; ETSI: Valbonne, France, 2020; Available online: https://www.etsi.org/images/files/ETSIWhitePapers/etsi_wp_41_FSG_ed1.pdf (accessed on 8 October 2023).
9. Jiang, W.; Han, B.; Habibi, M.A.; Schotten, H.D. The Road Towards 6G: A Comprehensive Survey. *IEEE Open J. Commun. Soc.* **2021**, *2*, 334–366. [\[CrossRef\]](#)
10. Calabretta, N.; Prifti, K.; Tessema, N.; Xue, X.; Pan, B.; Stabile, R. Photonic Integrated WDM Cross-Connects for Optical Metro and Data Center Networks. *Metro and Data Center Optical Networks and Short-Reach Links II*; International Society for Optics and Photonics: Washington, DC, USA, 2019; Volume 10946, Available online: https://www.researchgate.net/publication/330813789_Photonic_integrated_WDM_cross-connects_for_optical_metro_and_data_center_networks (accessed on 8 October 2023).
11. Pointurier, Y.; Benzaoui, N.; Lautenschlaeger, W.; Dembeck, L. End-to-End Time-Sensitive Optical Networking: Challenges and Solutions. *J. Light. Technol.* **2019**, *37*, 1732–1741. [\[CrossRef\]](#)
12. Benzaoui, N.; Gonzalez, M.S.; Estaran, J.M.; Mardoyan, H.; Lautenschlaeger, W.; Gebhard, U.; Dembeck, L.; Bigo, S.; Pointurier, Y. Deterministic Dynamic Networks (DDN). *J. Light. Technol.* **2019**, *37*, 3465–3474. [\[CrossRef\]](#)
13. Bigo, S.; Benzaoui, N.; Christodouloupoulos, K.; Miller, R.; Lautenschlaeger, W.; Frick, F. Dynamic Deterministic Digital Infrastructure for Time-Sensitive Applications in Factory Floors. *IEEE J. Sel. Top. Quantum Electron.* **2021**, *27*, 6000314. [\[CrossRef\]](#)

14. Richardson, D.J. New optical fibers for high-capacity optical communications. *Philos. Trans. R. Soc. A Math. Phys. Eng. Sci.* **2016**, *374*, 20140441. [CrossRef]
15. Saridis, G.M.; Alexandropoulos, D.; Zervas, G.; Simeonidou, D. Survey and Evaluation of Space Division Multiplexing: From Technologies to Optical Networks. *IEEE Commun. Surv. Tutor.* **2015**, *17*, 2136–2156. [CrossRef]
16. Papapavlou, C.; Paximadis, K.; Uzunidis, D.; Tomkos, I. Toward SDM-Based Submarine Optical Networks: A Review of Their Evolution and Upcoming Trends. *Telecom* **2022**, *3*, 234–280. [CrossRef]
17. Ji, P.N.; Qian, D.; Kanonakis, K.; Kachris, C.; Tomkos, I. Design and Evaluation of a Flexible-Bandwidth OFDM-Based Intra-Data Center Interconnect. *IEEE J. Sel. Top. Quantum Electron.* **2013**, *19*, 3700310. [CrossRef]
18. Marom, D.M.; Colbourne, P.D.; D’Errico, A.; Fontaine, N.K.; Ikuma, Y.; Proietti, R.; Zong, L.; Rivas-Moscoco, J.M.; Tomkos, I. Survey of Photonic Switching Architectures and Technologies in Support of Spatially and Spectrally Flexible Optical Networking. *J. Opt. Commun. Netw.* **2017**, *9*, 1–26. [CrossRef]
19. Rechtman, L.; Marom, D.M. Rectangular versus circular fiber core designs: New opportunities for mode division multiplexing? In Proceedings of the 2017 Optical Fiber Communications Conference and Exhibition (OFC), Anaheim, CA, USA, 17–21 March 2017; pp. 1–3.
20. Jinno, M. Spatial Channel Network (SCN): Opportunities and Challenges of Introducing Spatial Bypass Toward the Massive SDM Era [Invited]. *J. Opt. Commun. Netw.* **2019**, *11*, 1–14. [CrossRef]
21. Jones, N. The information factories. *Nature* **2018**, *561*, 163–166. [CrossRef]
22. Nazarathy, M.; Tomkos, I. Accurate Power-Efficient Format- Scalable Multi-Parallel Optical Digital-to-Analogue Conversion. *Photonics* **2021**, *8*, 38. [CrossRef]
23. Yariv, A. Dynamic analysis of the semiconductor laser as a current-controlled oscillator in the optical phased-lock loop: Applications. *Opt. Lett.* **2006**, *30*, 2191. [CrossRef]
24. Doerr, C. Silicon-Photonic Integrated Circuits with Enhanced Optical Functionality for Data-Center Applications. In Proceedings of the Optical Fiber Communication Conference (OFC), San Diego, CA, USA, 28 March 2023.
25. Nespola, A.; Franco, G.; Forghieri, F.; Traverso, M.; Anderson, S.; Webster, M.; Gaudino, R. Proof of Concept of Polarization-Multiplexed PAM Using a Compact Si-Ph Device. *IEEE Photon. Technol. Lett.* **2019**, *31*, 62–65. [CrossRef]
26. Tomkos, I.; Tolmachev, A.; Agmon, A.; Meltsin, M.; Nikas, T.; Nazarathy, M. Low-Cost/Power Coherent Transceivers for Intra-Datacenter Interconnections and 5G Fronthaul Links. In Proceedings of the 2019 21st International Conference on Transparent Optical Networks (ICTON), Angers, France, 9–13 July 2019; pp. 1–5. [CrossRef]
27. Morsy-Osman, M.; Sowailem, M.; El-Fiky, E.; Goodwill, T.; Hoang, T.; Lessard, S.; Plant, D.V. DSP-free ‘coherent-lite’ transceiver for next generation single wavelength optical intra-datacenter interconnects. *Opt. Express* **2018**, *26*, 8890–8903. [CrossRef]
28. Doerr, C.R.; Chen, L. Monolithic PDM-DQPSK receiver in silicon. In Proceedings of the 36th European Conference and Exhibition on Optical Communication, Turin, Italy, 19–23 September 2010.
29. Perin, J.K.; Shastri, A.; Kahn, J.M. Design of Low-Power DSP-Free Coherent Receivers for Data Center Links. *J. Light. Technol.* **2017**, *35*, 4650–4662. [CrossRef]
30. Erkilinc, M.S.; Lavery, D.; Thomsen, B.C.; Killey, R.I.; Bayvel, P.; Savory, S.J. Polarization-insensitive single-balanced photodiode coherent receiver for long-reach WDM-PONs. *J. Lightw. Technol.* **2016**, *34*, 2034–2041. [CrossRef]
31. Cano, I.N.; Lerin, A.; Polo, V.; Prat, J. Polarization independent single-PD coherent ONU receiver with centralized scrambling in WDM PONs. In Proceedings of the 2014 The European Conference on Optical Communication (ECOC), Cannes, France, 21–25 September 2014; pp. 1–3.
32. Kazovsky, L.; Meissner, P.; Patzak, E. ASK multipoint optical homodyne receivers. *J. Light. Technol.* **1987**, *5*, 770–791. [CrossRef]
33. Zhou, J.; Caponio, N. Operative characteristics and application aspects of synchronous intra-bit polarization spreading for polarization independent heterodyne detection. *IEEE Photon. Technol. Lett.* **1994**, *6*, 295–298. [CrossRef]
34. Ciaramella, E. Polarization-Independent Receivers for Low-Cost Coherent OOK Systems. *IEEE Photon. Technol. Lett.* **2014**, *26*, 548–551. [CrossRef]
35. Altabas, J.A.; Silva Valdecasa, G.; Didriksen, M.; Lazaro, J.A.; Garces, I.; Tafur Monroy, I.; Jensen, J.B. Real-time 10Gbps Polarization Independent Quasicoherent Receiver for NG-PON2 Access Networks. In Proceedings of the 2018 Optical Fiber Communications Conference and Exposition: OFC, Los Angeles, CA, USA, 19 March–23 March 2018; pp. 1–3.
36. Thomas, V.A.; Varughese, S.; Ralph, S.E. Quasicoherent Receivers for Access Networks Using Fullwave Rectification Based Envelope Detection. In Proceedings of the 2019 Conference on Lasers and Electro-Optics (CLEO), San Jose, CA, USA, 5–10 May 2019; pp. 1–2.
37. Murmann, B. ADC Performance Survey 1997–2021. Available online: <http://web.stanford.edu/~murmman/adcsurvey.html> (accessed on 8 October 2023).
38. Siegman, A.; Kuizenga, D. Proposed method for measuring picosecond pulsewidths and pulse shapes in CW mode-locked lasers. *IEEE J. Quantum Electron.* **1970**, *6*, 212–215. [CrossRef]
39. Valley, G.C. Photonic analog-to-digital converters. *Opt. Express* **2007**, *15*, 1955–1982. [CrossRef]
40. Khilo, A.; Spector, S.J.; Grein, M.E.; Nejadmayeri, A.H.; Holzwarth, C.W.; Sander, M.Y.; Dahlem, M.S.; Peng, M.Y.; Geis, M.W.; DiLello, N.A.; et al. Photonic ADC: Overcoming the bottleneck of electronic jitter. *Opt. Express* **2012**, *20*, 4454–4469.
41. Yariv, A.; Koumans, R. Time interleaved optical sampling for ultra-high speed A/D conversion. *Electron. Lett.* **1998**, *34*, 2012–2013.

42. Krueger, B.; Makon, R.E.; Landolt, O.; Hidri, O.; Schweiger, T.; Krune, E.; Knoll, D.; Lischke, S.; Schulze, J. A monolithically integrated, optically clocked 10 GS/s sampler with a bandwidth of >30 GHz and a jitter of <30 fs in photonic SiGe BiCMOS technology. In Proceedings of the 2017 IEEE Custom Integrated Circuits Conference (CICC), Austin, TX, USA, 30 April–3 May 2017.
43. Zazzi, A.; Müller, J.; Weizel, M.; Koch, J.; Fang, D.; Moscoso-Mártir, A.; Mashayekh, A.T.; Das, A.D.; Drayß, D.; Merget, F.; et al. Optically Enabled ADCs and Application to Optical Communications. *IEEE Open J. Solid-State Circuits Soc.* **2021**, *1*, 209–221. [[CrossRef](#)]
44. Nazarathy, M.; Shaham, O. Spatially distributed successive approximation register (SDSAR) photonic ADCs based on phase-domain quantization. *Opt. Express* **2012**, *20*, 7833–7869. [[CrossRef](#)]
45. Lopez, I.G.; Aimone, A.; Alreesh, S.; Rito, P.; Brast, T.; Hohns, V.; Fiol, G.; Gruner, M.; Fischer, J.K.; Honecker, J.; et al. DAC-Free Ultralow-Power Dual-Polarization 64-QAM Transmission at 32 Gbd With Hybrid InP IQ SEMZM and BiCMOS Drivers Module. *J. Light. Technol.* **2017**, *35*, 404–410.
46. Schell, M.; Fiol, G.; Aimone, A. DAC-free Generation of M-QAM Signals with InP Segmented Mach-Zehnder Modulators. In Proceedings of the 2017 Optical Fiber Communications Conference and Exhibition OFC, Los Angeles, CA, USA, 19–23 March 2017.
47. Patel, D.; Samani, A.; Veerasubramanian, V.; Ghosh, S.; Plant, D.V. Silicon Photonic Segmented Modulator-Based Electro-Optic DAC for 100 Gb/s PAM-4 Generation. *IEEE Photon. Technol. Lett.* **2015**, *27*, 2433–2436.
48. Sobu, Y.; Huang, G.; Tanaka, S.; Tanaka, Y.; Akiyama, Y.; Hoshida, T. High-Speed Optical Digital-to-Analog Converter Operation of Compact Two-Segment All-Silicon Mach-Zehnder Modulator. *J. Light. Technol.* **2020**, *39*, 1148–1154. [[CrossRef](#)]
49. Vanhoecke, M.; Argyris, N.; Aimone, A.; Dris, S.; Apostolopoulos, D.; Verheyen, K.; Vaernewyck, R.; Torfs, G.; Yin, X.; Bosman, E.; et al. Multi-level optical signal generation using a segmented-electrode InP IQ-MZM with integrated CMOS binary drivers. In Proceedings of the 42nd European Conference on Optical Communication, ECOC, Dusseldorf, Germany, 18–22 September 2016; pp. 352–354.
50. Aimone, A.; Lopez, I.G.; Alreesh, S.; Rito, P.; Brast, T.; Höhns, V.; Fiol, G.; Gruner, M.; Fischer, J.K.; Honecker, J.; et al. DAC-free ultra-low-power dual-polarization 64-QAM transmission with InP IQ segmented MZM module. In Proceedings of the 2016 Optical Fiber Communications Conference and Exhibition (OFC), Anaheim, CA, USA, 20–24 March 2016; pp. 1–3.
51. Aimone, A.; Frey, F.; Elschner, R.; Lopez, I.G.; Fiol, G.; Rito, P.; Gruner, M.; Ulusoy, A.C.; Kissinger, D.; Fischer, J.K.; et al. DAC-Less 32-Gb/s PDM-256-QAM Using Low-Power InP IQ Segmented MZM. *IEEE Photon. Technol. Lett.* **2017**, *29*, 221–223.
52. Ehrlichman, Y.; Amrani, O.; Ruschin, S. Improved Digital-to-Analog Conversion Using Multi-Electrode Mach-Zehnder Interferometer. *J. Light. Technol.* **2008**, *26*, 3567–3575.
53. Giuglea, A.; Belfiore, G.; Khafaji, M.; Henker, R.; Petousi, D.; Winzer, G.; Zimmermann, L.; Ellinger, F. Comparison of Segmented and Traveling-Wave Electro-Optical Transmitters Based on Silicon Photonics Mach-Zehnder Modulators. In Proceedings of the 2018 Photonics in Switching and Computing, PSC 2018, Limassol, Cyprus, 19–21 September 2018; pp. 2018–2020.
54. Verbist, J.; Verplaetse, M.; Lambrecht, J.; Srivinasan, S.A.; de Heyn, P.; de Keulenaer, T.; Pierco, R.; Vyncke, A.; Absil, P.; Yin, X.; et al. 100 Gb/s DAC-less and DSP-free transmitters using GeSi EAMs for short-reach optical interconnects. In Proceedings of the 2018 Optical Fiber Communications Conference and Exposition, OFC 2018-Proceedings, San Diego, CA, USA, 11–15 March 2018; pp. 1–3.
55. Yamazaki, H.; Yamada, T.; Goh, T.; Mino, S. Multilevel optical modulator with PLC and LiNbO₃ hybrid integrated circuit. In Proceedings of the OFC 2011, Los Angeles, CA, USA, 6–10 March 2011.
56. Sano, A.; Kobayashi, T.; Ishihara, K.; Masuda, H.; Yamamoto, S.; Mori, K.; Yamazaki, E.; Yoshida, E.; Miyamoto, Y.; Yamada, T.; et al. 240-Gb/s polarization-multiplexed 64-QAM modulation and blind detection using PLC-LN hybrid integrated modulator and digital coherent receiver. In Proceedings of the European Conference on Optical Communication, Vienna, Austria, 20–24 September 2009; Volume 2009.
57. Yamazaki, H.; Yamada, T.; Goh, T.; Kaneko, A. PDM-QPSK modulator with a hybrid configuration of silica PLCs and LiNbO₃ phase modulators. *J. Light. Technol.* **2011**, *29*, 721–727. [[CrossRef](#)]
58. Yamazaki, H.; Yamada, T.; Goh, T.; Kaneko, A. 64QAM Modulator with a Hybrid Configuration of Silica PLCs and LiNbO₃ Phase Modulators for 100-Gb/s Applications Hiroshi. In Proceedings of the ECOC 2009, Vienna, Austria, 20–24 September 2009; pp. 1–4.
59. Nazarathy, M.; Tomkos, I. Energy-Efficient Reconfigurable 4 | 16 | 64 | 256-QAM Transmitter Based on PAM2 | 4-Driven Optical DACs. *IEEE Photon. Technol. Lett.* **2022**, *34*, 1159–1162.
60. Bogaerts, W.; Pérez, D.; Capmany, J.; Miller, D.A.B.; Poon, J.; Englund, D.; Morichetti, F.; Melloni, A. Programmable photonic circuits. *Nature* **2020**, *586*, 207–216.
61. Pérez, D.; Gasulla, I.; Crudgington, L.; Thomson, D.J.; Khokhar, A.Z.; Li, K.; Cao, W.; Mashanovich, G.Z.; Capmany, J. Multipurpose silicon photonics signal processor core. *Nat. Commun.* **2017**, *8*, 636.
62. Perez, D.; Gasulla, I.; Capmany, J. Reconfigurable integrated waveguide meshes for photonic signal processing and emerging applications. *Integr. Opt. Devices Mater. Technol. XXII* **2018**, 10535, 197–209.
63. Ellis, A.D.; Mac Suibhne, N.; Saad, D.; Payne, D.N. Communication networks beyond the capacity crunch. *Philos. Trans. R. Soc. A Math. Phys. Eng. Sci.* **2016**, *374*, 20150191. [[CrossRef](#)] [[PubMed](#)]

64. Karanov, B.; Chagnon, M.; Thouin, F.; Eriksson, T.A.; Bulow, H.; Lavery, D.; Bayvel, P.; Schmalen, L. End-to-End Deep Learning of Optical Fiber Communications. *J. Light. Technol.* **2018**, *36*, 4843–4855. [\[CrossRef\]](#)
65. Essiambre, R.-J.; Kramer, G.; Winzer, P.J.; Foschini, G.J.; Goebel, B. Capacity Limits of Optical Fiber Networks. *J. Light. Technol.* **2010**, *28*, 662–701. [\[CrossRef\]](#)
66. Winzer, P.J.; Neilson, D.T. From Scaling Disparities to Integrated Parallelism: A Decathlon for a Decade. *J. Light. Technol.* **2017**, *35*, 1099–1115. [\[CrossRef\]](#)
67. Winzer, P.J.; Neilson, D.T.; Chraplyvy, A.R. Fiber-optic transmission and networking: The previous 20 and the next 20 years. *Opt. Express* **2018**, *26*, 24190–24239. [\[CrossRef\]](#)
68. Aguiar, R.L.; Bourse, D.; Hecker, A.; Huusko, J.; Pouttu, A. Strategic Research and Innovation Agenda 2022. NetworkEurope; Zenodo: Honolulu, HI, USA, 2022. [\[CrossRef\]](#)
69. Nagatani, M.; Wakita, H.; Yamazaki, H.; Ogiso, Y.; Mutoh, M.; Ida, M.; Hamaoka, F.; Nakamura, M.; Kobayashi, T.; Miyamoto, Y.; et al. A Beyond-1-Tb/s Coherent Optical Transmitter Front-End Based on 110-GHz-Bandwidth 2:1 Analog Multiplexer in 250-nm InP DHBT. *IEEE J. Solid State Circuits* **2020**, *55*, 2301–2315. [\[CrossRef\]](#)
70. Eppenberger, M.; Bitachon, B.I.; Messner, A.; Heni, W.; Habegger, P.; Destraz, M.; De Leo, E.; Meier, N.; Del Medico, N.; Hoessbacher, C.; et al. Plasmonic Racetrack Modulator Transmitting 220 Gbit/s OOK and 408 Gbit/s 8PAM. In Proceedings of the 2021 European Conference on Optical Communication (ECOC), Bordeaux, France, 13–16 September 2021.
71. Pittalà, F.; Braun, R.-P.; Boecherer, G.; Schulte, P.; Schaedler, M.; Bettelli, S.; Calabrò, S.; Kuschnerov, M.; Gladisch, A.; Westphal, F.-J.; et al. Single-Carrier Coherent 930G, 1.28T and 1.60T Field Trial. In Proceedings of the 2021 European Conference on Optical Communication (ECOC), Bordeaux, France, 13–16 September 2021.
72. Xiang, L. Evolution of Fiber-Optic Transmission and Networking toward the 5G Era. *iScience* **2019**, *22*, 489–506.
73. Agrell, E.; Karlsson, M.; Chraplyvy, A.R.; Richardson, D.J.; Krummrich, P.M.; Winzer, P.; Roberts, K.; Fischer, J.K.; Savory, S.J.; Eggleton, B.J.; et al. Roadmap of optical communications. *J. Opt.* **2016**, *18*, 063002. [\[CrossRef\]](#)
74. Uzunidis, D.; Apostolopoulou, F.; Pagiatakis, G.; Stavdas, A. Analysis of Available Components and Performance Estimation of Optical Multi-Band Systems. *Eng* **2021**, *2*, 531–543. [\[CrossRef\]](#)
75. Knittle, C. IEEE 50 Gb/s EPON (50G-EPON). In Proceedings of the 2020 Optical Fiber Communications Conference and Exhibition (OFC), San Diego, CA, USA, 8–12 March 2020; pp. 1–3.
76. ENA. 100G PON; XENA Networks, White Paper; ENA: Schaumburg, IL, USA, 2017.
77. Available online: https://www.zte.com.cn/global/about/magazine/zte-technologies/2017/5/en_734/465612.html (accessed on 8 October 2023).
78. Available online: <https://www.telcotitans.com/vodafonewatch/vodafone-tests-100g-pon-waters-with-nokia/2990.article> (accessed on 8 October 2023).
79. Shaddad, R.; Mohammad, A.; Al-Gailani, S.; Al-Hetar, A.; Elmagzoub, M. A survey on access technologies for broadband optical and wireless networks. *J. Netw. Comput. Appl.* **2014**, *41*, 459–472. [\[CrossRef\]](#)
80. Horvath, T.; Munster, P.; Oujezsky, V.; Bao, N.-H. Passive Optical Networks Progress: A Tutorial. *Electronics* **2020**, *9*, 1081. [\[CrossRef\]](#)
81. Kanonakis, K.; Cvijetic, N.; Tomkos, I.; Wang, T. Dynamic Software-Defined Resource Optimization in Next-Generation Optical Access Enabled by OFDMA-Based Meta-MAC Provisioning. *J. Light. Technol.* **2013**, *31*, 2296–2306. [\[CrossRef\]](#)
82. Reis, J.D.; Ferreira, R.M.; Rossi, S.M.; Suzigan, G.J.; Pinto, T.M.S.; Shahpari, A.; Teixeira, A.L.; Gonzalez, N.G.; Oliveira, J.R.F. Bidirectional coherent WDM-PON performance with real-time Nyquist 16QAM transmitter. In Proceedings of the 2015 Optical Fiber Communications Conference and Exhibition (OFC), Los Angeles, CA, USA, 22–26 March 2015.
83. Available online: <https://www.infinera.com/innovation/xr-optics> (accessed on 8 October 2023).
84. Xu, Z.; Tan, Z.; Yang, C. Research on Performances of Coherent Nyquist-WDM-PON and WDM-OFDM-PON Using Effective Phase Noise Suppression Methods. In Proceedings of the 2016 Asia Communications and Photonics Conference (ACP), Wuhan, China, 2–5 November 2016.
85. Fehenberger, T.; Alvarado, A.; Bocherer, G.; Hanik, N. On Probabilistic Shaping of Quadrature Amplitude Modulation for the Nonlinear Fiber Channel. *J. Light. Technol.* **2016**, *34*, 5063–5073. [\[CrossRef\]](#)
86. Cho, J.; Winzer, P.J. Probabilistic Constellation Shaping for Optical Fiber Communications. *J. Light. Technol.* **2019**, *37*, 1590–1607. [\[CrossRef\]](#)
87. Poggiolini, P.; Nespola, A.; Jiang, Y.; Bosco, G.; Carena, A.; Bertignono, L.; Bilal, S.M.; Abrate, S.; Forghieri, F. Analytical and Experimental Results on System Maximum Reach Increase Through Symbol Rate Optimization. *J. Light. Technol.* **2016**, *34*, 1872–1885. [\[CrossRef\]](#)
88. Nikolaou, K.F.; Uzunidis, D.; Stavdas, A.; Pagiatakis, G. Quantifying the Impact of Physical Layer Effects in an Optical Multi-Band System. In Proceedings of the 29th Telecommunications forum TELFOR, Serbia, Belgrade, 23–24 November 2021.
89. Uzunidis, D.; Matrakidis, C.; Stavdas, A.; Lord, A. Power Optimization Strategy for Multi-Band Optical Systems. In Proceedings of the European Conference of Optical Communications, ECOC'20, Brussels, Belgium, 6–10 December 2020.
90. Uzunidis, D.; Kosmatos, E.; Matrakidis, C.; Stavdas, A.; Lord, A. Strategies for Upgrading an Operator's Backbone Network Beyond the C-Band: Towards Multi-Band Optical Networks. *IEEE Photon. J.* **2021**, *13*, 1–18. [\[CrossRef\]](#)

91. Uzunidis, D.; Matrakidis, C.; Kosmatos, E.; Stavdas, A.; Petropoulos, P.; Lord, A. Connectivity Challenges in E, S, C and L Optical Multi-Band Systems. In Proceedings of the 2021 European Conference on Optical Communication (ECOC), Bordeaux, France, 13–16 September 2021; pp. 1–4.
92. Sano, A.; Masuda, H.; Kobayashi, T.; Fujiwara, M.; Horikoshi, K.; Yoshida, E.; Miyamoto, Y.; Matsui, M.; Mizoguchi, M.; Yamazaki, H.; et al. 69.1-Tb/s (432×171 -Gb/s) C- and extended L-band transmission over 240 km Using PDM-16-QAM modulation and digital coherent detection. In Proceedings of the 2010 Conference on Optical Fiber Communication (OFC/NFOEC), Collocated National Fiber Optic Engineers Conference, San Diego, CA, USA, 21–25 March 2010; pp. 1–3.
93. Qian, D.; Huang, M.-F.; Ip, E.; Huang, Y.-K.; Shao, Y.; Hu, J.; Wang, T. 101.7-Tb/s (370×294 -Gb/s) PDM-128QAM-OFDM transmission over 3×55 -km SSMF using pilot-based phase noise mitigation. In Proceedings of the 2011 Optical Fiber Communication Conference and Exposition and the National Fiber Optic Engineers Conference, Los Angeles, CA, USA, 6–10 March 2011; pp. 1–3.
94. Kobayashi, T.; Yamanaka, S.; Matsuura, A.; Kawakami, H.; Miyamoto, Y.; Ishihara, K.; Masuda, H. 102.3-Tb/s (224×548 -Gb/s) C- and extended L-band all-Raman transmission over 240 km using PDM-64QAM single carrier FDM with digital pilot tone. In Proceedings of the OFC/NFOEC, Los Angeles, CA, USA, 4–8 March 2012; pp. 1–3.
95. Zhu, B.; Xie, C.; Nelson, L.E.; Jiang, X.; Peckham, D.; Lingle, R.; Yan, M.F.; Wisk, P.W.; DiGiovanni, D.J. 70 nm seamless band transmission of 17.3 Tb/s over 40×100 km of fiber using complementary Raman/EDFA. In Proceedings of the 2015 Optical Fiber Communications Conference and Exhibition (OFC), Los Angeles, CA, USA, 22–26 March 2015; pp. 1–3.
96. Cai, J.-X.; Sun, Y.; Zhang, H.; Batshon, H.G.; Mazurczyk, M.V.; Sinkin, O.V.; Foursa, D.G.; Pilipetskii, A. 49.3 Tb/s Transmission Over 9100 km Using C + L EDFA and 54 Tb/s Transmission Over 9150 km Using Hybrid-Raman EDFA. *J. Light. Technol.* **2015**, *33*, 2724–2734. [[CrossRef](#)]
97. Okamoto, S.; Horikoshi, K.; Hamaoka, F.; Minoguchi, K.; Hirano, A. 5-band (O, E, S, C, and L) WDM Transmission with Wavelength Adaptive Modulation Format Allocation. In Proceedings of the ECOC 2016, 42nd European Conference on Optical Communication, Dusseldorf, Germany, 18–22 September 2016; pp. 1–3.
98. Saavedra, G.; Tan, M.; Elson, D.J.; Galdino, L.; Semrau, D.; Iqbal, A.; Phillips, I.D.; Harper, P.; Ellis, A.; Thomsen, B.C.; et al. Experimental Analysis of Nonlinear Impairments in Fibre Optic Transmission Systems up to 7.3 THz. *J. Light. Technol.* **2017**, *35*, 4809–4816. [[CrossRef](#)]
99. Ghazisaeidi, A.; Ruiz, I.F.d.J.; Rios-Muller, R.; Schmalen, L.; Tran, P.; Brindel, P.; Meseguer, A.C.; Hu, Q.; Buchali, F.; Charlet, G.; et al. Advanced C + L-Band Transoceanic Transmission Systems Based on Probabilistically Shaped PDM-64QAM. *J. Light. Technol.* **2017**, *35*, 1291–1299. [[CrossRef](#)]
100. Renaudier, J.; Meseguer, A.C.; Ghazisaeidi, A.; Tran, P.; Muller, R.R.; Brenot, R.; Verdier, A.; Blache, F.; Mekhazni, K.; Duval, B.; et al. First 100-nm Continuous-Band WDM Transmission System with 115Tb/s Transport over 100km Using Novel Ultra-Wideband Semiconductor Optical Amplifiers. In Proceedings of the 2017 European Conference on Optical Communication (ECOC), Gothenburg, Sweden, 17–21 September 2017; pp. 1–3.
101. Cai, J.-X.; Batshon, H.G.; Mazurczyk, M.V.; Sinkin, O.V.; Wang, D.; Paskov, M.; Davidson, C.R.; Patterson, W.W.; Bolshtyansky, M.A.; Foursa, D.G. 51.5 Tb/s Capacity over 17,107 km in C + L Bandwidth Using Single Mode Fibers and Nonlinearity Compensation. In Proceedings of the 2017 European Conference on Optical Communication (ECOC), Gothenburg, Sweden, 17–21 September 2017; pp. 1–3.
102. Cai, J.-X.; Batshon, H.G.; Mazurczyk, M.V.; Sinkin, O.V.; Wang, D.; Paskov, M.; Patterson, W.W.; Davidson, C.R.; Corbett, P.C.; Wolter, G.M.; et al. 70.46 Tb/s Over 7600 km and 71.65 Tb/s Over 6970 km Transmission in C + L Band Using Coded Modulation with Hybrid Constellation Shaping and Nonlinearity Compensation. *J. Light. Technol.* **2018**, *36*, 114–121. [[CrossRef](#)]
103. Cai, J.-X.; Batshon, H.G.; Mazurczyk, M.V.; Davidson, C.R.; Sinkin, O.V.; Wang, D.; Paskov, M.; Patterson, W.W.; Bolshtyansky, M.A.; Foursa, D.G. 94.9 Tb/s Single Mode Capacity Demonstration over 1900 km with C + L EDFAs and Coded Modulation. In Proceedings of the 2018 European Conference on Optical Communication (ECOC), Rome, Italy, 23–27 September 2018; pp. 1–3.
104. Ionescu, M.; Galdino, L.; Edwards, A.; James, J.; Pelouch, W.; Sillekens, E.; Semrau, D.; Lavery, D.; Killey, R.I.; Barnes, S.; et al. 91 nm C + L Hybrid Distributed Raman–Erbium-Doped Fibre Amplifier for High Capacity Subsea Transmission. In Proceedings of the 2018 European Conference on Optical Communication (ECOC), Rome, Italy, 23–27 September 2018; pp. 1–3.
105. Galdino, L.; Edwards, A.; Ionescu, M.; James, J.; Pelouch, W.; Sillekens, E.; Semrau, D.; Lavery, D.; Killey, R.I.; Barnes, S.; et al. 120 Tbit/s Transmission over Single Mode Fibre using Continuous 91 nm Hybrid Raman-EDFA Amplification. *arXiv* **2018**, arXiv:1804.01845.
106. Hamaoka, F.; Minoguchi, K.; Sasai, T.; Matsushita, A.; Nakamura, M.; Okamoto, S.; Yamazaki, E.; Kisaka, Y. 150.3-Tb/s Ultra-Wideband (S, C, and L Bands) Single-Mode Fibre Transmission over 40-km Using >519 Gb/s/A PDM-128QAM Signals. In Proceedings of the 2018 European Conference on Optical Communication (ECOC), Rome, Italy, 23–27 September 2018; pp. 1–3.
107. Lopez, V.; Zhu, B.; Moniz, D.; Costa, N.; Pedro, J.; Xu, X.; Kumpera, A.; Dardis, L.; Rahn, J.; Sanders, S. Optimized Design and Challenges for C&L Band Optical Line Systems. *J. Light. Technol.* **2020**, *38*, 1080–1091.
108. Ionescu, M.; Lavery, D.; Edwards, A.; Sillekens, E.; Galdino, L.; Semrau, D.; Killey, R.I.; Pelouch, W.; Barnes, S.; Bayvel, P. 74.38 Tb/s Transmission Over 6300 km Single Mode Fiber with Hybrid EDFA/Raman Amplifiers. In Proceedings of the 2019 Optical Fiber Communications Conference and Exhibition (OFC), San Diego, CA, USA, 3–7 March 2019; pp. 1–3.
109. Hamaoka, F.; Nakamura, M.; Okamoto, S.; Minoguchi, K.; Sasai, T.; Matsushita, A.; Yamazaki, E.; Kisaka, Y. Ultra-Wideband WDM Transmission in S-, C-, and L-Bands Using Signal Power Optimization Scheme. *J. Light. Technol.* **2019**, *37*, 1764–1771. [[CrossRef](#)]

110. Iqbal, A.; Di Rosa, G.; Krzczanowicz, L.; Phillips, I.; Harper, P.; Richter, A.; Forysiak, W. Impact of pump-signal overlap in S + C + L band discrete Raman amplifiers. *Opt. Express* **2020**, *28*, 18440–18448. [\[CrossRef\]](#)
111. Kato, T.; Watanabe, S.; Yamauchi, T.; Nakagawa, G.; Muranaka, H.; Tanaka, Y.; Akiyama, Y.; Hoshida, T. Real-time transmission of 240×200 -Gb/s signal in S + C + L triple-band WDM without S- or L-band transceivers. In Proceedings of the 45th European Conference on Optical Communication (ECOC 2019), Dublin, Ireland, 22–26 September 2019; pp. 1–4.
112. Arnould, A.; Ryf, R.; Chen, H.; Achouche, M.; Renaudier, J.; Ghazisaeidi, A.; Le Gac, D.; Brindel, P.; Makhsiyan, M.; Mekhazni, K.; et al. 103 nm Ultra-Wideband Hybrid Raman/SOA Transmission Over 3×100 km SSMF. *J. Light. Technol.* **2020**, *38*, 504–508. [\[CrossRef\]](#)
113. Renaudier, J.; Arnould, A.; Ghazisaeidi, A.; Le Gac, D.; Brindel, P.; Awwad, E.; Makhsiyan, M.; Mekhazni, K.; Blache, F.; Boutin, A.; et al. Recent Advances in 100+ nm Ultra-Wideband Fiber-Optic Transmission Systems Using Semiconductor Optical Amplifiers. *J. Light. Technol.* **2020**, *38*, 1071–1079. [\[CrossRef\]](#)
114. Galdino, L.; Edwards, A.; Yi, W.; Sillekens, E.; Wakayama, Y.; Gerard, T.; Pelouch, W.S.; Barnes, S.; Tsuritani, T.; Killey, R.I.; et al. Optical Fibre Capacity Optimisation via Continuous Bandwidth Amplification and Geometric Shaping. *IEEE Photon. Technol. Lett.* **2020**, *32*, 1021–1024. [\[CrossRef\]](#)
115. Le Gac, D.; Bendimerad, D.; Demirtzioglou, I.; De Jauregui Ruiz, I.F.; Lorences-Riesgo, A.; El Dahdah, N.; Gallet, A.; Elfaiki, H.; Yu, S.; Gao, G.; et al. 63.2Tb/s Real-time Transmission Through Discrete Extended C- and L-Band Amplification in a 440 km SMF Link. In Proceedings of the 2021 European Conference on Optical Communication (ECOC), Bordeaux, France, 13–16 September 2021; pp. 1–4.
116. Demirtzioglou, I.; Bendimerad, D.F.; de Jauregui Ruiz, I.F.; Le Gac, D.; Lorences-Riesgo, A.; El Dahdah, N.; Gallet, A.; Elfaiki, H.; Yu, S.; Gao, G.; et al. 107.6 Tb/s GMI Throughput over 220 km SSMF using Discrete C- and L-Band Amplification across >12 THz. In Proceedings of the 2021 Optical Fiber Communications Conference and Exhibition (OFC), San Francisco, CA, USA, 6–10 June 2021; pp. 1–3.
117. Mizuno, T.; Shibahara, K.; Ye, F.; Sasaki, Y.; Amma, Y.; Takenaga, K.; Jung, Y.; Pulverer, K.; Ono, H.; Abe, Y.; et al. Long-Haul Dense Space-Division Multiplexed Transmission Over Low-Crosstalk Heterogeneous 32-Core Transmission Line Using a Partial Recirculating Loop System. *J. Light. Technol.* **2017**, *35*, 488–498. [\[CrossRef\]](#)
118. Hayashi, T.; Tamura, Y.; Hasegawa, T.; Taru, T. Record-Low Spatial Mode Dispersion and Ultra-Low Loss Coupled Multi-Core Fiber for UltraLong-Haul Transmission. *J. Light. Technol.* **2017**, *35*, 450–457. [\[CrossRef\]](#)
119. Milione, G.; Ip, E.; Li, M.-J.; Stone, J.; Peng, G.; Wang, T. Mode crosstalk matrix measurement of a 1 km elliptical core few-mode optical fiber. *Opt. Lett.* **2016**, *41*, 2755–2758. [\[CrossRef\]](#)
120. Jain, S.; Castro, C.; Jung, Y.; Hayes, J.; Sandoghchi, R.; Mizuno, T.; Sasaki, Y.; Amma, Y.; Miyamoto, Y.; Bohn, M.; et al. 32-core erbium/ytterbium-doped multicore fiber amplifier for next generation space-division multiplexed transmission system. *Opt. Express* **2017**, *25*, 32887–32896. [\[CrossRef\]](#)
121. Ip, E.; Li, M.J.; Bennett, K.; Huang, Y.K.; Tanaka, A.; Korolev, A.; Koreshkov, K.; Wood, W.; Mateo, E.; Hu, J.; et al. $146\lambda \times 6 \times 19$ -Gbaud wavelength- and mode division multiplexed transmission over 10×50 -km spans of few-mode fiber with a gain-equalized few-mode EDFA. *J. Light. Technol.* **2013**, *32*, 790–797. [\[CrossRef\]](#)
122. Gnauck, A.H.; Winzer, P.J.; Jopson, R.M.; Burrows, E.C. Efficient pumping scheme for amplifier arrays with shared pump laser. In Proceedings of the ECOC 2016; 42nd European Conference on Optical Communication, Dusseldorf, Germany, 18–22 September 2016.
123. Du, J.; Zheng, L.; Xu, K.; Chen, G.; Ma, L.; Liu, Y.; He, Z. High speed and small footprint silicon micro-ring modulator assembly for space-division-multiplexed 100-Gbps optical interconnection. *Opt. Express* **2018**, *26*, 13721–13729. [\[CrossRef\]](#) [\[PubMed\]](#)
124. Ferrari, A.; Napoli, A.; Fischer, J.K.; Costa, N.; D’Amico, A.; Pedro, J.; Forysiak, W.; Pincemin, E.; Lord, A.; Stavdas, A.; et al. Assessment on the achievable throughput of multi-band ITU-T G. 652. D fiber transmission systems. *J. Light. Technol.* **2020**, *38*, 4279–4291. [\[CrossRef\]](#)
125. Rajana, K.; Mitra, A.; Pradhan, A.; Grattan, K.; Srivastava, A.; Mukherjee, B.; Lord, A. When Is Operation C + L Bands More Economical than Multifiber for Capacity Upgrade of an Optical Backbone Network? In Proceedings of the 2020 European Conference on Optical Communications (ECOC), Brussels, Belgium, 6–10 December 2020; IEEE: Piscataway, NJ, USA, 2020.
126. Kobayashi, T.; Nakamura, M.; Hamaoka, F.; Shibahara, K.; Mizuno, T.; Sano, A.; Kawakami, H.; Isoda, A.; Nagatani, M.; Yamazaki, H.; et al. 1-Pb/s (32 SDM/46 WDM/768 Gb/s) C-band dense SDM transmission over 205.6-km of single-mode heterogeneous multi-core fiber using 96-Gbaud PDM-16QAM channels. In Proceedings of the 2017 Optical Fiber Communications Conference and Exhibition (OFC), Los Angeles, CA, USA, 19–23 March 2017; pp. 1–3.
127. Pulverer, K.; Tanaka, T.; Häbel, U.; Castro, C.; Bohn, M.; Mizuno, T.; Isoda, A.; Shibahara, K.; Inui, T.; Miyamoto, Y.; et al. First Demonstration of Single-Mode MCF Transport Network with Crosstalk-Aware In-Service Optical Channel Control. In Proceedings of the 2017 European Conference on Optical Communication (ECOC), Gothenburg, Sweden, 17–21 September 2017; pp. 1–3. [\[CrossRef\]](#)
128. Takasaka, S.; Maeda, K.; Kawasaki, K.; Yoshioka, K.; Oshio, H.; Sugizaki, R.; Kawaguchi, Y.; Takahashi, H.; Tsuritani, T.; Shiino, M. Increase of Cladding Pump Power Efficiency by a 19 Core Erbium Doped Fibre Amplifier. In Proceedings of the 2017 European Conference on Optical Communication (ECOC), Gothenburg, Sweden, 17–21 September 2017; pp. 1–3.

129. Thouras, J.; Pincemin, E.; Amar, D.; Gravey, P.; Morvan, M.; Moulinard, M.-L. Introduction of 12 Cores Optical Amplifiers in Optical Transport Network: Performance Study and Economic Impact. In Proceedings of the 2018 20th International Conference on Transparent Optical Networks (ICTON), Bucharest, Romania, 1–5 July 2018; pp. 1–4.
130. Jinno, M.; Kodama, T. Spatial Channel Network (SCN): Introducing Spatial Bypass Toward the SDM Era. In Proceedings of the Optical Fiber Communication Conference (OFC), San Diego, CA, USA, 8–12 March 2020; pp. 1–3.
131. Luis, R.S.; Puttnam, B.J.; Rademacher, G.; Eriksson, T.A.; Hirota, Y.; Shinada, S.; Ross-Adams, A.; Gross, S.; Withford, M.; Maruyama, R.; et al. Demonstration of a 1 Pb/s spatial channel network node. In Proceedings of the 45th European Conference on Optical Communication (ECOC 2019), Dublin, Ireland, 22–26 September 2019; pp. 1–4.
132. Marom, D.M.; Blau, M. Switching solutions for WDM-SDM optical networks. *IEEE Commun. Mag.* **2015**, *53*, 60–68. [\[CrossRef\]](#)
133. Miyamoto, Y.; Suzuki, K.; Nakajima, K. Multicore fiber transmission system for high-capacity optical transport network. *Next-Gener. Opt. Commun. Compon. Sub-Syst. Syst. VIII* **2019**, 10947, 1094703.
134. Pecci, P.; Jovanovski, L.; Barezzani, M.; Kamalov, V.; Marcerou, J.F.; Cantono, M. Pump Farming as enabling factor to increase subsea cable. *Proc. SubOptic.* **2019**, 2019, 1–7.
135. Bolshtyansky, M.A.; Sinkin, O.V.; Paskov, M.; Hu, Y.; Cantono, M.; Jovanovski, L.; Pilipetskii, A.N.; Mohs, G.; Kamalov, V.; Vusirikala, V. Single-Mode Fiber SDM Submarine Systems. *J. Light. Technol.* **2019**, *38*, 1296–1304. [\[CrossRef\]](#)
136. Papapavlou, C.; Paximadis, K.; Tzimas, G. Design and Analysis of a new SDM submarine optical network for Greece. In Proceedings of the 2021 12th International Conference on Information, Intelligence, Systems & Applications (IISA), Chania Crete, Greece, 12–14 July 2021.
137. Lagkas, T.; Klonidis, D.; Sarigiannidis, P.; Tomkos, I. 5G/NGPON Evolution and Convergence: Developing on Spatial Multiplexing of Optical Fiber Links for 5G Infrastructures. *Fiber Integr. Opt.* **2020**, *39*, 4–23. [\[CrossRef\]](#)
138. Desurvire, E.B. Capacity Demand and Technology Challenges for Lightwave Systems in the Next Two Decades. *J. Light. Technol.* **2006**, *24*, 4697–4710. [\[CrossRef\]](#)
139. Fontaine, N.K.; Mazur, M.; Ryf, R.; Chen, H.; Dallachiesa, L.; Neilson, D.T. 36-THz Bandwidth Wavelength Selective Switch. In Proceedings of the 2021 European Conference on Optical Communication (ECOC), Bordeaux, France, 13–16 September 2021; pp. 1–4.
140. Jatoba-Neto, A.C.; Mello, D.A.A.; Rothenberg, C.E.; Arik, S.; Kahn, J.M. Scaling SDM Optical Networks Using Full-Spectrum Spatial Switching. *J. Opt. Commun. Netw.* **2018**, *10*, 991–1004. [\[CrossRef\]](#)
141. Chen, K.; Ye, T.; He, H.; Guo, Z. Modula Optical Cross-Connect (OXCs) for Large-Scale Optical Networks. *IEEE Photon. Technol. Lett.* **2019**, *31*, 763–766. [\[CrossRef\]](#)
142. Hasegawa, H.; Sato, K.I. Switching Granularity and intra-node interconnection optimization for large scale optical nodes. In Proceedings of the 2019 24th OptoElectronics and Communications Conference (OECC) and 2019 International Conference on Photonics in Switching and Computing (PSC), Fukuoka, Japan, 7–11 July 2019.
143. Kuno, T.; Mori, Y.; Hasegawa, H. A 2.15 Pbps Throughput Optical Cross-Connect with Flexible Waveband Routing. In Proceedings of the 2020 IEEE 8th International Conference on Photonics (ICP), Kota Bharu, Malaysia, 12 May–30 June 2020; pp. 28–29. [\[CrossRef\]](#)
144. Kuno, T.; Mori, Y.; Subramaniam, S.; Jinno, M.; Hasegawa, H. Experimental Evaluation of Optical Cross-Connects with Flexible Waveband Routing Function for SDM Networks. In Proceedings of the 2021 Optical Fiber Communications Conference and Exhibition (OFC), San Francisco, CA, USA, 6–10 June 2021.
145. Zhang, J.; Zhu, B.; Yan, X.; Chen, C.; Jiang, M.; Hu, F. A novel multi-granularity two-layer SDM ROADM architecture. *Opt. Commun.* **2021**, *479*, 126473. [\[CrossRef\]](#)
146. Ding, S.; Yin, S.; Zhang, Z.; Huang, S. Evaluation of the Flexibility of Switching Node Architectures for Spaced Division Multiplexed Elastic Optical Network. In Proceedings of the 2020 Optical Fiber Communications Conference and Exhibition (OFC), San Diego, CA, USA, 8–12 March 2020; pp. 1–3.
147. Ge, D.; Guo, B.; Yang, Y.; Chen, Z.; He, Y.; He, J.; Li, J. Layered OXC With Intermodulation Switching Bridge for Optical SDM-WDM Networks. *J. Light. Technol.* **2019**, *37*, 3918–3924. [\[CrossRef\]](#)
148. Paximadis, K.; Papapavlou, C. Towards an all-New Submarine Optical Network for the Mediterranean Sea: Trends, Design and Economics. In Proceedings of the 2021 12th International Conference on Network of the Future (NoF), Coimbra, Portugal, 6–8 October 2021. [\[CrossRef\]](#)
149. “FLEX-SCALE” Project. Available online: <https://6g-flexscale.eu/> (accessed on 8 October 2023).
150. Benzaoui, N.; Soudais, G.; Angot, O.; Robineau, P.; Bigo, S. DDX Add-On Card: Transforming Any Optical Legacy Network into a Deterministic Infrastructure. In Proceedings of the 2021 European Conference on Optical Communication (ECOC), Bordeaux, France, 13–16 September 2021.
151. Zhou, S.; Liu, X.; Effenberger, F.; Chao, J. Low-Latency High-Efficiency Mobile Fronthaul With TDM-PON (Mobile-PON). *J. Opt. Commun. Netw.* **2018**, *10*, A20–A26. [\[CrossRef\]](#)

Disclaimer/Publisher’s Note: The statements, opinions and data contained in all publications are solely those of the individual author(s) and contributor(s) and not of MDPI and/or the editor(s). MDPI and/or the editor(s) disclaim responsibility for any injury to people or property resulting from any ideas, methods, instructions or products referred to in the content.